# THE IRRADIATED HUMAN MANDIBLE

Hannah Dekker

# THE IRRADIATED HUMAN MANDIBLE

**Hannah Dekker**

Financial support for printing and distribution of this thesis was kindly supported by:
ACTA, NVMKA, van Velthuysen Liebrecht, Straumann, Dam Medical, ExamVision.

ISBN/EAN: 978-94-6496-118-8

Cover design and Lay-Out: Hannah Dekker, Wendy Bour-van Telgen
Cover illustration: 'Skull and book, 1885' by Paul Cézanne
Copyright: Detroit Institute of Arts
Printed by: Gildeprint, Enschede

VRIJE UNIVERSITEIT

# THE IRRADIATED HUMAN MANDIBLE

ACADEMISCH PROEFSCHRIFT

ter verkrijging van de graad Doctor aan
de Vrije Universiteit Amsterdam,
op gezag van de rector magnificus
prof.dr. J.J.G. Geurts,
in het openbaar te verdedigen
ten overstaan van de promotiecommissie
van de Faculteit der Tandheelkunde
op vrijdag 14 juni 2024 om 11.45 uur
in een bijeenkomst van de universiteit,
De Boelelaan 1105

door

Hannah Dekker

geboren te Hoorn

| | |
|---|---|
| promotoren: | prof.dr. E.A.J.M. Schulten<br>prof.dr. E. Bloemena |
| copromotoren: | dr. N. Bravenboer<br>prof.dr. C.M. ten Bruggenkate |
| promotiecommissie: | prof.dr. J. Klein Nulend<br>prof.dr. R. de Bree<br>prof.dr. J.P.R. van Merkesteyn<br>prof.dr. J.G.A.M. de Visscher<br>prof.dr.dr. P.A.W.H. Kessler |

Voor mijn ouders

# CONTENTS

# 1

# General introduction and outline of the thesis

In the Netherlands, approximately 3% of all new cases of cancer are localized in the head and neck area. It is the 8th most common cancer in men and the 9th in women.[1] Radiotherapy is an important treatment modality in head and neck cancer, which, depending on tumor site and stage, can be administered as a primary therapy or adjuvant to surgery. However, radiotherapy in the head and neck region is associated with oral sequelae that are the result of the deleterious effects of radiation on the surrounding tissues. The clinical consequences of radiotherapy include mucositis, hyposalivation, loss of taste, radiation caries, trismus and osteoradionecrosis (ORN).[2] ORN is a severe complication and is characterized by a non-healing area of exposed bone of at least three months duration.[3] As a late complication of irradiation, it can develop at any time from a few months to many years after radiotherapy.[4] ORN is associated with pain, drainage and fistulae of the mucosa or skin, pathological fracture, and usually has a high morbidity. In advanced stages, ORN typically requires surgical resection and reconstruction.[5]

There is no general consensus about the pathophysiology -and consequently, the prevention and management- of ORN. Historically, there are two main theories for the pathogenesis of ORN with two different therapeutic approaches based on the presumed underlying mechanisms. In 1983, Marx proposed the theory that a sequence of radiation-induced cellular injury leads to the formation of hypoxic, hypocellular and hypovascular tissue, and subsequent tissue breakdown through persistent hypoxia can cause a chronic, non-healing wound that can ultimately result in ORN.[6] Marx developed a treatment protocol consisting of a combination of hyperbaric oxygen therapy and surgical resection and reconstruction with microvascular flap surgery based on his concept, that the trias hypovascularity, hypocellularity and hypoxia (the 'triple H' theory) is the main pathophysiologic event in ORN. However, the importance of hypoxia in tissues affected by ORN has never been proven.[7]

In 2004, Delanian and Lefaix proposed a theory for the pathogenesis of ORN that emphasizes the role of a radiation-induced fibro-atrophic process[8]. Three subsequent phases are described. First, a pre-fibrotic phase, characterized by non-specific chronic local inflammation, destruction of endothelial cells and vascular thrombosis. Second, a constitutive organized phase, characterized by inappropriate fibroblastic activity, leading

to a fibrotic remodeling of the extracellular matrix. Third, the late fibro-atrophic phase, characterized by poorly vascularized and acellular fibrous tissue, present up to decades after radiotherapy. The resulting fragile tissue could, especially in combination with trauma, result in ORN.[9] Based on this theory, a treatment protocol using pentoxifylline, tocopherol and clodronate has been introduced as a means to prevent and treat ORN by means of an anti-oxidant effect (pentoxifylline), improving local microcirculation (tocopherol) and inhibition of osteoclasts (clodronate). Although studies have shown that the combination of pentoxifylline plus tocopherol with or without clodronate was found to be effective for the treatment of mandibular ORN, data are generally scarce and mostly derived from retrospective case series.[10,11]

In search of scientific evidence of the two main theories by Marx and Delanian and Lefaix, the proceeds are scarce. In Marx´ publication presenting his ´triple H´ hypothesis, he sought to demonstrate tissue hypoxia by measuring oxygen tension in the skin in the radiation field and compared it to that in the intercostal space and found the oxygen tension to be lower in the radiated area. However, Rudolph et al. found similar transcutaneous oxygen pressure values in irradiated and non-irradiated skin.[12]

The literature has heretofore not been able to demonstrate a clear and quantitative degradation of bone microvasculature in the irradiated human mandible. Most studies on vascularity in irradiated mandibles were carried out in animal models.[13-20] In animal studies, the radiation doses and regimens vary greatly, as well as timing of sacrifice and methods of vascularity assessment. Moreover, it is unclear to what extent animal models can accurately represent events in human bone. Impairment of vascularity in irradiated mandibles is a common finding. Most studies focusing on vascularity in irradiated mandibular bone use qualitative assessment, which is not suitable to specify the extent and characteristics of vascular degradation, or flow studies which measure changes in blood flow but do not directly determine the quantitative changes in the vessel number and size.[13]

The consequences of irradiation for bone and bone marrow adipose tissue have been investigated in animal models and in vitro studies. High dose irradiation in rodent models leads to early osteocyte death, initial increase of osteoclast activity and decreased

osteoblast activity with subsequent loss of bone volume and increased bone marrow adiposity.[14,21-28] After high dose irradiation, an initial increase in osteoclastic activity is followed by long term depletion and inhibition of osteoclastogenesis potential.[25,26] In vitro experiments have shown that skeletal stem cells harvested from the iliac crest are capable of maintaining their proliferation, differentiation, and regenerative properties at low-dose irradiation exposure, but at a lower capacity than non-irradiated skeletal stem cells. However, after high-dose exposure skeletal stem cells lose their stem cell characteristics or experience cell death.[29]

Radiation damage to mandibular bone tissue is a dynamic and multifactorial process, which makes it difficult to investigate. In search of evidence supporting the different theories of the pathogenesis of ORN, quantitative histological research data is indispensable. As mentioned, most histological studies on radiation damage to (mandibular) bone have been performed in animal models. Studies on human tissue are limited and have typically been performed on tissue specimens derived from ORN lesions or oncological resections in previously irradiated patients.[30-36] A disadvantage of these studies is that the investigated tissue has been subjected to pathologic processes (e.g. tumor, ORN) that could potentially bias the results.

Bras et al.[30] compared mandibles of non-irradiated, irradiated non-ORN patients (irradiated with 60 Gy, resected due to recurrent tumor) and ORN patients in a qualitative descriptive histological analysis. Two non-ORN irradiated mandibular specimens obtained from patients undergoing segmental mandibulectomy due to recurrent tumor, resected 1 and 9 months after irradiation with 60 Gy were used in this study. Between the non-irradiated and the irradiated, non-ORN mandibles, the only differences found were the fibrosis of the periosteum and intimal thickening of the inferior alveolar artery observed in the irradiated non-ORN mandibles. The irradiated mandibles did not show fibrosis of the bone marrow, and cortical and trabecular bone were vital. The authors concluded from the findings in ORN mandibles (obliteration of the inferior alveolar artery and necrosis of the buccal cortex with mostly vital lingual and inferior cortex, bone marrow and periosteal fibrosis) that ORN is an ischemic necrosis rather than a radiation induced bone necrosis. The conclusion that ORN is an ischemic necrosis, however, cannot frankly be drawn from the data presented. When a

patient undergoes segmental mandibular resection for ORN, a situation of prolonged exposed bone with severe infection has been present for a period of time. It is impossible to conclude whether the vascular obliteration and marrow fibrosis preceded the occurrence of ORN or resulted from the extensive bacterial contamination and inflammatory response typically seen in ORN lesions.

McGregor et al. investigated the inferior alveolar artery and periosteal vessels in 22 irradiated (external beam irradiation) non-ORN mandibular samples from tumor resections, without signs of mandibular ORN, and demonstrated a radiation-induced increase in the number of periosteal blood vessels but no significant effect on the inferior alveolar artery.[33] Interval between radiotherapy and resection was 21.8 months (range 2-84 months) and the total radiation dose was 50-60 Gy. Furthermore, in a different study, the authors state that atrophy of the inferior alveolar artery in edentulous patients is a common finding and in combination with atherosclerosis can cause stenosis of this artery, also in non-irradiated patients.[37] These findings imply that the hypothesis of Bras et al. that obliteration of the alveolar inferior artery leads to an ischemic necrosis of the mandible is less plausible.

Curi et al. investigated mandibular bone specimens from ORN patients and compared these with non-irradiated specimens from mandibular samples obtained from tumor resection.[31] A quantitative analysis showed a decrease in bone marrow cellularity and vascularity and increased fibrosis in the samples of ORN patients. However, a control group of irradiated, non-ORN mandibular bone was not included in this study.

Store et al. studied the vascular channels, resorption and regeneration areas in cortical bone sites of mandibular samples from non-irradiated, irradiated and ORN patients.[36] Vascular channels in the mandibular cortical bone did not significantly differ between non-irradiated and irradiated mandibles but were increased in ORN samples. Cortical bone of non-irradiated and irradiated mandibles showed no resorption nor regeneration sites, whereas in ORN samples high metabolic activity with active resorption and regeneration of bone was observed. Apparently, in the (subperiosteal) cortical bone, bone formation is not impaired, which corresponds with the finding of Bras et al.[30] that

on the lingual and inferior cortex of ORN samples, subperiosteal bone apposition is observed.

Three different studies aimed to distinguish ORN, medication-related osteonecrosis of the jaw (MRONJ) and osteomyelitis of the jaw (OMJ) histologically.[32,34,35] It appeared in two out of these three studies,[34,35] that histopathological assessment of ORN, MRONJ, and OMJ failed to identify distinctive microscopic characteristics in any of the three entities that could be used to differentiate between ORN, MRONJ, and OMJ. All three entities show signs of chronic inflammation and bacterial colonization, presence of Actinomyces, reactive bone formation and a depletion of osteoclasts.

## OUTLINE AND AIM OF THE STUDY

To better understand the events leading up to the development of ORN, we should first focus on what happens in the irradiated mandible, and investigate the effect of irradiation on the individual cells and tissues in the bone and bone marrow. The general aim of the present study was to thoroughly investigate the effects of radiotherapy on the human mandible at the tissue level, in order to elucidate the processes that occur in irradiated human mandibular bone, that might precede and contribute to the development of ORN. The goal was to broaden the current perspective by focusing on all aspects of the bone tissue: the trabecular structure, the vascularity, the bone turnover and the bone marrow.

In order to investigate the effect of radiation we compared bone specimens taken from mandibles of edentulous patients during dental implant surgery, with and without a history of radiotherapy on the mandible (Chapters 4, 5 and 6). Because all these patients were edentulous, there was another issue to address first. Edentulism in itself initiates a process of resorption that changes the properties of the mandibular bone. In order to correctly interpret the findings in the mandibles of irradiated patients, we needed to first define the characteristics of mandibular bone affected by resorption due to edentulism (Chapters 2 and 3). The available literature was unable to provide this definition and, therefore, the first part of this thesis describes the changes in bone

microstructure and turnover in the edentulous mandible including differences between men and women and progressive stages of bone resorption.

In ***Chapters 2 and 3*** the non-irradiated, edentulous human mandible was studied with respect to the cellular and structural aspects in bone biopsies using histology and micro-CT (Chapter 2). The dimensions, mineralization and microstructure were investigated using micro-CT in larger segments of mandibular bone from human cadavers (Chapter 3).

In ***Chapter 4*** the microvascular system in the irradiated mandibular bone marrow was quantitatively assessed by immunohistomorphometry.

In ***Chapter 5*** bone from healthy individuals was compared with that from previously irradiated individuals. The effect of radiotherapy on the trabecular structure and turnover in trabecular mandibular bone and its relation with radiation dose was assessed by micro-CT and histomorphometrical analysis.

In ***Chapter 6*** the effect of radiotherapy on osteocyte apoptosis, osteocyte death and bone marrow adipocytes in the human mandible was further investigated by immunohistochemical and histomorphometrical analyses, giving a perspective on the possible contribution of the findings to the pathophysiology of radiation damage and ORN.

# REFERENCES


1. IKNL. Hoofd-hals kanker. (https://www.iknl.nl/kankersoorten/hoofd-halskanker).
2. Vissink A, Jansma J, Spijkervet FK, Burlage FR, Coppes RP. Oral sequelae of head and neck radiotherapy. Crit Rev Oral Biol Med 2003;14(3):199-212.
3. Chrcanovic BR, Reher P, Sousa AA, Harris M. Osteoradionecrosis of the jaws--a current overview--part 1: Physiopathology and risk and predisposing factors. Oral Maxillofac Surg 2010;14(1):3-16. DOI: 10.1007/s10006-009-0198-9.
4. Moon DH, Moon SH, Wang K, et al. Incidence of, and risk factors for, mandibular osteoradionecrosis in patients with oral cavity and oropharynx cancers. Oral Oncol 2017;72:98-103. DOI: 10.1016/j.oraloncology.2017.07.014.
5. Jereczek-Fossa BA, Orecchia R. Radiotherapy-induced mandibular bone complications. Cancer Treat Rev 2002;28(1):65-74. DOI: 10.1053/ctrv.2002.0254.
6. Marx RE. Osteoradionecrosis: a new concept of its pathophysiology. J Oral Maxillofac Surg 1983;41(5):283-8.
7. Jegoux F, Malard O, Goyenvalle E, Aguado E, Daculsi G. Radiation effects on bone healing and reconstruction: interpretation of the literature. Oral Surg Oral Med Oral Pathol Oral Radiol Endod 2010;109(2):173-84. DOI: 10.1016/j.tripleo.2009.10.001.
8. Delanian S, Lefaix JL. The radiation-induced fibroatrophic process: therapeutic perspective via the antioxidant pathway. Radiother Oncol 2004;73(2):119-31. DOI: 10.1016/j.radonc.2004.08.021.
9. Lyons A, Ghazali N. Osteoradionecrosis of the jaws: current understanding of its pathophysiology and treatment. Br J Oral Maxillofac Surg 2008;46(8):653-60. DOI: 10.1016/j.bjoms.2008.04.006.
10. Martos-Fernandez M, Saez-Barba M, Lopez-Lopez J, Estrugo-Devesa A, Balibrea-Del-Castillo JM, Bescos-Atin C. Pentoxifylline, tocopherol, and clodronate for the treatment of mandibular osteoradionecrosis: a systematic review. Oral Surg Oral Med Oral Pathol Oral Radiol 2018;125(5):431-439. DOI: 10.1016/j.oooo.2018.02.004.
11. Kolokythas A, Rasmussen JT, Reardon J, Feng C. Management of osteoradionecrosis of the jaws with pentoxifylline-tocopherol: a systematic review of the literature and meta-analysis. Int J Oral Maxillofac Surg 2019;48(2):173-180. DOI: 10.1016/j.ijom.2018.08.007.
12. Rudolph R, Tripuraneni P, Koziol JA, McKean-Matthews M, Frutos A. Normal transcutaneous oxygen pressure in skin after radiation therapy for cancer. Cancer 1994;74(11):3063-70. DOI: 10.1002/1097-0142(19941201)74:11<3063::aid-cncr2820741126>3.0.co;2-c.
13. Deshpande SS, Donneys A, Farberg AS, Tchanque-Fossuo CN, Felice PA, Buchman SR. Quantification and characterization of radiation-induced changes to mandibular vascularity using micro-computed tomography. Ann Plast Surg 2014;72(1):100-3. DOI: 10.1097/SAP.0b013e318255a57d.
14. Fenner M, Park J, Schulz N, et al. Validation of histologic changes induced by external irradiation in mandibular bone. An experimental animal model. J Craniomaxillofac Surg 2010;38(1):47-53. DOI: 10.1016/j.jcms.2009.07.011.
15. Xu J, Zheng Z, Fang D, et al. Early-stage pathogenic sequence of jaw osteoradionecrosis in vivo. J Dent Res 2012;91(7):702-8. DOI: 10.1177/0022034512448661.
16. Yachouh J, Breton P, Roux JP, Goudot P. Osteogenic capacity of vascularised periosteum: an experimental study on mandibular irradiated bone in rabbits. J Plast Reconstr Aesthet Surg 2010;63(12):2160-7. DOI: 10.1016/j.bjps.2010.01.015.
17. Sonstevold T, Johannessen AC, Stuhr L. A rat model of radiation injury in the mandibular area. Radiat Oncol 2015;10:129. DOI: 10.1186/s13014-015-0432-6.
18. Poort LJ, Ludlage JHB, Lie N, et al. The histological and histomorphometric changes in the mandible after radiotherapy: An animal model. J Craniomaxillofac Surg 2017;45(5):716-721. DOI: 10.1016/j.jcms.2017.02.014.
19. Bodard AG, Debbache S, Langonnet S, Laffay F, Fleury B. A model of mandibular irradiation in the rabbit: preliminary results. Bull Group Int Rech Sci Stomatol Odontol 2013;52(1):e17-22.

**20.** Blery P, Espitalier F, Hays A, et al. Development of mandibular osteoradionecrosis in rats: Importance of dental extraction. J Craniomaxillofac Surg 2015;43(9):1829-36. DOI: 10.1016/j.jcms.2015.08.016.

**21.** Wright LE, Buijs JT, Kim HS, et al. Single-Limb Irradiation Induces Local and Systemic Bone Loss in a Murine Model. J Bone Miner Res 2015;30(7):1268-79. DOI: 10.1002/jbmr.2458.

**22.** Willey JS, Lloyd SA, Robbins ME, et al. Early increase in osteoclast number in mice after whole-body irradiation with 2 Gy X rays. Radiat Res 2008;170(3):388-92. DOI: 10.1667/RR1388.1.

**23.** Spiegelberg L, Braks JA, Groeneveldt LC, Djasim UM, van der Wal KG, Wolvius EB. Hyperbaric oxygen therapy as a prevention modality for radiation damage in the mandibles of mice. J Craniomaxillofac Surg 2015;43(2):214-9. DOI: 10.1016/j.jcms.2014.11.008.

**24.** Damek-Poprawa M, Both S, Wright AC, Maity A, Akintoye SO. Onset of mandible and tibia osteoradionecrosis: a comparative pilot study in the rat. Oral Surg Oral Med Oral Pathol Oral Radiol 2013;115(2):201-11. DOI: 10.1016/j.oooo.2012.09.008.

**25.** Zhai J, He F, Wang J, Chen J, Tong L, Zhu G. Influence of radiation exposure pattern on the bone injury and osteoclastogenesis in a rat model. Int J Mol Med 2019;44(6):2265-2275. DOI: 10.3892/ijmm.2019.4369.

**26.** Oest ME, Franken V, Kuchera T, Strauss J, Damron TA. Long-term loss of osteoclasts and unopposed cortical mineral apposition following limited field irradiation. J Orthop Res 2015;33(3):334-42. DOI: 10.1002/jor.22761.

**27.** Tchanque-Fossuo CN, Monson LA, Farberg AS, et al. Dose-response effect of human equivalent radiation in the murine mandible: part I. A histomorphometric assessment. Plast Reconstr Surg 2011;128(1):114-21. DOI: 10.1097/PRS.0b013e31821741d4.

**28.** Jackson RS, Voss SG, Wilson ZC, et al. An Athymic Rat Model for Mandibular Osteoradionecrosis Allowing for Direct Translation of Regenerative Treatments. Otolaryngol Head Neck Surg 2015;153(4):526-31. DOI: 10.1177/0194599815593278.

**29.** Costa S, Reagan MR. Therapeutic Irradiation: Consequences for Bone and Bone Marrow Adipose Tissue. Front Endocrinol (Lausanne) 2019;10:587. DOI: 10.3389/fendo.2019.00587.

**30.** Bras J, de Jonge HK, van Merkesteyn JP. Osteoradionecrosis of the mandible: pathogenesis. Am J Otolaryngol 1990;11(4):244-50.

**31.** Curi MM, Cardoso CL, de Lima HG, Kowalski LP, Martins MD. Histopathologic and Histomorphometric Analysis of Irradiation Injury in Bone and the Surrounding Soft Tissues of the Jaws. J Oral Maxillofac Surg 2016;74(1):190-9. DOI: 10.1016/j.joms.2015.07.009.

**32.** Marx RE, Tursun R. Suppurative osteomyelitis, bisphosphonate induced osteonecrosis, osteoradionecrosis: a blinded histopathologic comparison and its implications for the mechanism of each disease. Int J Oral Maxillofac Surg 2012;41(3):283-9. DOI: 10.1016/j.ijom.2011.12.016.

**33.** McGregor AD, MacDonald DG. Post-irradiation changes in the blood vessels of the adult human mandible. Br J Oral Maxillofac Surg 1995;33(1):15-8.

**34.** De Antoni CC, Matsumoto MA, Silva AAD, et al. Medication-related osteonecrosis of the jaw, osteoradionecrosis, and osteomyelitis: A comparative histopathological study. Braz Oral Res 2018;32:e23. DOI: 10.1590/1807-3107bor-2018.vol32.0023.

**35.** Shuster A, Reiser V, Trejo L, Ianculovici C, Kleinman S, Kaplan I. Comparison of the histopathological characteristics of osteomyelitis, medication-related osteonecrosis of the jaw, and osteoradionecrosis. Int J Oral Maxillofac Surg 2018. DOI: 10.1016/j.ijom.2018.07.002.

**36.** Store G, Granstrom G. Osteoradionecrosis of the mandible: a microradiographic study of cortical bone. Scand J Plast Reconstr Surg Hand Surg 1999;33(3):307-14.

**37.** McGregor AD, MacDonald DG. Age changes in the human inferior alveolar artery--a histological study. Br J Oral Maxillofac Surg 1989;27(5):371-4. DOI: 10.1016/0266-4356(89)90075-2.

# 2

# Resorption of the mandibular residual ridge: A micro-CT and histomorphometrical analysis

Hannah Dekker, Engelbert A.J.M. Schulten, Christiaan M. ten Bruggenkate, Elisabeth Bloemena, Leo van Ruijven, Nathalie Bravenboer

**Published in:** Gerodontology 2018; 35: 221-228

## ABSTRACT

Objectives: The aim of this study was to investigate whether the extent of mandibular resorption and gender is related to the bone turnover and microarchitecture of the edentulous mandible.

Participants and methods: A mandibular bone sample was obtained at canine position from 36 edentulous participants (50% women; mean age: 65 years) during dental implant surgery. All female participants were postmenopausal. Mandibular height, duration of edentulous state and resorption pattern (Cawood classification) were recorded. Microcomputed tomography was used to determine bone mineral density, bone volume fraction, trabecular connectivity density, trabecular number, trabecular thickness and trabecular separation. Histomorphometric analysis was used to assess bone turnover: osteoid area and surface were measured as a parameter for bone formation and osteoclast numbers were determined as a parameter for bone resorption. Correlations between micro-CT, histomorphometrical parameters and clinical data were analyzed with correlation coefficients and parametric and non-parametric tests.

Results: Lower mandibular height was strongly associated with higher bone mineral density in trabecular bone. Women showed higher osteoclast numbers in trabecular bone than men. In trabecular bone of women, bone volume was significantly related to osteoclast numbers, osteoid surface and osteoid area.

Conclusions: The higher trabecular bone mineral density found in the edentulous mandible could either indicate a restructuring process of the resorbed mandible or suggests that the inferior region of the mandible is more highly mineralized. In women, higher bone turnover is associated with lower bone volume, suggesting an effect of postmenopausal estrogen deficiency on bone turnover in the edentulous mandible.

# INTRODUCTION

Edentulism is a condition that affects many individuals worldwide. In Europe, the prevalence of edentulism ranges from 3 to 27% in the population over the age of 45 years.[1] After tooth loss, the residual ridge of the jaw decreases in a vertical and horizontal dimension in a process known as residual ridge resorption. The extent of resorption is four times greater in the mandible than in the maxilla.[2] In progressive stages of resorption, the mandible loses up to 60% of its original bone substanceee. Consequently, the denture-bearing area decreases and the retention of conventional dentures is compromised.[3] Although the introduction of dental implant supported prosthetics has significantly improved the outcomes of prosthetic care in the resorbed edentulous mandible[4,5,6], implant surgery in severely resorbed mandibles has proven to be a clinical challenge.[7]

Whether teeth are present or not, and independent of the gender of the individual, the mandible shows great variability in size, shape and in the fraction of its volume occupied by bone.[8] In the process of resorption, the pattern and extent of bone loss in the edentulous mandible vary greatly within and between individuals.[2,9,10] Studies focusing on the cortical and trabecular layers of the mandibular bone have shown that this variability is reflected in the apparent density and micro-architecture of the mandible.[8,11,12,13]

A definitive solution for preventing ridge resorption has yet to be discovered. Understanding mandibular bone physiology after tooth loss is essential for improvement and innovation of prosthetic care. Furthermore, a detailed documentation of normal variations in mandibular bone of healthy edentulous individuals is of great importance to correctly interpret findings in pathological situations predisposing the mandible such as peri-implantitis, osteomyelitis and osteo(radio)necrosis.

Studies focusing on mandibular bone microarchitecture are limited. No previous human studies have been carried out focusing on bone formation and resorption in edentulous mandibles. Bone loss occurs when the net bone resorption exceeds net formation, either as a result of increased resorption, decreased formation or both.[14] Changes in

bone turnover are bound to occur in residual ridge resorption of the mandible, resulting in its altered structure and shape after tooth loss. This led us to investigate the processes that occur in the resorbing edentulous mandible on a histological and morphological level. To the authors' knowledge, this is the first non-cadaver study using a combination of micro-CT and bone histomorphometry to assess bone microarchitecture and turnover in edentulous mandibles in an attempt to elucidate the physiological processes that occur after tooth loss in the mandible. The aim of this study was to investigate whether the extent of mandibular resorption and gender is related to the bone turnover and microarchitecture of the edentulous mandible.

## PARTICIPANTS AND METHODS

Participants in good general physical (ASA I and II) and mental health, fully edentulous in the lower jaw with an indication for dental implant surgery participated in the study. Exclusion criteria were previous bone augmentation surgery of the mandible, a history of bisphosphonate medication, impaired bone metabolism (e.g., hyperparathyroidism, osteomalacia) or systemic immunosuppressive medication up to 3 months prior to the dental implant surgery. Thirty-six participants (18 men and 18 women) were included in this study. All participants were of White Caucasian descent. All participants were included between 1-8-2012 and 31-12-2014 at the Alrijne Hospital in Leiderdorp. All female participants were postmenopausal and had no recorded history of osteoporosis. To confirm normal blood calcium, phosphate, parathyroid hormone and HbA1c levels, blood samples were drawn from all participants. Duration of edentulous state in the anterior mandible was recorded (self-reported). Resorption was measured in terms of interforaminal mandibular height and the Cawood classification of the resorption pattern.[15] Mandibular height was measured on a panoramic radiograph in the mental foramen region. The Cawood classification was registered from lateral cephalograms. All participants were fully informed and signed a written consent form. Prior to the study, approval for the research was provided by the Medical Ethical Committee of the VU University Medical Center, Amsterdam (registration number 2011/220).

*Dental implant surgery and bone biopsy retrieval*

All participants were treated in the Alrijne Hospital in Leiderdorp by a single oral and maxillofacial surgeon (CtB). Participants were given antibiotic prophylaxis (amoxicillin 3 gr orally) prior to dental implant surgery. The procedure was performed under local anaesthesia. A crestal incision was made in the interforaminal region with a buccal release incision at the symphysis. A full thickness mucoperiosteal flap was raised to expose the alveolar ridge and, if necessary, levelled by an alveolotomy. Implant preparations were made with a 2.5 mm (inner) diameter hollow trephine burr (Straumann) to a depth of 10 or 12 mm at left and right canine positions. After collection of the bone samples, additional cylindrical drills were used for alveolar preparation. All drilling phases were conducted under copious irrigation with sterile saline. Regular neck Straumann dental implants with a diameter of 4.1 mm and a length of 10 or 12 mm, and a SLA surface were inserted into the preparations. All implants showed good primary stability. The implants were placed in a single-staged surgical procedure, mounted with healing caps and the mucosa was sutured with non-resorbable sutures (Gore-Tex 4-0).

*Processing of the bone biopsies*

The most intact bone cylinder from each participant was selected for analysis. Bone cylinders were immediately fixed by immersion in 4% phosphate-buffered formaldehyde, dehydrated in ascending series of ethanols, and embedded in 80% methylmethacrylate (BDH Chemicals) supplemented with 20% dibuthylphtalate (Merck), 8 g/L lucidol CH-50L (Akzo Nobel) and 22 µl/10 ml N,Ndimethyl-p-toluidine (Merck).

*Micro-CT analysis*

Micro-CT analysis was performed to determine parameters of the bone microarchitecture. Embedded samples were scanned with a micro-computed tomography system (µCT 40; Scanco Medical AG) using 55 kV, 145 µA, 600 ms integration time, and a resolution of 8 µm. The polychromatic source and cone-shaped beam of the scanner was filtered with a 0.5 mm aluminum filter. The beam hardening effect was further reduced by applying a correction algorithm developed by the manufacturer. The system was calibrated weekly with a reference phantom (QRM GmbH).

Grey values were considered to be proportional to the local bone mineral density, equivalent to the concentration of hydroxyapatite (HA).[16,17] Imaging processing included Gaussian filtering and segmentation with sigma 0.3, support 1, threshold 560 mg HA/cm3. This threshold was used for each measurement. Volumes of interest (VOI) of cortical and trabecular regions were chosen by visual inspection. Transformation zones with no distinct trabecular or cortical characteristics were not included. In all VOI's bone volume fraction (BV/TV; %) and bone mineral density (BMD; mg HA/$cm^{-3}$) were determined. Additionally, in trabecular VOI's the trabecular number (Tb.N; 1/mm-1), separation (Tb.S; μm), thickness (Tb.Th; μm) and trabecular connectivity density were determined. The manufacturer's morphometric software uct_evaluation v6.5-3 (Scanco Medical AG) was used for this analysis.

*Histological procedure*

Following the scanning procedure, biopsies were cut into 5-micrometre-thick undecalcified sections with Polycut 2500 S Microtome (Reichert-Jung). Per biopsy, on 3 evenly spaced out sections a Goldner trichrome staining[18] and a Tartrate Resistant Acid Phosphatase (TRAP) reaction was performed.[19] Goldner's trichrome staining colors osteoid and demineralized bone matrix red, mineralized bone matrix blue and nuclei dark blue. The TRAP cytochemical activity reaction identifies osteoclasts by coloring TRAP-positive cells red while mineralized bone matrix and connective tissue colors green by green background stain.

*Histomorphometrical analysis*

Histomorphometry was used to determine parameters of bone turnover. Trabecular and cortical regions of interest were chosen by visual inspection conform VOI selection in micro-CT analysis. Histomorphometry measurements were performed automatically using NIS-Elements AR 4.10.01 (Nikon GmbH) at 400x magnification according to the ASBMR nomenclature.[20,21] Osteoid volume fraction (osteoid volume/bone volume OV/BV; %) and osteoid surface fraction (osteoid surface/bone surface OS/BS; %) were measured as parameters associated with bone formation. Bone resorption was assessed as osteoclast number per millimeter bone surface (n.Ocl/BS;/mm), which was measured using an integrated eye piece (Zeiss II, Zeiss). All measurements were performed by a single investigator (HD).

*Statistical analysis*

Correlations between micro-CT, histomorphometrical parameters and clinical data were analyzed with correlation coefficients and parametric and non-parametric tests. Pearson's correlation coefficient and Student's *t*-test were used for normally distributed variables to compare the mean; Spearman's correlation coefficient and Mann Whitney non-parametric test for abnormally distributed variables to compare the median of the parameters against the hypothetical value 1.0 (no difference in parameter between two groups; e.g., men/women). All statistical analyses were performed using SPSS software (version 22). $P<.05$ was considered statistically significant.

# RESULTS

Of 36 bone biopsies, 16 contained both trabecular and cortical bone compartments, 19 only contained trabecular bone, and one biopsy only contained cortical bone. Accordingly, 35 sections of trabecular bone (18 men, 17 women) and 17 sections of cortical bone (8 men, 9 women) were analyzed. Participant characteristics are shown in Table 1. A strong correlation was seen between the mandibular height and the Cawood classification (Spearman correlation $r = -0.848$, $p < 0.001$), as seen in Figure 1A, and between the mandibular height and the duration of edentulism (Pearson correlation $r = -0.571$, $p < 0.001$), as seen in Figure 1B. Mandibular height was selected as parameter for the extent of ridge resorption.

A strong relationship was seen between the mandibular height and bone mineral density (Spearman's correlation $r = -0.620$, $p < 0.001$) as seen in Figure 2A, bone biopsies from mandibles with lower height had a higher trabecular BMD, as seen in Figure 2B.

The trabecular bone in women contained a greater number of osteoclasts per millimeter bone surface than in men ($p = 0.032$). In women, but not in men, lower bone volume fraction (BV/TV) in trabecular bone correlated significantly with higher osteoclast number (Ocl.N/mmBS) (Spearman correlation $r = -0.750$, $p=0.001$), as seen in Figure 3A, osteoid volume fraction (OV/BV) (Spearman correlation $r = -0.654$, $p = 0.004$), as seen in Figure 3B, and osteoid surface fraction (OS/BS) (Spearman's correlation $r = -0.654$, $p = 0.004$), as seen in Figure 3C. There was no significant difference between men and women for any of the other measured parameters in cortical nor trabecular bone, as seen in Table 2.

Table 1. Participant characteristics. No significant differences were seen between men and women (Student's t-test).

| | **Men (n=18)** *Mean (min-max)* | | **Women (n=18)** *Mean (min-max)* | |
|---|---|---|---|---|
| **Age (years)** | 65 | (34-79) | 65 | (51-78) |
| **Edentulous state (years)** | 16.9 | (0.5-45) | 20.9 | (0.2-55) |
| **Mandibular height (mm)** | 21 | (12-30) | 18 | (8-30) |



Table 2. Median and interquartile range (IQR) for cortical and trabecular bone parameters in men and women. Non-parametric test (Mann Whitney) showed a significant difference between genders in osteoclast number.

| | **Unit** | **Men (n=8)** *Median (IQR)* | **Women (n=9)** *Median (IQR)* |
|---|---|---|---|
| **Bone volume fraction** | BV/TV (%) | 91.4 (9.89) | 93.4 (7.50) |
| **Bone mineral density** | BMD (mg HA/cm$^3$) | 1020 (98) | 1069 (54) |
| **Osteoid surface fraction** | OS/BS (%) | 37.5 (55.8) | 7.65 (39.8) |
| **Osteoid area fraction** | OV/TV (%) | 0.575 (2.89) | 0.0145 (1.24) |
| **Osteoclasts per mm** | N.Ocl/BS (/mm) | 0.113 (1.93) | 0.364 (0.480) |
| | | | |
| **Trabecular Measure** | **Unit** | **Men (n=18)** *Median (IQR)* | **Women (n=17)** *Median (IQR)* |
| **Bone volume fraction** | BV/TV (%) | 35.1 (21.3) | 27.4 (25.8) |
| **Bone mineral density** | BMD (mg HA/cm$^3$) | 958 (92) | 946 (90) |
| **Connectivity density** | Conn. Dens | 5.51 (6.90) | 6.76 (14) |
| **Trabecular number** | Tb.N (1/mm$^{-1}$) | 1.80 (0.76) | 2.08 (0.99) |
| **Trabecular thickness** | Tb.Th (μm) | 253 (57.4) | 237 (82.9) |
| **Trabecular separation** | Tb.Sp (μm) | 608 (30) | 461 (23) |
| **Osteoid surface fraction** | OS/BS (%) | 29.1 (61.0) | 11.3 (34.8) |
| **Osteoid area fraction** | OV/TV (%) | 3.68 (6.44) | 9.47 (11.9) |
| **Osteoclasts per mm** | N.Ocl/BS (/mm) | 0.379 (0.506) | 0.396 (1.675)* |

*p = 0.032

Abbreviations: IQR, interquartile range; BV, bone volume; TV, total volume; BMD, bone mineral density; OS, osteoid surface; BS, bone surface; OV, osteoid volume; N.Ocl, osteoclast number; BS, bone surface.

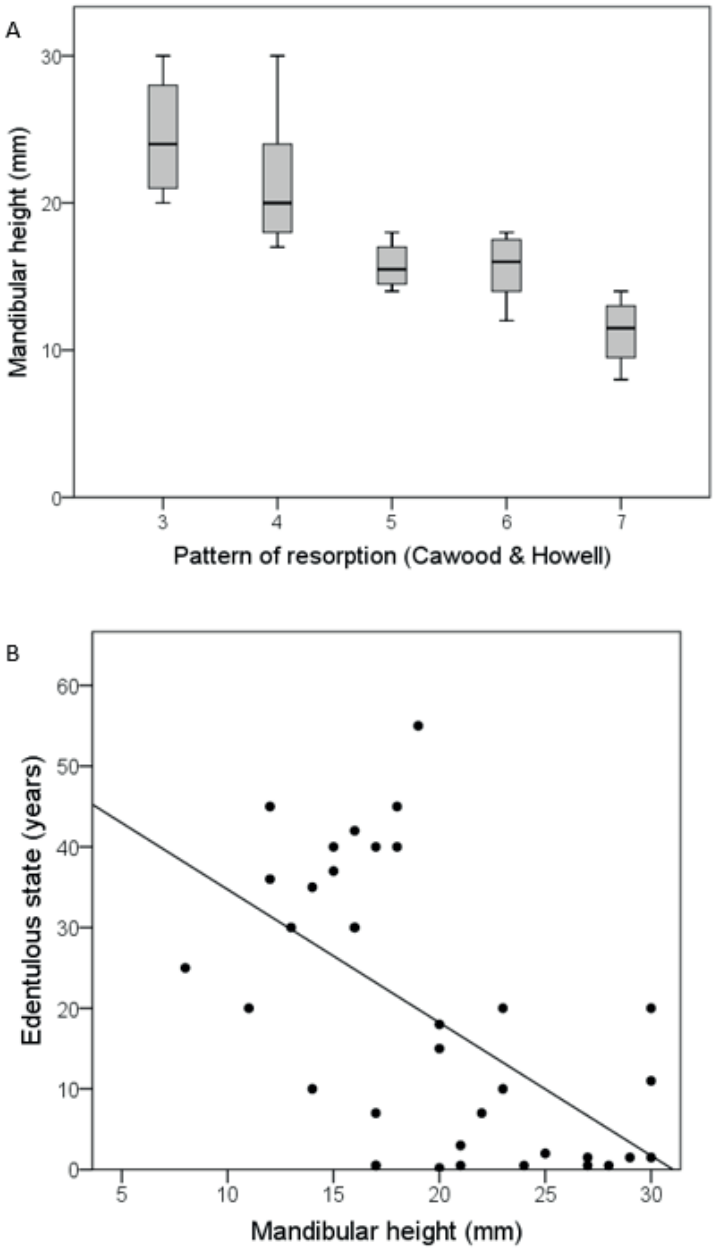


Figure 1.

A. Correlation between the Cawood classification and the mandibular height (Spearman's correlation r = -0.848 $p < 0.001$).

B. Correlation between mandibular height and duration of the edentulous state (Pearson's correlation r = -0.571, $p < 0.001$).

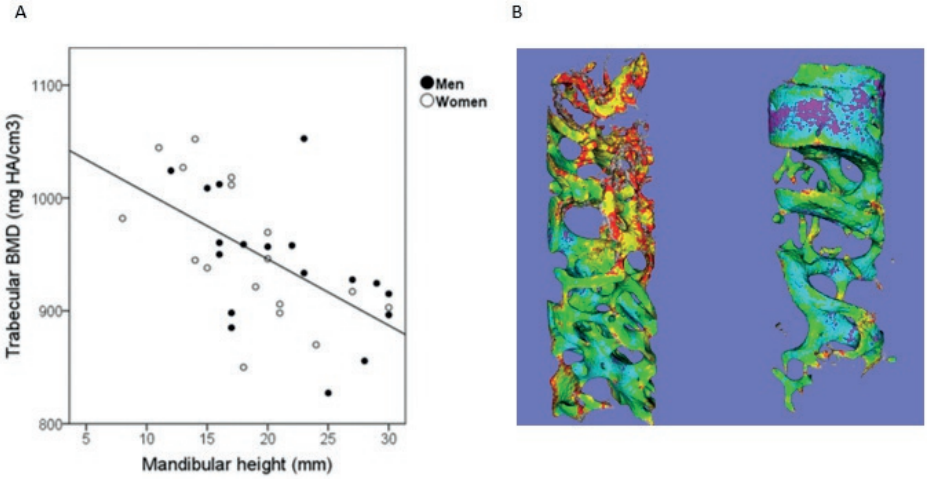


Figure 2.

A. Correlation between mandibular height and bone mineral density (Spearman's correlation r = -0.620, p <0.001)

B. Micro-CT image with bone mineral density in color scale for 2 biopsies from a mandible with a height of 30 mm (left) and 8 mm (right). Colors represent bone mineral density values (mmHA/cm3): red: 650-750, yellow: 750-850, green: 850-950, blue: 950-1050, magenta: 1050-1150. The biopsy from the mandible with lower height has a higher bone mineral density. Within the biopsy of the 30 mm mandible, the bone mineral density seems to increase gradually towards the basal part. Image obtained with uct_ evaluation v6.5-3 (Scanco Medical AG ).

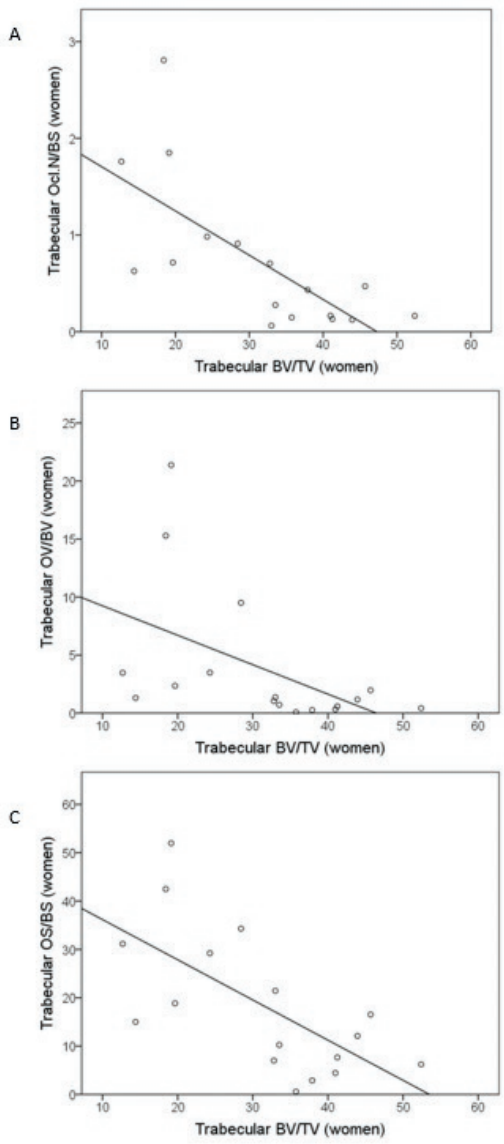


Figure 3.

A. Correlation between osteoclast number (Ocl.N/mmBS) and bone volume (BV/TV) in women (Spearman's correlation r = -0.750, p = 0.001).

B. Correlation between osteoid volume fraction (OV/TV) and bone volume (BV/TV) in women (Spearman's correlation r = -0.654 p = 0.004).

C. Correlation between osteoid surface fraction (OS/BS) and bone volume (BV/TV) in women (Spearman's correlation r = -0.654 p = 0.004).

# DISCUSSION

As expected, this study demonstrated a large variation in trabecular bone microarchitecture. This profound variability in trabecular microarchitecture has been described in various studies.[10,11,12,22,23] Ulm et al. found a coarsening of the trabecular microarchitecture in progressive atrophy, as well as an increased apposition to the inner cortex of bone with reduction in the trabecular compartment.[12,24] Towards the mandibular base, a denser trabecular microarchitecture is found compared to the alveolar area.[11] Ulm et al. also found a large variation in cortical thickness, and assumed that the stability of the mandible is more likely to depend on cortical bone than on trabecular bone. Several authors suggested the contribution of the trabecular bone compartment to structural strength is negligible.[25]

The micro-CT results of this study show that biopsies from mandibles with lower height have higher trabecular BMD. The increase of trabecular BMD with decreasing mandibular height could indicate that the trabecular microarchitecture to some extent does contribute to the structural strength of the resorbed mandible. This observation could be an effect of a restructuring process, where the progressively resorbed mandible compensates for loss of volume with an increase in trabecular BMD. Micro-CT has proven to be valuable in the assessment of different three-dimensional microarchitectural data including trabecular microarchitecture. With proper calibration, it can be used to reliably measure BMD.[22] The advantage of measuring BMD with micro-CT is that it measures a three-dimensional volume of bone, as opposed to two-dimensional techniques that measure density from radiographs which do not allow density to be calculated as a volumetric measurement.

Our samples were limited in size and did not provide a full volume measurement of the edentulous mandible. All biopsies were taken from the canine position and variations may occur in different regions of the mandible, although Monje et al. found that bone volume appears not to differ between defined anatomical locations.[26] The mineralization density tends to reduce in the more superior the site is sampled on the mandible, with the alveolar portion having the lowest density at the mental foramen and midline regions.[8,27] Biopsies from mandibles with lower height will contain a relatively larger

portion of bone from the inferior region than biopsies from higher mandibles. In other words, BMD is likely to increase gradually from the alveolar part towards the inferior region independent of the process of ridge resorption. Kingsmill et al.[28] found that areas of lowest density match the sites known to undergo the greatest net resorption following tooth loss, and found relatively high densities towards the inferior region at midline and interforaminal sites, which are thought to experience the highest strains.

No relationship between trabecular bone volume fraction and mandibular height was seen. This result corresponds with previous studies suggesting that the height of the mandible does not correlate with the trabecular bone volume.[8,11,12,29,30]

All women in this study are postmenopausal. Although no women had a recorded history of osteoporosis and estrogen levels were not measured, the majority of post-menopausal women have to some extent diminished bone density at postcranial skeletal sites.[30] Estrogen deficiency after menopause affects bone metabolism which leads to diminished BMD and bone volume and ultimately osteoporosis.[31] According to the literature, approximately 30% of post-menopausal women have osteoporosis. Estrogen deficiency increases osteoclast formation by increasing hematopoietic progenitors and providing a larger recruited osteoclast precursor pool. The upregulated formation and activation of osteoclasts lead to cortical porosity and enlarged resorption areas in trabecular surfaces.[32] Increased bone turnover in post-menopausal women is associated with osteoporosis.[13] This association has not been investigated specifically for mandibular bone as this is not a common site used to evaluate osteoporosis. In the present study, significantly higher number of osteoclasts was found in the trabecular compartment in women. This indicates that post-menopausal estrogen depletion leads to increased osteoclast numbers in the mandible. Although no significant difference in trabecular bone volume was found between genders, in women, but not in men, lower bone volume was associated with higher osteoclast numbers, osteoid surface and osteoid volume, which reflects a relationship between increased bone turnover and lower bone volume fraction.

Whether bone mass at the skeletal sites usually studied to evaluate osteoporosis is associated with alveolar bone resorption has long been a matter of debate.[33] Some

studies found a relationship between bone mass and density at other skeletal sites, most of which relied on two-dimensional scanning techniques such as Dual X-ray absorptiometry. This indirect measure of bone status gives a BMD value that consists of both cortical and trabecular volumes. In mandibles, the ratio between cortical and trabecular bone is highly variable, and in traditional X-rays, both halves of the mandible are often superimposed. Bodic et al.[34] analyzed iliac and mandibular bone samples with DXA, conventional CT and micro-CT, and found no relationships between mandibular and iliac bone, when considering mineral density, cortical thickness, bone volume or microarchitecture. The DXA method as currently available may therefore not be the most reliable method to assess BMD in the mandible.[25,35]

Techniques that provide the possibility of separate assessment of trabecular and cortical bone volume such as micro-computed tomography and histomorphometry can produce more reliable measurements of trabecular BMD and bone volume fraction.[24] Although present study shows no differences between men and women in trabecular bone volume fraction, several cadaver histomorphometric studies on cross sectional planes of edentulous mandibles have demonstrated a higher trabecular bone area fraction in men compared to women.[11,12,29] Our results suggest that post-menopausal women have an increase in mandibular bone turnover, which indicates that estrogen depletion affects mandibular bone turnover. Because the variability in bone volume in men as well as women, the dimension of our samples and the sample size of our study might be insufficient to demonstrate differences in trabecular bone volume between men and women.

The mandible differs in several ways from bones commonly affected by osteoporosis, for instance, it consists largely of cortical bone with a variable trabecular compartment, it may get more compact with age rather than less compact, it is more highly mineralized and it is of different embryological origin.[25] Pathological conditions with a strong predisposition for the mandible, such as antiresorptive drug related osteonecrosis of the jaw and osteoradionecrosis, suggest different bone dynamics in the mandible compared to other skeletal sites. This is supported by findings in animal studies, showing a different osteoclastogenesis and a different response of bone mass to ageing in mandibles compared to long bones.[36, 37]

No significant relationships were found between mandibular height and trabecular structure parameters (connectivity density, Tb.Th, Tb.N and Tb.Sp). To represent trabecular bone architecture accurately, the measured volume of interest should contain at least three to five intertrabecular lengths.[38] Standard bone biopsies for metabolic bone diseases are performed with a 7 mm diameter bone trephine. As our biopsies had a diameter of 2.5 mm, trabecular microarchitecture measurements may be biased.

Cortical bone measurements did not correlate with resorption parameters. This could be, in part, due to the smaller sample size. Only 17 out of 36 obtained bone samples contained sufficient cortical bone for analysis. Cortical bone varies greatly in thickness at the occlusal surface of the alveolar ridge. After extraction, a trabecular tract is observed at the healed extraction sites.[9] When the trephine drill enters the bone at this tract, no cortical bone is likely to be present in this biopsy. In addition, the alveolar ridge was leveled by alveolotomy prior to implantation, removing a small amount of the superficial (cortical) bone from the alveolar ridge.

## CONCLUSIONS

In conclusion, bone mineral density is higher in the trabecular bone of the more severely resorbed edentulous mandibles, although the clinical significance of this finding calls for further investigation. Only in women, bone volume was negatively associated with turnover, which suggests a similar relationship between a post-menopausal estrogen depletion and osteoporosis to that found in postcranial skeletal sites.

# REFERENCES


1. Guarnizo-Herreno CC, Watt RG, Pikhart H, Sheiham A, Tsakos G. Socioeconomic inequalities in oral health in different European welfare state regimes. J Epidemiol Community Health 2013;67:728-735.
2. Atwood DA, Coy WA. Clinical, cephalometric, and densitometric study of reduction of residual ridges. J Prosthet Dent 1971;26:280-295.
3. Jahangiri L, Devlin H, Ting K, Nishimura I. Current perspectives in residual ridge remodeling and its clinical implications: a review. J Prosthet Dent 1998;80:224-237.
4. Feine JS, Carlsson GE, Awad MA, Chehade A, Duncan WJ, Gizani S, et al. The McGill consensus statement on overdentures. Mandibular two-implant overdentures as first choice standard of care for edentulous patients. Gerodontology 2002;19:3-4.
5. Meiffert RM, Langer B, Fritz ME. Dental implants: a review. J Periodontol 1992;63:859-870.
6. Guillaume B. Dental Implants: a review. Morphologie 2016;100:189-198.
7. Stellingsma C, Vissink A, Meijer HJ, Kuiper C, Raghoebar GM. Implantology and the severely resorbed edentulous mandible. Crit Rev Oral Biol Med 2004;15:240-248.
8. Kingsmill VJ, Boyde A. Variation in the apparent density of human mandibular bone with age and dental status. J Anat 1998;192:233-244.
9. Pietrokovski J, Starinsky R, Arensburg B, Kaffe I. Morphologic characteristics of bony edentulous jaws. J Prosthodont 2007;16:141-147.
10. Tallgren A. The continuing reduction of the residual alveolar ridges in complete denture wearers: a mixed-longitudinal study covering 25 years. 1972. J Prosthet Dent 2003;89:427-435.
11. Ulm C, Tepper G, Blahout R, Rausch-Fan X, Hienz S, Matejka M. Characteristic features of trabecular bone in edentulous mandibles. Clin Oral Implants Res 2009;20:594-600.
12. Ulm CW, Kneissel M, Hahn M, Solar P, Matejka M, Donath K. Characteristics of the cancellous bone of edentulous mandibles. Clin Oral Implants Res 1997;8:125-130.
13. Bodic F, Hamel L, Lerouxel E, Basle MF, Chappard D. Bone loss and teeth. Joint Bone Spine 2005;72:215-221.
14. Atwood DA. Some clinical factors related to rate of resorption of residual ridges. 1962. J Prosthet Dent 2001;86:119-125.
15. Cawood JI, Howell RA. A classification of the edentulous jaws. Int J Oral Maxillofac Surg 1988;17:232-236.
16. Nuzzo S, Peyrin F, Cloetens P, Baruchel J, Boivin G. Quantification of the degree of mineralization of bone in three dimensions using synchrotron radiation microtomography. Med Phys 2002;29:2672-2681.
17. Mulder L, Koolstra JH, van Eijden TM. Accuracy of microCT in the quantitative determination of the degree and distribution of mineralization in developing bone. Acta Radiol 2004;45:769-777.
18. Goldner J. A modification of the masson trichrome technique for routine laboratory purposes. Am J Pathol 1938;14:237-243.
19. van de Wijngaert FP, Burger EH. Demonstration of tartrate-resistant acid phosphatase in un-decalcified, glycolmethacrylate-embedded mouse bone: a possible marker for (pre)osteoclast identification. J Histochem Cytochem 1986;34:1317-1323.
20. Parfitt AM, Drezner MK, Glorieux FH, Kanis JA, Malluche H, Meunier PJ et al. Bone histomorphometry: standardization of nomenclature, symbols, and units. Report of the ASBMR Histomorphometry Nomenclature Committee. J Bone Miner Res 1987;2:595-610.
21. Dempster DW, Compston JE, Drezner MK, Glorieux FH, Kanis JA, Malluche H et al. Standardized nomenclature, symbols, and units for bone histomorphometry: a 2012 update of the report of the ASBMR Histomorphometry Nomenclature Committee. J Bone Miner Res 2013;28:2-17.

**22.** Kim YJ, Henkin J. Micro-computed tomography assessment of human alveolar bone: bone density and three-dimensional micro-architecture. Clin Implant Dent Relat Res 2015;17:307-313.

**23.** Parfitt GJ. An investigation of the normal variation in alveolar bone trabeculation. Oral Surg Oral Med Oral Pathol 1962;15:1453-1463.

**24.** Ulm C, Solar P, Blahout R, Matejka M, Gruber H. Reduction of the compact and cancellous bone substances of the edentulous mandible caused by resorption. Oral Surg Oral Med Oral Pathol 1992;74:131-136.

**25.** Kingsmill VJ. Post-extraction remodeling of the adult mandible. Crit Rev Oral Biol Med 1999;10:384-404.

**26.** Monje A, Chan HL, Galindo-Moreno P, Elnayef B, Suarex-Lopez del Amo F, Wang F et al. Alveolar bone architecture: a systematic review and meta-analysis. J Periodontol 2015;86:1231-1248.

**27.** Landini G. Videodensitometrical study of the alveolar bone crest in periodontal disease. J Periodontol 1991;62:528-534.

**28.** Kingsmill VJ, Boyde A . Mineralisation density of human mandibular bone: quantitative backscattered electron image analysis. J Anat 1998;192:245-256.

**29.** Bertl K, Subotic M, Heimel P, Schwarze UY, Tangl S, Ulm C. Morphometric characteristics of cortical and trabecular bone in atrophic edentulous mandibles. Clin Oral Implants Res 2015;26:780-787.

**30.** Kanis JA, Melton LJ, Christiansen C, Johnston CC, Khaltaev N. The diagnosis of osteoporosis. J Bone Miner Res 1994;9:1137-1141.

**31.** Consensus development conference: prophylaxis and treatment of osteoporosis. Am J Med 1991;90:107-110.

**32.** Faienza MF, Ventura A, Marzano F, Cavallo L. Postmenopausal osteoporosis: the role of immune system cells. Clin Dev Immunol 2013;2013:575936.

**33.** Garnero P, Sornay-Rendu E, Chapuy MC, Delmas PD. Increased bone turnover in late postmenopausal women is a major determinant of osteoporosis. J Bone Miner Res 1996;11:337-349.

**34.** Bodic F, Amouriq Y, Gayet-Delacroix M, Maugars Y, Hamel L, Basle MF, et al. Relationships between bone mass and micro-architecture at the mandible and iliac bone in edentulous subjects: a dual X-ray absorptiometry, computerised tomography and microcomputed tomography study. Gerodontology 2012;29:585-594

**35.** Schwartz-Dabney CL, Dechow PC. Edentulation alters material properties of cortical bone in the human mandible. J Dent Res 2002;81:613-617.

**36.** Nenda MM, Lewicki M, Mandalunis PM. Histomorphometry of the tibia and mandible of healthy female Wistar rats at different stages of growth. Exp Anim 2016;65:109-116.

**37.** Chaichanasakul T, Kang B, Bezouglaia O, Aghaloo TL, Tetradis S. Diverse osteoclastogenesis of bone marrow from mandible versus long bone. J Periodontol 2014;85:829-836.

**38.** Bouxsein ML, Boyd SK. Christiansen BA, Guldberg RE, Jepsen KJ, Müller R. Guidelines for assessment of bone microstructure in rodents using micro-computed tomography. J Bone Miner Res 2010;25:1468-1486.

# 3

# Regional differences in microarchitecture and mineralization of the atrophic edentulous mandible: A microcomputed tomography study

Hannah Dekker, Engelbert A.J.M. Schulten, Christiaan M. ten Bruggenkate, Elisabeth Bloemena, Leo van Ruijven, Nathalie Bravenboer

**Published in:** Archives of Oral Biology 2022; 133: 105302

## ABSTRACT

Objective**:** The aim of the present study was to assess mineralization and trabecular microarchitecture in atrophic edentulous mandibles and to identify regional differences and relations with the extent of resorption.

Methods**:** Cortical and trabecular bone volumes in anterior, premolar and molar regions of 10 edentulous cadaveric mandibles (5 males and 5 females; mean age ± SD: 85.4 ± 8.3 years) were assessed by microcomputed tomography. Mandibular height and Cawood & Howell classes were recorded. Concerning trabecular volumes, bone mineral density (BMD), bone volume fraction, trabecular tissue volume fraction, connectivity density, trabecular number, trabecular thickness, trabecular separation, degree of anisotropy, and structural model index were measured; concerning cortical volumes porosity, BMD and cortical thickness were measured.

Results**:** In molar regions, the bone volume fraction and trabecular number were lower, whereas trabecular separation, degree of anisotropy and cortical BMD were higher compared to anterior regions. In premolar regions, mandibular height correlated negatively with trabecular number (Spearman's correlation $r = 0.73$, $p = 0.017$) and connectivity density (Spearman's correlation $r = 0.82$, $p = 0.004$), and correlated positively with trabecular separation (Spearman's correlation $r = -0.65$, $p = 0.04$). Cortical BMD was higher at bucco-inferior cortex of molar and inferior border of premolar region and lower at anterior cranial buccal and lingual surface.

Conclusions**:** In the premolar region, increased resorption coincides with local impairment of trabecular bone quality. Cortical bone BMD is higher in areas with highest strains and lower in areas with most mandibular resorption. Trabecular bone volume and quality is superior in the anterior region of the edentulous mandible, which might explain improved primary stability of dental implants in this region.

# INTRODUCTION

Following tooth loss, resorption of the mandibular residual ridge is an irreversible physiological process, leading to a decrease in mandibular volume. The altered shape of the edentulous mandible gives rise to problems with retention and function of a lower denture. Therefore, dental implant surgery is particularly indicated in edentulous patients, and is a challenging procedure in progressively resorbed mandibles.[1]



The success and survival of dental implants depend on multiple factors, which can be patient-, implant-, and surgery-related. Mineral density, bone volume and trabecular microarchitecture of the encasing bone is crucial for primary stability of the dental implant and a predictor of osseointegration and implant success.[2]

Most reports that assessed the microarchitecture of the mandibular residual ridge relied on two-dimensional techniques, as traditional histomorphometry has been for long the gold standard for assessment of trabecular bone microarchitecture.[3-5] Although traditional histomorphometry remains the designated method for analysis of cellularity and dynamic bone remodeling indices, for assessment of structural parameters of bone microarchitecture this method has its limitations.[6] Microcomputed tomography (micro-CT) allows a three-dimensional quantitative analysis of bone microarchitecture without the limitations involved in sectional techniques relying on two-dimensional models.[7,8]

Various micro-CT studies that investigated the bone microarchitecture at dental implant sites, used core biopsies from living as well as cadaveric specimens.[9-13] However, the outcomes of trabecular microarchitecture at these sites cannot readily be generalized for the entire mandibular ridge as great inter- and intra-individual variability is a well-known feature of mandibular trabecular bone.[4,14,15] The small dimension of core biopsies provide insufficient volumes to appreciate regional differences.

For assessing bone mineral density of the mandible 'in vivo', conventional CT-scanning is the most reliable and widely used method.[16-18] Mineral density measurements of conventional CT scanning correlate well with those of micro-CT.[19-21] Micro-CT is not

suitable for clinical ´in vivo´ use, but for ex-vivo bone samples the mineral density distribution can reliably be assessed.[22]

So far, no detailed micro-CT studies that appreciate the full cross-sectional volume at the different anatomical regions of the edentulous mandibular residual ridge are available.[23] The present study aimed to assess the mineralization distributions and trabecular microarchitecture characteristics in different regions of the edentulous mandible through a systematic three-dimensional evaluation by means of micro-CT to identify regional differences and relations with the extent of mandibular resorption.

## MATERIALS AND METHODS

Ten edentulous mandibles were prepared from ten human cadavers (5 males and 5 females; mean age ± SD: 85.4 ± 8.3 years). Specimens were obtained from the anatomic dissection course for medical students. According to their legal testaments, donors provided their bodies to the Department of Anatomy, Physiology and Embryology of the Amsterdam University Medical Centers after death for the purposes of science and research. Embalming was performed upon arrival at the department with an intra-arterial solution of water, alcohol, salicylic acid, carolinum, thymol, chloral hydrate and formaldehyde. Usage of these specimens conformed to a written protocol that was reviewed and approved by the Department of Anatomy Physiology and Embryology. This protocol forbids the disclosure of any medical records of the donors other than age and sex, and was conducted in accordance to the Declaration of Helsinki.

After preparation, the edentulous mandibles were photographed for documentation purposes. To determine the extent of mandibular resorption the classification according to Cawood & Howell was used.[24] All mandibles were classified by an experienced oral and maxillofacial surgeon (ES). All specimens had identical left and right posterior Cawood & Howell classes.

Each edentulous mandible was divided in three segments with an automatic band sawing machine (Ferm FLZ-275, Zwolle, The Netherlands) (Figure 1):

1. Anterior region (A): 15 mm anteriorly to the anterior margin of the mental foramen on both sides.
2. Premolar region (PM) (right side): 15 mm anteriorly to the anterior margin of the mental foramen on the right side and 5 mm posteriorly to the posterior margin of the mental foramen on the right side.
3. Molar (M) region (right side): 5 mm posteriorly to the posterior margin of the mental foramen on the right side and 30 mm posteriorly to the posterior margin of the mental foramen on the right side.



The mental foramen is located between the first and second premolar or apical of the second premolar in approximately 90% of cases.[25] We chose this reference point to ensure the inclusion of the premolar area. Mean premolar width is approximately 7 millimeters and a cutoff point 5 mm posteriorly to the posterior margin and 15 mm anterior to the anterior margin was chosen for the segmentation of the premolar region, which would include the canine position. However, volumes of interest (VOI's) were always chosen in the center of each segment so no sawing planes were included, with a maximal dimension of 1 cm. In the premolar region the VOI would always contain the foramen. The canine position therefore was never included in the VOI.

The machine had a table leaf with a device for measuring angles. It was used to standardize the different cutting angles, so that all specimens were cut in the same manner.

Mandibular height was measured in each section with a precision caliper at three points evenly distributed along the segment, the mean value was recorded.


Figure 1. Photograph (cranial view) of a human cadaveric edentulous mandible, schematically illustrating the investigated regions: A=Anterior region, PM=premolar region, M=molar region. The red circles mark the mental foramen.

*Micro-CT*

The thirty specimens were scanned with a high-resolution micro-CT system (μCT 40, Scanco Medical AG, Brüttisellen, Switzerland). The polychromatic source and cone-shaped beam of the scanner was filtered with a 0.05 mm aluminum filter to remove the lowest energies from the X-ray spectrum. The beam hardening effect was further reduced by applying a correction algorithm developed by the manufacturer. The system was calibrated weekly using reference phantoms with densities of 0, 100, 200, 400 and 800 mg HA/cm$^3$ (QRM GmbH). Specimens were scanned in a polyetheramide tube with a diameter of 36 mm and a length of 75 mm, fixed with synthetic foam to prevent movements. Scanner settings for all specimens were voltage: 70 kVp, intensity: 114 μa, integration time: 500 ms and resolution: 18 μm. Grey values were considered to be proportional to the local bone mineral density, equivalent to the concentration of hydroxyapatite (HA).[26,27] Imaging processing included Gaussian filtering (sigma=0.8, support=1) and segmentation (threshold 515.9 mg HA/cm$^3$).

All VOI's were evaluated with morphometric software uct_evaluation v6.5-3 (Scanco Medical AG, Bruttisellen, Switzerland). The mandibular bone segments had their central axis aligned with the Z-axis. For analysis, the images were oriented along their Z-axis in the X-axis plane. In each specimen multiple VOIs were selected (Figure 2). To select a VOI, the frame halfway along the Z-axis was selected (representing the middle of the segment) and 300 frames on either side of this frame were selected. In the anterior region, due to the natural curvature of the mandible, the lingual surface of the specimen was narrower than the buccal surface. Selecting 600 frames in this area would include sawing planes in the VOI, so in anterior region, a minimum of 300 frames was selected. This way, sawing planes were never included in the VOI. To represent trabecular bone architecture accurately, the measured VOI should contain at least three to five intertrabecular lengths [8]. Each VOI measured ≥ 5 mm in all three dimensions. An intertrabecular length in mandibular bone is reportedly 1.05-1.15 mm[28], so this VOI covers a representative amount of trabecular bone.

The first VOI (VOI1) contained only the trabecular tissue volume, which was drawn manually at the endocortical surface. In PM and M specimens, the cavities of the mandibular canal and mental foramen were not selected in the VOI. For these VOIs,

six parameters were determined: the bone mineral density (BMD; mgHA/cm$^3$), trabecular bone volume fraction (BV/TV; %) as the relative volume of the bony tissue in the trabecular tissue volume, the connectivity density (ConnD; 1/mm$^3$) as the number of connections within the bone per volume unit, the trabecular number (Tb.N; mm-1) as the average number of trabeculae within one millimeter distance, trabecular separation (Tb.Sp; mm) as the average distance between trabeculae, trabecular thickness (Tb.Th; mm), the degree of anisotropy (DA) and structural model index. Degree of anisotropy is defined as the preference in orientation of the trabeculae. Random, disorganized orientation of trabeculae has a DA of 1, higher values imply that a higher fraction of trabeculae run parallel to each other and the bone structure is more organized. Structure Model Index (SMI) is used to quantify the characteristic form of a three-dimensionally described structure in terms of the amount of plates and rod composing the structure.[29] For an ideal plate and rod structure the SMI value is 0 and 3, respectively, independent of the physical dimensions. For a structure with both plates and rods of equal thickness the value lies between 0 and 3, depending on the volume ratio of rods and plates. Although commonly used in micro-CT research, the reliability of this parameter is controversial.[30]

The second VOI (VOI2) was taken in identical frames as VOI1, including both the trabecular and cortical bone volumes. VOI2 was used to calculate the fraction of trabecular tissue volume in total volume (trabecular tissue volume fraction, Tb.TV/TV, %), the cortical porosity (Ct.Po, %) and cortical BMD. To evaluate the trabecular microarchitecture in craniocaudal direction, the trabecular volume was divided in three VOIs (VOI 3-5). The craniocaudal axis was divided in three equal segments, two lines perpendicular to this axis were drawn to divide trabecular volume in an upper, middle and basal part, and a cubic VOI was selected within each part. BV/TV and BMD was calculated for each of these VOIs.

To evaluate the thickness of the cortex on buccal, inferior and lingual surfaces, seven VOIs (VOI 6-12) were selected on upper buccal (UB), mid-buccal (MB), lower buccal (LB), inferior border (IB), lower lingual (LL), mid-lingual (ML) and upper lingual (UL) cortex. As the mandibular ridge, following tooth loss, never develops a complete cortex[14], this 'trabecular track' running over the occlusal surface of the edentulous mandible is

thought to be the remaining scar after tooth extraction.[31] Therefore, the ridge-crest of the mandible was excluded from the VOIs. BMD was calculated for each of these VOIs. For each of these VOIs, three cortical thickness measurements were made and the mean of these three measurements was documented as cortical thickness at that site.

*Statistical analysis*

SPSS (Version 25.0, IBM Corp., Armonk, NY) was used to perform all statistical analyses. Spearman's Rho 2-tailed correlation coefficients (*r*) were used to check correlations between the morphological parameters and the correlation between the mandibular height and the parameters. A Mann-Whitney *U* test for was used for comparisons between sexes. Differences between anterior, premolar and molar regions were not further analyzed statistically due to the small sample size.

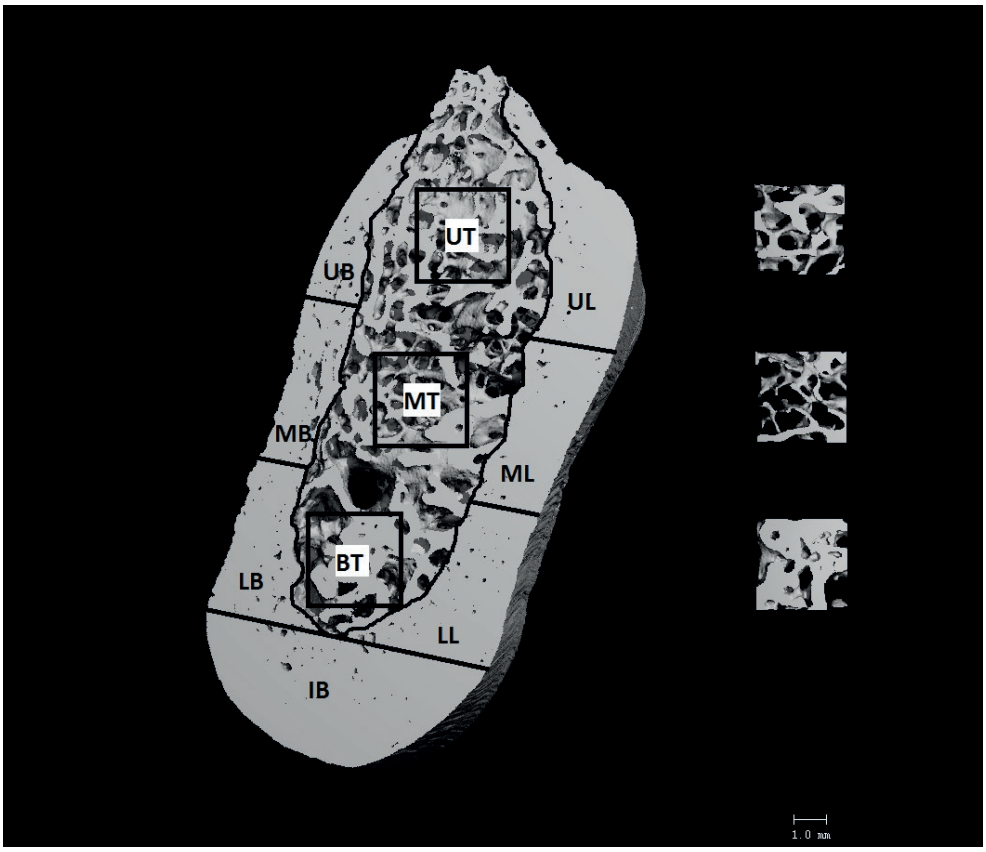


Figure 2. Schematic drawing of the different volumes of interest (VOIs). The trabecular bone volume is outlined. Within the trabecular bone volume, three VOIs were selected, respectively the upper third trabecular volume (UT), middle third trabecular volume (MT) and basal third trabecular volume (BT). Along the cortex, bone mineral density measurements were performed at seven subsites: upper buccal (UB), midbuccal (MB), lower buccal (LB), inferior border (IB), lower lingual (LL), midlingual (ML) and upper lingual (UL).

## RESULTS

On visual inspection, all specimens exhibited an area on the top of the residual ridge, where the cortical layer was either interrupted by an area of trabecular bone or increasingly porous compared to the surrounding cortex. The lingual cortex in the anterior region contained the mental spine and a gradual thickening of the cortex was observed in the area surrounding the mental spine. In Figure 2 the micro-CT images of the anterior, premolar and molar sections of two specimens are shown. In Table 1 the

characteristics of the mandibular specimens are shown. Age, mandibular height and the Cawood & Howell classification did not differ significantly between the sexes (Mann Whitney-*U*). No significant differences were found between the sexes in any of the measured regions (Mann Whitney-*U*, data not shown). The variability in trabecular bone microarchitecture parameters is shown in Table 2.

Only in the premolar region, significant correlations were found between mandibular height and trabecular microarchitectural parameters connectivity density (Spearman's correlation r = 0.82, p = 0.004) (Figure 4A), trabecular number (Spearman's correlation r = 0.73, p = 0.017) (Figure 4B) and trabecular separation (Spearman's correlation r = -0.65, p = 0.04) (Figure 4C). Spearman's correlations between posterior Cawood class and connectivity density (Spearman's correlation r = -0.86, p = 0.002), trabecular number (Spearman's correlation r = -0.82, p = 0.004) and trabecular separation (Spearman's correlation r = 0.78, p = 0.008) were significant as well. Furthermore, Cawood classes (anterior and posterior) correlated with the cortical BMD in the premolar area (Cawood anterior: Spearman's correlation r = 0.67 p = 0.034; Cawood posterior: Spearman's correlation r = 0.70 p = 0.025). The relationship between mandibular height and cortical BMD in the premolar area was not significant (Spearman's correlation r = -0.59 p = 0.074).

In Table 3 the measurements in the trabecular and cortical bone parameters between the anterior, premolar and molar regions are shown. Trabecular bone volume values were lower in the premolar and molar region compared to the anterior region. Trabecular number values are lower and trabecular separation values were higher in the premolar and molar region compared to the anterior region. The degree of anisotropy values were higher in the premolar and molar region compared to the anterior region. In general, the BMD increased towards the posterior sites, with the exception of the upper lingual cortex in the molar area. Cortical thickness of the lingual surface and inferior border was thicker in the premolar region compared to the molar region. The upper buccal cortical thickness was thinner in the premolar and anterior regions compared to the molar region.

In Figures 5A-F the cortical BMD and cortical thickness measured at seven sites in the mandibular cortex are shown. Measured points were: upper buccal, mid-buccal, lower buccal, inferior border, lower lingual, mid-lingual and upper lingual sites. In all three mandibular regions the BMD and cortical thickness peaked at the inferior border. However, this peak was most profound in the premolar region. In the anterior region, BMD decreased gradually in cranial direction on both lingual and buccal surfaces. The cortex was thicker on the lingual surface than buccal surface at the lower lingual and mid-lingual site. In the premolar region, cortical thickness and BMD increased in craniocaudal direction on the buccal surface to peak at the inferior border. The cortical thickness and BMD of the lingual cortical surface decreased from inferior border towards mid-lingual and had a slight increase in thickness and BMD at the upper lingual site. In the molar region, only minor variability in cortical thickness at the different sites was seen. BMD tended to be higher on the buccal surface with a small peak at the inferior border and a decrease in BMD over the lingual cortical surface in cranial direction.

Table 1. Characteristics of 10 human cadaveric edentulous mandibles.

| | **Age (years)** | **Cawood & Howell class anterior** | **Cawood & Howell class posterior** | **Height Anterior (mm)** | **Height Premolar (mm)** | **Height Molar (mm)** |
|---|---|---|---|---|---|---|
| **Female** | 95 | VII | VII | 18 | 15 | 14 |
| **Female** | 92 | V | VI | 25 | 25 | 19 |
| **Female** | 90 | VI | VII | 20 | 15 | 14 |
| **Female** | 98 | V | VI | 26 | 26 | 21 |
| **Female** | 79 | V | VI | 24 | 23 | 16 |
| **Male** | 83 | V | V | 29 | 30 | 27 |
| **Male** | 71 | VI | VII | 15 | 14 | 14 |
| **Male** | 79 | VII | VII | 25 | 23 | 23 |
| **Male** | 83 | V | VI | 25 | 25 | 22 |
| **Male** | 84 | V | V | 28 | 27 | 25 |

Table 2. Variability defined by minimum and maximum values and corresponding range in trabecular microarchitectural parameters in the anterior (A), premolar (PM) and molar (M) region.

| Trabecular bone parameter (unit) | A min-max (range) | PM min-max (range) | M min-max (range) |
|---|---|---|---|
| **Bone volume fraction (BV/TV; %)** | 22-66 (44) | 10-35 (26) | 7-35 (28) |
| **Connectivity density (ConnD; 1/mm³)** | 3.7-9.81 (6.11) | 2.19-9.51 (7.31) | 1.74-7.41 (5.67) |
| **Trabecular number (Tb.N; 1/mm)** | 0.96-2.43 (1.47) | 0.66-1.39 (0.73) | 0.29-1.27 (0.97) |
| **Trabecular thickness (Tb.Th; mm)** | 0.22-0.49 (0.27) | 0.21-0.37 (0.16) | 0.17-0.34 (0.17) |
| **Trabecular separation (Tb.Sp; mm)** | 0.38-1.06 (0.68) | 0.71-1.54 (0.83) | 0.79-3.51 (2.72) |
| **Trabecular tissue volume fraction (Tb.TV/TV; %)** | 29-57 (0.28) | 30-55 (25) | 39-57 (18) |



Table 3. Differences in trabecular and cortical bone parameters between anterior (A), premolar (PM) and molar (M) regions.

| | Unit | A (n=10) *Median (IQR)* | PM (n=10) *Median (IQR)* | M (n=10) *Median (IQR)* |
|---|---|---|---|---|
| **TRABECULAR BONE** | | | | |
| **Trabecular bone volume fraction** | **BV/TV (%)** | 31 (33) | 21 (16) | 17 (15) |
| **Trabecular tissue volume fraction** | **Tb.TV/TV (%)** | 45 (18) | 46 (9) | 50 (11) |
| **Upper third trabecular bone volume fraction** | **BV/TV (%)** | 27 (40) | 18 (19) | 14 (25) |
| **Middle third trabecular bone volume fraction** | **BV/TV (%)** | 26 (35) | 17 (12) | 4.8 (13) |
| **Basal third trabecular bone volume fraction** | **BV/TV (%)** | 48 (27) | 27 (26) | 7.3 (14) |
| **Connectivity Density** | **normed by TV (1/mm³)** | 5.84 (4.07) | 4.02 (2.87) | 4.49 (2.69) |
| **Trabecular number** | **Tb.N (1/mm)** | 1.53 (0.75) | 1.02 (0.49) | 0.85 (0.24) |
| **Trabecular thickness** | **Tb.Th (mm)** | 0.31 (0.12) | 0.24 (0.11) | 0.25 (0.08) |
| **Trabecular separation** | **Tb.Sp (mm)** | 0.69 (0.36) | 1.01 (0.50) | 1.22 (0.37) |
| **Degree of anisotropy** | **DA** | 1.24 (0.10) | 1.37 (0.18) | 1.63 (0.47) |
| **Structure model index** | **SMI** | 0.35 (3.35) | 1.17 (1.42) | 1.34 (0.98) |
| **Trabecular Bone Mineral Density (BMD)** | **BMD (mgHA/mm³)** | 825 (48) | 831 (44) | 849 (47) |
| **BMD upper third trabecular volume** | **BMD (mgHA/mm³)** | 789 (115) | 792 (86) | 816 (56) |

Table 3. Differences in trabecular and cortical bone parameters between anterior (A), premolar (PM) and molar (M) regions. *(Continued)*

| | Unit | A (n=10) *Median (IQR)* | PM (n=10) *Median (IQR)* | M (n=10) *Median (IQR)* |
|---|---|---|---|---|
| **BMD middle third trabecular volume** | **BMD (mgHA/ mm³)** | 802 (66) | 785 (79) | 762 (58) |
| **BMD lower third trabecular volume** | **BMD (mgHA/ mm³)** | 825 (78) | 836 (60) | 776 (65) |
| **CORTICAL BONE** | | | | |
| **Cortical porosity** | **Ct.Po (%)** | 12 (4) | 10 (5.3) | 9.5 (5.5) |
| **Cortical BMD** | **BMD (mgHA/ mm³)** | 953 (25) | 975 (18) | 989 (40) |
| **BMD upper buccal cortex** | **BMD (mgHA/ mm³)** | 929 (88) | 939 (51) | 1022 (76) |
| **BMD midbuccal cortex** | **BMD (mgHA/ mm³)** | 949 (57) | 948 (113) | 1017 (57) |
| **BMD lower buccal cortex** | **BMD (mgHA/ mm³)** | 977 (61) | 1011 (104) | 1036 (41) |
| **BMD inferior border** | **BMD (mgHA/ mm³)** | 1005 (23) | 1056 (20) | 1061 (43) |
| **BMD lower lingual cortex** | **BMD (mgHA/ mm³)** | 996 (42) | 1010 (35) | 1016 (52) |
| **BMD mid lingual cortex** | **BMD (mgHA/ mm³)** | 956 (97) | 955 (64) | 963 (100) |
| **BMD upper lingual cortex** | **BMD (mgHA/ mm³)** | 932 (93) | 988 (42) | 950 (90) |
| **Cortical thickness upper buccal** | **Ct.Th, mm** | 1.1 (1.3) | 1.25 (0.45) | 2.2 (1.23) |
| **Cortical thickness mid buccal** | **Ct.Th mm** | 1.65 (1.98) | 1.4 (0.83) | 2.15 (0.88) |
| **Cortical thickness lower buccal** | **Ct.Th mm** | 2.1 (2.53) | 2.15 (1.48) | 2.1 (0.77) |
| **Cortical thickness inferior border** | **Ct.Th mm** | 3.15 (3.18) | 3.9 (0.98) | 2.65 (1.03) |
| **Cortical thickness lower lingual** | **Ct.Th mm** | 2.75 (2.52) | 2.8 (0.88) | 1.85 (0.78) |
| **Cortical thickness midlingual** | **Ct.Th mm** | 3.1 (2.4) | 2.2 (0.68) | 1.45 (0.92) |

Table 3. Differences in trabecular and cortical bone parameters between anterior (A), premolar (PM) and molar (M) regions. *(Continued)*

| | Unit | **A (n=10)** *Median (IQR)* | **PM (n=10)** *Median (IQR)* | **M (n=10)** *Median (IQR)* |
|---|---|---|---|---|
| **Cortical thickness upper lingual** | **Ct.Th mm** | 1.45 (0.85) | 2.40 (1.28) | 1.55 (0.95) |

IQR = interquartile range.

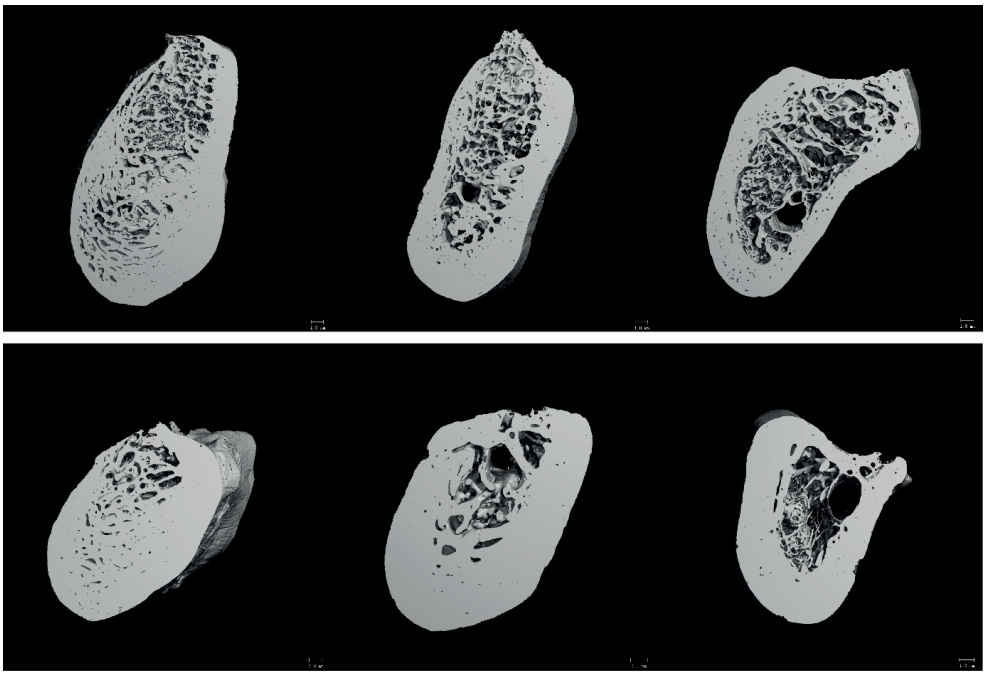

Figure 3. Micro-CT images (from left to right) of the anterior, premolar and molar regions of two mandibular specimens. The buccal surface is oriented on the left side of the image. The upper image is from a female specimen, aged 79 years-old, anterior Cawood class V and posterior Cawood class VI. The lower image is from a male specimen, aged 79 years-old, anterior Cawood class VII and posterior Cawood class VII.

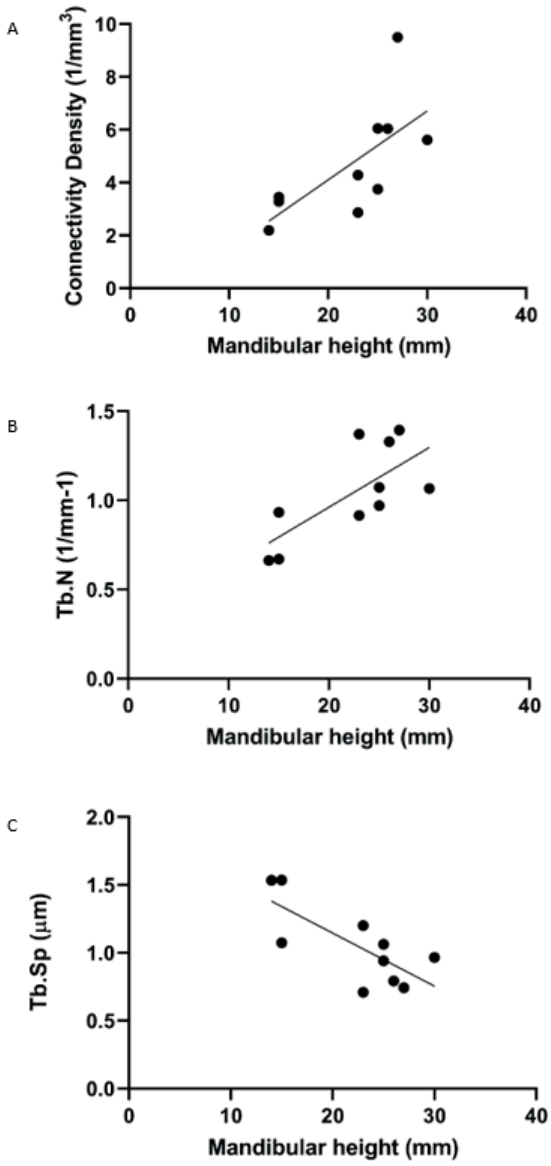


Figure 4.

A. Spearman's correlation between connectivity density and mandibular height (millimeter) in the premolar region of the mandible (r=0.82, p=0.004). (n=10)

B. Spearman's correlation between trabecular number (1/millimeter-1) and mandibular height (millimeter) in the premolar region of the mandible (r=0.73, p=0.017). (n=10)

C. Spearman's correlation between trabecular number (µm) and mandibular height (millimeter) in the premolar region of the mandible (r=-0.65, p=0.04). (n=10)

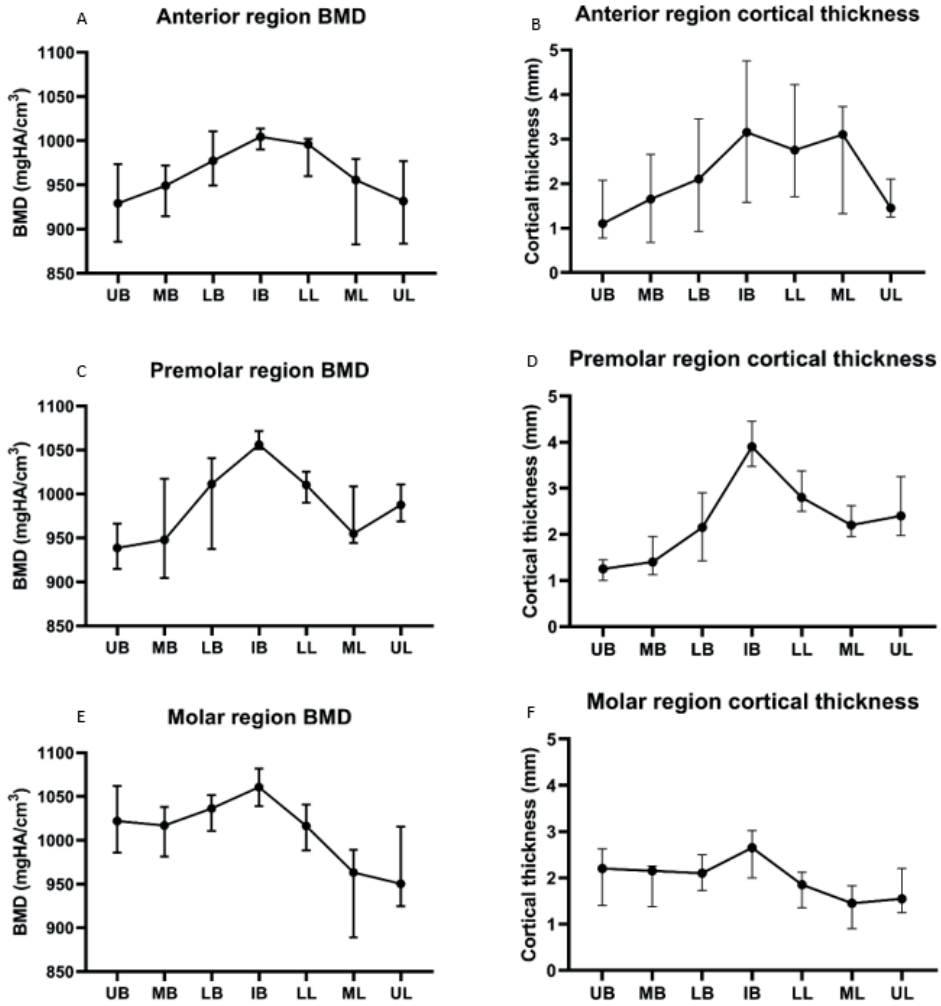


Figure 5.

A. Bone mineral density (median, interquartile range) measured in upper buccal (UB), mid-buccal (MB), lower buccal (LB), inferior border (IB), lower lingual (LL), mid-lingual (ML) and upper lingual (UL) sites in the cortex of the anterior region of the mandible (n=10).

B. Cortical thickness (median, interquartile range) measured in UB, MB, LB, IB, LL, ML and UL sites in the cortex of the anterior region of the mandible (n=10).

C. Bone mineral density (median, interquartile range) measured in UB, MB, LB, IB, LL, ML and UL sites in the cortex of the premolar region of the mandible (n=10).

D. Cortical thickness (median, interquartile range) measured in UB, MB, LB, IB, LL, ML and UL sites in the cortex of the premolar region of the mandible (n=10).

E. Bone mineral density (median, interquartile range) measured in UB, MB, LB, IB, LL, ML and UL sites in the cortex of the molar region of the mandible (n=10).

F. Cortical thickness (median, interquartile range) measured in UB, MB, LB, IB, LL, ML and UL sites in the cortex of the molar region of the mandible (n=10).

# DISCUSSION

The specimens exhibited overall great variability in trabecular bone volume fraction, trabecular number, trabecular separation and connectivity density, inter- as well as intra-individually. However, when the range is appreciated for each mandibular region separately, the variability is less profound. Only the variability in trabecular bone volume fraction of the anterior region and variability in trabecular spacing of the molar region was substantially higher than what could be expected based on observations in other skeletal sites.[32] Our data are consistent with the study by Kim et al., who analyzed human cadaveric mandibles with micro-CT and found a variability in trabecular bone volume fraction ranging from 2.4-48.9%.[33] In their study the trabecular thickness was very consistent as well, although in our study higher values were found. A possible explanation is that they did not study fully edentulous mandibles, and they analyzed only a small VOI at the alveolar part of the mandible, which is completely resorbed in our specimens. A micro-CT study by Moon et al. in the premolar area of dentate cadaveric mandibles found that trabecular bone volume fraction and trabecular number were significantly higher and trabecular separation significantly lower in alveolar bone as opposed to basal bone, with lowest values measured in the basal area below the mandibular canal.[34] This is different from our study, which showed that the premolar sites of the resorbed mandibles have the highest trabecular bone volume fraction in the basal third part, which is in contrast with Moon's findings in dentate situations. This finding suggest a structural remodeling in the trabecular microarchitecture in the edentulous mandible which may be a result of the physiological process of mandibular resorption and/or changes in mechanical forces exerted on the bone.

Blok et al. analyzed alveolar bone in dentate cadavers and chose VOIs in the periapical bone.[15] Their data also showed great variability in trabecular bone volume fraction but overall the volume fraction was high compared to other skeletal sites. These data suggest that in dentate situations, regional differences are observed, however, these seem to be distributed differently than in edentulous situations. The alveolar portion of the mandible is found to have superior bone quality, which is possibly due to forces exerted on the mandibular bone in this area. The alveolar bone portion in the edentulous mandible is obviously resorbed, the occlusal loading forces are reduced and force

distributions are different compared to dentate situations, causing a change in structural and mechanical properties of the mandibular bone after tooth loss.[35-37]

The present study shows that trabecular bone volume is decreased in posterior sites with a significant decrease in the molar regions compared to the anterior regions. This is in agreement with Monje et al. who systematically reviewed the available literature on alveolar bone microarchitecture and concluded, that the total bone volume is greater in the anterior sites compared to posterior sites and lower in atrophic sites compared to non-atrophic sites of the mandible.[23] Ulm et al. also demonstrated this difference between the anterior and posterior regions and postulated that this might be due to molars being lost earlier in life than anterior and premolar teeth, perhaps this is the reason for the less pronounced atrophy in the anterior region.[4]

This higher trabecular bone volume, trabecular number and lower trabecular separation in the anterior as opposed to posterior regions, implies a better bone quality in the anterior region which seems to be independent to the degree of mandibular resorption, and might explain the reported favorable dental implant stability in the anterior mandible.[38-41]

In the premolar region, decreased mandibular height correlated with decreased connectivity density, trabecular number and increased trabecular separation, suggesting an impaired bone quality after more severe resorption at premolar sites. No relation was found between the trabecular bone volume and mandibular height or Cawood & Howell class. It must be noted, however, that all investigated specimens had moderate to severe atrophy (Cawood & Howell classes V-VII), and no definitive relation between resorption and bone quality can be demonstrated here, as earlier stages of resorption were not represented in the current study.

Cortical bone mineral density was lower in the upper buccal and upper lingual site in the anterior region, upper buccal site in the premolar region and upper lingual site in the molar region. The highest values were found inferior-lingually at the midline, inferiorly at the mental foramen region and at the inferior-buccal surface in the molar area. Kingsmill and Boyde used quantitative backscattered electron imaging in a scanning

electron microscope to investigate regional differences in mandibular mineralization densities in dentate, partially dentate and edentulous situations.[42] Measurements were made in the midline anterior, premolar and third molar area sections of the buccal, inferior, lingual cortices and trabecular zones. Although their cortical mineral densities are not directly comparable due to the different technique for measuring mineral density, cortical mineralization distributions are in agreement with the outcomes of the present study. The anterior sites were less mineralized than the premolar and third molar sites. In the molar area the buccal surface is more mineralized than the lingual surface. In general, the mineralization tends to decrease the more cranial the site sampled in the mandible. At anterior and premolar sites the alveolar area showed the lowest density. In the third molar region, the superior-lingual site showed the lowest density. In their study the highest densities were found inferior-lingually at the midline and inferiorly at the mental foramen region as well, and buccally in posterior sites. The areas of lower mineralization density seem to match the areas of majority of bone loss that follows the loss of teeth.[14,43,44] The regions of highest mineralization mirror sites thought to experience the highest strains.[42]



Schwartz-Dabney et al. studied cortical cylinders from human cadaveric edentulous mandibles on the lingual and buccal surface and compared thickness and density with dentate mandibles.[37] For cortical thickness, generally the thickest sites were described lingually in the mandibular body. In the anterior region, thicker cortex is likely to be present at the lingual surface, due to the presence of the mental spine and the cortex gradually thickens towards the spine.

Bertl et al. measured cortical thickness of incisor, premolar and molar regions in atrophic edentulous mandibles and found a decrease in cortical thickness from mesial to distal region for lingual, inferior and buccal cortex.[5] In the present study a similar gradient was found for the mid- and lower points in the lingual surface but not for inferior and buccal mid- and lower surfaces. This discrepancy might be due to the different manner of measurement, as in the present study the mean of three measurements along each subsite was taken as opposed to the maximum thickness at each subsite. Bertl's study had a greater sample size and also less resorbed mandibles (Cawood III and IV) were included.

Several limitations concerning our study should be mentioned. The sample size in the present study was 10, which is a relatively low number. Potential significant relations and sex differences might be missed because of this.

For this study, formalin-embalmed specimens were used. Nägele et al. concluded that micro-CT data are highly reproducible in formalin-embalmed specimens.[32] Although embalming may have a small but significant effect on the mechanical properties of bones, there is no known effect on bone morphology or bone mineral density.[45,46]

One common limitation in cadaveric studies is the lack of information on medical and dental history, such as systemic diseases and medication that may affect bone health, the duration of the edentulous state, and the use of dentures. This information, therefore, could not be obtained and considered in the interpretation of the results.

## CONCLUSIONS

In conclusion, in the premolar region increased resorption coincides with local impairment of trabecular bone quality. Cortical BMD is higher in areas with highest strains and lower in areas subject to the most mandibular resorption. Trabecular bone volume is higher and trabecular bone quality is superior in the anterior region of the edentulous mandible which might explain improved primary stability of dental implants in this region.

## ACKNOWLEDGEMENTS

The authors thank Inez Lichters and the Department of Anatomy, Embryology and Physiology from the Amsterdam University Medical Centers, location AMC, for providing and preparing the anatomical specimens. Furthermore, the authors thank Jorieke Grooten for her valuable contribution to the study execution and Birgit Lissenberg-Witte for her input in the statistical analyses.

# REFERENCES


1. Stellingsma C, Vissink A, Meijer HJ, Kuiper C, Raghoebar GM. Implantology and the severely resorbed edentulous mandible. Crit Rev Oral Biol Med 2004;15(4):240-8. DOI: 10.1177/154411130401500406.
2. Chrcanovic BR, Albrektsson T, Wennerberg A. Bone Quality and Quantity and Dental Implant Failure: A Systematic Review and Meta-analysis. Int J Prosthodont 2017;30(3):219-237. DOI: 10.11607/ijp.5142.
3. Ulm CW, Kneissel M, Hahn M, Solar P, Matejka M, Donath K. Characteristics of the cancellous bone of edentulous mandibles. Clin Oral Implants Res 1997;8(2):125-30. DOI: 10.1034/j.1600-0501.1997.080207.x.
4. Ulm C, Tepper G, Blahout R, Rausch-Fan X, Hienz S, Matejka M. Characteristic features of trabecular bone in edentulous mandibles. Clin Oral Implants Res 2009;20(6):594-600. DOI: 10.1111/j.1600-0501.2008.01701.x.
5. Bertl K, Subotic M, Heimel P, Schwarze UY, Tangl S, Ulm C. Morphometric characteristics of cortical and trabecular bone in atrophic edentulous mandibles. Clin Oral Implants Res 2015;26(7):780-7. DOI: 10.1111/clr.12340.
6. Parfitt AM, Drezner MK, Glorieux FH, et al. Bone histomorphometry: standardization of nomenclature, symbols, and units. Report of the ASBMR Histomorphometry Nomenclature Committee. J Bone Miner Res 1987;2(6):595-610. DOI: 10.1002/jbmr.5650020617.
7. Thomsen JS, Laib A, Koller B, Prohaska S, Mosekilde L, Gowin W. Stereological measures of trabecular bone structure: comparison of 3D micro computed tomography with 2D histological sections in human proximal tibial bone biopsies. J Microsc 2005;218(Pt 2):171-9. DOI: 10.1111/j.1365-2818.2005.01469.x.
8. Bouxsein ML, Boyd SK, Christiansen BA, Guldberg RE, Jepsen KJ, Muller R. Guidelines for assessment of bone microstructure in rodents using micro-computed tomography. J Bone Miner Res 2010;25(7):1468-86. DOI: 10.1002/jbmr.141.
9. Dekker H, Schulten E, Ten Bruggenkate CM, Bloemena E, van Ruijven L, Bravenboer N. Resorption of the mandibular residual ridge: A micro-CT and histomorphometrical analysis. Gerodontology 2018. DOI: 10.1111/ger.12343.
10. de Oliveira RC, Leles CR, Lindh C, Ribeiro-Rotta RF. Bone tissue microarchitectural characteristics at dental implant sites. Part 1: identification of clinical-related parameters. Clin Oral Implants Res 2012;23(8):981-6. DOI: 10.1111/j.1600-0501.2011.02243.x.
11. Ribeiro-Rotta RF, de Oliveira RC, Dias DR, Lindh C, Leles CR. Bone tissue microarchitectural characteristics at dental implant sites part 2: correlation with bone classification and primary stability. Clin Oral Implants Res 2014;25(2):e47-53. DOI: 10.1111/clr.12046.
12. Fu MW, Shen EC, Fu E, Lin FG, Wang TY, Chiu HC. Assessing Bone Type of Implant Recipient Sites by Stereomicroscopic Observation of Bone Core Specimens: A Comparison With the Assessment Using Dental Radiography. J Periodontol 2017;88(6):593-601. DOI: 10.1902/jop.2017.160446.
13. Stoppie N, Pattijn V, Van Cleynenbreugel T, Wevers M, Vander Sloten J, Ignace N. Structural and radiological parameters for the characterization of jawbone. Clin Oral Implants Res 2006;17(2):124-33. DOI: 10.1111/j.1600-0501.2005.01204.x.
14. Kingsmill VJ. Post-extraction remodeling of the adult mandible. Crit Rev Oral Biol Med 1999;10(3):384-404. DOI: 10.1177/10454411990100030801.
15. Blok Y, Gravesteijn FA, van Ruijven LJ, Koolstra JH. Micro-architecture and mineralization of the human alveolar bone obtained with microCT. Arch Oral Biol 2013;58(6):621-7. DOI: 10.1016/j.archoralbio.2012.10.001.
16. Norton MR, Gamble C. Bone classification: an objective scale of bone density using the computerized tomography scan. Clin Oral Implants Res 2001;12(1):79-84. DOI: 10.1034/j.1600-0501.2001.012001079.x.

**17.** Naitoh M, Takada ST, Kurosu Y, Inagaki K, Mitani A, Ariji E. Relationship between findings of mandibular cortical bone in inferior border and bone mineral densities of lumbar vertebrae in postmenopausal women. Okajimas Folia Anat Jpn 2014;91(3):49-55. DOI: 10.2535/ofaj.91.49.

**18.** Bassi F, Procchio M, Fava C, Schierano G, Preti G. Bone density in human dentate and edentulous mandibles using computed tomography. Clin Oral Implants Res 1999;10(5):356-61. DOI: 10.1034/j.1600-0501.1999.100503.x.

**19.** Bodic F, Amouriq Y, Gayet-Delacroix M, et al. Relationships between bone mass and micro-architecture at the mandible and iliac bone in edentulous subjects: a dual X-ray absorptiometry, computerised tomography and microcomputed tomography study. Gerodontology 2012;29(2):e585-94. DOI: 10.1111/j.1741-2358.2011.00527.x.

**20.** Dall'Ara E, Varga P, Pahr D, Zysset P. A calibration methodology of QCT BMD for human vertebral body with registered micro-CT images. Med Phys 2011;38(5):2602-8. DOI: 10.1118/1.3582946.

**21.** Parsa A, Ibrahim N, Hassan B, van der Stelt P, Wismeijer D. Bone quality evaluation at dental implant site using multislice CT, micro-CT, and cone beam CT. Clin Oral Implants Res 2015;26(1):e1-7. DOI: 10.1111/clr.12315.

**22.** Mashiatulla M, Ross RD, Sumner DR. Validation of cortical bone mineral density distribution using micro-computed tomography. Bone 2017;99:53-61. DOI: 10.1016/j.bone.2017.03.049.

**23.** Monje A, Chan HL, Galindo-Moreno P, et al. Alveolar Bone Architecture: A Systematic Review and Meta-Analysis. J Periodontol 2015;86(11):1231-1248. (In English). DOI: 10.1902/jop.2015.150263.

**24.** Cawood JI, Howell RA. A classification of the edentulous jaws. Int J Oral Maxillofac Surg 1988;17(4):232-6. DOI: 10.1016/s0901-5027(88)80047-x.

**25.** Zmyslowska-Polakowska E, Radwanski M, Ledzion S, Leski M, Zmyslowska A, Lukomska-Szymanska M. Evaluation of Size and Location of a Mental Foramen in the Polish Population Using Cone-Beam Computed Tomography. Biomed Res Int 2019;2019:1659476. DOI: 10.1155/2019/1659476.

**26.** Nuzzo S, Peyrin F, Cloetens P, Baruchel J, Boivin G. Quantification of the degree of mineralization of bone in three dimensions using synchrotron radiation microtomography. Med Phys 2002;29(11):2672-81. DOI: 10.1118/1.1513161.

**27.** Mulder L, Koolstra JH, Van Eijden TM. Accuracy of microCT in the quantitative determination of the degree and distribution of mineralization in developing bone. Acta Radiol 2004;45(7):769-77. (https://www.ncbi.nlm.nih.gov/pubmed/15624521).

**28.** Kim JE, Shin JM, Oh SO, et al. The three-dimensional microstructure of trabecular bone: Analysis of site-specific variation in the human jaw bone. Imaging Sci Dent 2013;43(4):227-33. DOI: 10.5624/isd.2013.43.4.227.

**29.** Hildebrand T, Ruegsegger P. Quantification of Bone Microarchitecture with the Structure Model Index. Comput Methods Biomech Biomed Engin 1997;1(1):15-23. DOI: 10.1080/01495739708936692.

**30.** Salmon PL, Ohlsson C, Shefelbine SJ, Doube M. Structure Model Index Does Not Measure Rods and Plates in Trabecular Bone. Front Endocrinol (Lausanne) 2015;6:162. DOI: 10.3389/fendo.2015.00162.

**31.** Pietrokovski J. The bony residual ridge in man. J Prosthet Dent 1975;34(4):456-62. DOI: 10.1016/0022-3913(75)90166-3.

**32.** Nagele E, Kuhn V, Vogt H, et al. Technical considerations for microstructural analysis of human trabecular bone from specimens excised from various skeletal sites. Calcif Tissue Int 2004;75(1):15-22. DOI: 10.1007/s00223-004-0151-8.

**33.** Kim YJ, Henkin J. Micro-computed tomography assessment of human alveolar bone: bone density and three-dimensional micro-architecture. Clin Implant Dent Relat Res 2015;17(2):307-13. DOI: 10.1111/cid.12109.

**34.** Moon HS, Won YY, Kim KD, et al. The three-dimensional microstructure of the trabecular bone in the mandible. Surg Radiol Anat 2004;26(6):466-73. DOI: 10.1007/s00276-004-0247-x.

**35.** Mahnama A, Tafazzoli-Shadpour M, Geramipanah F, Mehdi Dehghan M. Verification of the mechanostat theory in mandible remodeling after tooth extraction: animal study and numerical modeling. J Mech Behav Biomed Mater 2013;20:354-62. DOI: 10.1016/j.jmbbm.2013.02.013.

**36.** Dechow PC, Wang Q, Peterson J. Edentulation alters material properties of cortical bone in the human craniofacial skeleton: functional implications for craniofacial structure in primate evolution. Anat Rec (Hoboken) 2010;293(4):618-29. DOI: 10.1002/ar.21124.

**37.** Schwartz-Dabney CL, Dechow PC. Edentulation alters material properties of cortical bone in the human mandible. J Dent Res 2002;81(9):613-7. DOI: 10.1177/154405910208100907.

**38.** Mesa F, Munoz R, Noguerol B, de Dios Luna J, Galindo P, O'Valle F. Multivariate study of factors influencing primary dental implant stability. Clin Oral Implants Res 2008;19(2):196-200. DOI: 10.1111/j.1600-0501.2007.01450.x.

**39.** Turkyilmaz I, Sennerby L, McGlumphy EA, Tozum TF. Biomechanical aspects of primary implant stability: a human cadaver study. Clin Implant Dent Relat Res 2009;11(2):113-9. DOI: 10.1111/j.1708-8208.2008.00097.x.

**40.** Boronat-Lopez A, Penarrocha-Diago M, Martinez-Cortissoz O, Minguez-Martinez I. Resonance frequency analysis after the placement of 133 dental implants. Med Oral Patol Oral Cir Bucal 2006;11(3):E272-6. (https://www.ncbi.nlm.nih.gov/pubmed/16648767).

**41.** Tricio J, Laohapand P, van Steenberghe D, Quirynen M, Naert I. Mechanical state assessment of the implant-bone continuum: a better understanding of the Periotest method. Int J Oral Maxillofac Implants 1995;10(1):43-9. (https://www.ncbi.nlm.nih.gov/pubmed/7615316).

**42.** Kingsmill VJ, Boyde A. Mineralisation density of human mandibular bone: quantitative backscattered electron image analysis. J Anat 1998;192 ( Pt 2):245-56. DOI: 10.1046/j.1469-7580.1998.19220245.x.

**43.** Fish EW. Tongue space in full denture construction. Br Dent J 1947;83(7):137-42. (https://www.ncbi.nlm.nih.gov/pubmed/20266580).

**44.** Watt DM, Likeman PR. Morphological changes in the denture bearing area following the extraction of maxillary teeth. Br Dent J 1974;136(6):225-35. DOI: 10.1038/sj.bdj.4803165.

**45.** Boskey AL, Cohen ML, Bullough PG. hard tissue biochemistry: a comparison of fresh-frozen and formalin-fixed tissue samples. Calcif Tissue Int 1982;34(4):328-31. DOI: 10.1007/BF02411262.

**46.** Currey JD, Brear K, Zioupos P, Reilly GC. Effect of formaldehyde fixation on some mechanical properties of bovine bone. Biomaterials 1995;16(16):1267-71. DOI: 10.1016/0142-9612(95)98135-2.

# 4

# The irradiated human mandible: A quantitative study on bone vascularity

Hannah Dekker, Nathalie Bravenboer, Dennis van Dijk, Elisabeth Bloemena, Derek H.F. Rietveld, Christiaan M. ten Bruggenkate, Engelbert A.J.M. Schulten

**Published in :** Oral Oncology 2018; 87: 126-130

## ABSTRACT

Objectives**:** Hypovascularisation is thought to play an important role in the pathogenesis of osteoradionecrosis. The objective of this study was to assess the microvascular system in the irradiated mandibular bone marrow.

Materials and methods**:** Mandibular bone biopsies were taken from 20 irradiated patients and 24 controls. Blood vessels were visualized using CD34 antibody stain to detect endothelial cells. The vascular density (VD) and vascular area fraction (VAF) were measured. Mean vessel lumen area, perimeter and diameter of the vessels were calculated for each vessel. A distinction was made between large and small vessels (cut-off point<400 μm2).

Results**:** Vascular density and vascular area fraction were lower in the irradiated group. The mean vascular perimeter and mean vascular diameter were higher in samples with a local radiation dose of ≥50 Gy, whereas the percentage of small vessels was lower. Larger vessel perimeter is associated with higher radiation dose. A longer interval between biopsy and radiotherapy is associated with a larger mean vessel perimeter and a lower percentage of small vessels.

Conclusions**:** Radiation dosages higher than 50 Gy mainly affect the smaller vessels. With increased time after irradiation, the share of smaller vessels in the mandibular bone marrow seems to decrease. In search of the exact mechanisms of irradiation damage and osteoradionecrosis of the mandible, the role of the microvascular system in the mandibular bone marrow should be further explored.

# INTRODUCTION

Radiotherapy plays an important role in the treatment of head and neck malignancies, either as adjuvant or primary treatment modality. Osteoradionecrosis (ORN), usually occurring in the mandible, is a late and severe complication after radiotherapy in head and neck cancer patients. ORN is defined by a non-healing area of exposed bone of at least three months duration.[1] ORN is often characterized by pain, suppuration and oral or orocutaneous fistulae and usually has a high morbidity. In advanced stages, ORN typically requires extensive surgical resection and reconstruction. Despite a considerable decrease from 20% in patients irradiated for oral and oropharyngeal cancer several decades ago to 4-8% in recent studies, ORN still presents a difficult clinical and therapeutic challenge.[2]



In 1983, Marx proposed the theory that a sequence of radiation-induced cellular injury leading to the formation of hypoxic-hypocellular and hypovascular tissue, and subsequent tissue breakdown through persistent hypoxia can cause a chronic, non-healing wound and can ultimately result in ORN.[3] This theory is currently widely accepted. However, the importance of hypoxia in tissues affected by ORN has not been proven.[4] More recently, Delanian and Lefaix[5] proposed another theory that emphasises the role of a radiation-induced fibro-atrophic process. Three subsequent phases are described. First, there is a pre-fibrotic phase, which is characterized by non-specific chronic local inflammation, destruction of endothelial cells and vascular thrombosis. Second, a constitutive organised phase takes place, which is characterized by abnormal fibroblastic activity, leading to a fibrotic remodelling of the extracellular matrix. The third late fibro-atrophic phase is characterized by poorly vascularized and cellularized tissue and can last up to decades after radiotherapy. Poor vascularisation is a common feature in both theories. A possible role for irradiation-induced damage of oral mucosa in the pathogenesis of osteoradionecrosis, through alterations of the mucosal cell surface and subsequent dysfunction of the oral mucosal barrier, has been proposed by Asikainen et al.[6]

Multiple methods have been employed to investigate the vascularity of irradiated mandibular bone. The vascularity of bone can be analyzed through quantitative or

qualitative histology or with micro-CT analysis. Most of these studies have been carried out in animal models.[7-15] Studies on human tissue are limited and have been typically performed on tissue specimens derived from ORN lesions or oncological resections in previously irradiated patients.[16-19] A disadvantage of these studies is that tissue has been subjected to pathological processes (e.g. recurrent tumor, osteoradionecrosis) that could potentially bias the histological findings on bone vascularity. Another common method to assess bone vascularity in animal as well as human studies, is laser Doppler flowmetry. However, this method measures blood flow by measuring the backscatter of passing erythrocytes and is unable to quantify the vascular microarchitecture.[7]

The pathophysiology of radiation-induced tissue injury and its consequences in the mandible are still poorly understood. To unravel the exact pathophysiological process of radiation damage to the mandible and ORN, quantitative studies of the vascularity in irradiated mandibular tissue are essential. The primary objective of this study was to investigate the vascularity in mandibular bone marrow following radiotherapy of the bone tissue in patients without evidence of recurrent tumor or ORN.

## PATIENTS AND METHODS

*Patients*

The irradiated group consisted of fully edentulous patients (14 males and 6 females; age range 54-76 years, mean age 65 years) with a history of radiotherapy for head and neck malignancy who underwent dental rehabilitation with dental implants in the mandible between August 1, 2012 and April 1, 2016 in Amsterdam University Medical Centers (UMC), location VUmc. Patients with radiation fields that did not include the mandible and patients who had undergone mandibular reconstruction with bone grafts were excluded.

The control group consisted of 24 fully edentulous patients (14 males and 10 females; age range 34-79 years, mean age 65 years) who underwent dental implant surgery, with no history of oral cancer or radiotherapy. Patients in the control group were included between August 1, 2012 and December 31, 2014 in the Alrijne Hospital in Leiderdorp, The Netherlands.

Exclusion criteria were a history of bisphosphonate medication, impaired bone metabolism (e.g. hyperparathyroidism, osteomalacia) or systemic immunosuppressive medication up to three months prior to the dental implant surgery. All participants had blood calcium, phosphate, parathyroid hormone and HbA1c levels within the normal range.

All patients were fully informed and signed a written consent form. Prior to the study, approval for the research was provided by the Medical Ethical Committee of the Amsterdam UMC (location VUmc), Amsterdam, The Netherlands (registration number 2011/220).



*Hyperbaric oxygen therapy*

Hyperbaric oxygen therapy is the standard procedure in our clinic and it is administered to patients who undergo surgical procedures in the area of the maxilla or mandible that have been irradiated with 50 Gy or more. For all irradiated patients the radiotherapist was consulted pre-operatively to estimate the radiation dose in the anterior mandible. Patients who had received an estimated dose of 50 Gy or higher on the anterior mandible, were treated with 20 sessions hyperbaric oxygen therapy preoperatively and 10 sessions postoperatively (Marx-protocol).

*Dental implant surgery and bone biopsy retrieval*

All patients from the irradiated group were treated by a single oral and maxillofacial surgeon (ES). Patients in this study group were treated under general anesthesia, no local anesthesia was administered during the surgical procedure. Patients were given antibiotic prophylaxis following the ORN-protocol (amoxicillin/clavulanic acid 500/125 mg 3 times daily, starting 24 hours prior to surgery and continuing until 10 days after surgery). In the study group patients, four dental implants were placed in the interforaminal region of the edentulous mandible, equally distributed on positions 44-42-32-34.

Patients from the control group were treated by a single oral and maxillofacial surgeon (CtB). Patients were given a single dose antibiotic prophylaxis (amoxicillin 3 gr orally) prior to dental implant surgery. The surgical procedure was performed under local

anesthesia. Patients in the control group received two dental implants in the edentulous mandible, in the left and right canine position.

The dental implant surgical procedure was the same in both groups. A crestal incision was made in the interforaminal region of the mandible with a mid-line buccal release incision. A full thickness mucoperiosteal flap was raised to expose the alveolar ridge and, if necessary, levelled by vertical alveolotomy. Implant preparations were made with a 3.5 mm trephine burr (2.5 mm inner diameter) (Straumann® Dental Implant System, Straumann Holding AG, Basel, Switzerland) to a depth of 10 or 12 mm at left and right canine positions. An ejector pin was used to carefully remove the bone cylinder from the trephine drill. After collection of the bone samples, additional spiral drills were used to finish the alveolar osteotomy. All drilling phases were conducted under copious irrigation with sterile saline. Regular neck Straumann dental implants with a diameter of 4.1 mm and a length of 10 or 12 mm, and an SLA surface (Straumann® Dental Implant System, Straumann Holding AG, Basel, Switzerland) were inserted into the prepared sites. All dental implants were placed in a single-staged surgical procedure, mounted with healing caps and the mucosa was sutured with non-resorbable sutures (Gore-Tex 4-0). One bone cylinder (biopsy specimen) per patient was selected and prepared for further analysis.

*Processing and measurements of the bone biopsies*

The bone cylinders were immediately fixed by immersion in 4% phosphate-buffered formaldehyde for 24 hours. Subsequently the biopsies were rinsed with phosphate-buffered saline and immersed in EDTA solution for decalcification. After 3 weeks of decalcification the samples were embedded in paraffin and cut in 5 μm sections using a Leitz microtome (Leitz, Wetzlar, Germany). Blood vessels were visualized using CD34 antibody stain to detect endothelial cells (Dako M7165), using the BenchMark ULTRA IHC/ISH Staining module (Ventana).

Bone samples were blinded by encoding. A minimum area of 1 $mm^2$ bone marrow was measured, using 6-7 photographs of bone marrow sections at 200x magnification (0,46 $mm^2$ per photo) with NIS Elements AR 4.10.01. All morphological structures with a lumen surrounded by CD34-positive endothelial cells were identified as blood vessels.

The vascular density (VD) was calculated as the number of vessels per bone marrow area (N.Ve./Ma.Ar. = number of counted vessels/bone marrow area in $mm^2$). The vascular area fraction (VAF) was calculated as the percentage vascular area of the bone marrow (Ve.Ar./Ma.Ar. = [vascular area/studied bone marrow area] x 100). Furthermore the vessel lumen area, perimeter and diameter of the vessels were calculated for each vessel. The cut-off point for what is referred to as small vessels was a lumen surface area of $<400\ \mu m^2$. Ten random samples were analyzed by two independent observers (DvD, HD). Interobserver variance was less than 5%.

*Determination of radiation dose*

To determine the radiation dose at the site of the dental implant in patients treated with intensity modulated radiotherapy (IMRT), the radiotherapy treatment planning CT image was merged with a postoperative cone-beam CT image. In this way the exact point dose (Dmax) administered at the site of the implant (corresponding with the site of the biopsy) was determined. In patients who were treated with conventional conformal 3D radiotherapy, the radiotherapist estimated the local dose based on the treatment plans.



Two patients were treated with radiotherapy in clinics outside the Amsterdam UMC, despite efforts to contact these clinics to gather treatment plans, this information could not be retrieved. Therefore, in these two patients, the local dose could not be calculated.

*Statistical analysis*

SPSS software (IBM SPSS statistics, version 22, New York, United States) was used for statistical evaluation. Median VAF, VD, vessel lumen, vessel perimeter, vessel diameter and percentage of small vessels of the irradiated and non-irradiated group were compared using the Mann-Whitney U test with two tails. P-values of $<0.05$ were considered statistically significant. Spearman Rho correlations were used to analyze the correlation between radiation dose and the vascularity characteristics in the irradiated group.

# RESULTS

Patient and treatment characteristics of the irradiated group are summarized in Table 1. The mean total radiation dose (n=20) was 66.7 Gy (range 54-70 Gy) and the mean local radiation dose, Dmax, (n=18) was 38.11 Gy (range 4-72 Gy).

The number and size of blood vessel profiles was demonstrated by the endothelial cell marker CD34 (Figures 1 and 2). The vascular measurements of the irradiated patients versus non-irradiated (control) patients are summarized in Table 2. Vascular density as well as vascular area fraction were significantly lower in the irradiated group. No significant differences were observed in mean vessel lumen, perimeter, diameter and percentage of small vessels.

The correlation of radiation dose with vascular measurements in the irradiated group are summarized in Table 3. Vessel perimeter was positively associated with radiation dose. Time between biopsy and last day of radiotherapy correlated positively with the mean vessel perimeter (Spearman correlation $r = 0.489$, $p = 0.029$), but negatively with the percentage of small vessels (Spearman correlation $r = -0.548$, $p = 0.012$).

In Table 4, the vascular measurements in the irradiated group with a local radiation dose of $<50$ Gy versus a local radiation dose of $\geq 50$ Gy are shown separately. The mean vascular perimeter and mean vascular diameter are significantly higher in the samples with a local radiation dose of $\geq 50$ Gy, whereas the percentage of small vessels is significantly lower.

Table 1. Patient and treatment characteristics of the irradiated group (N=20)

| Age/sex | Tumor site | RT-technique | RT dose total (Gy) | RT dose local (Gy) | Interval RT – biopsy (months) |
|---|---|---|---|---|---|
| 74/Male | Floor of mouth | 3D-CRT | 55 | 55 | 199 |
| 73/Female | Base of tongue | IMRT | 70 | 47 | 21 |
| 61/Female | Uvula | IMRT | 70 | 20 | 16 |
| 54/Male | Oral tongue | IMRT | 70 | 72 | 85 |
| 64/Male | Soft palate | IMRT | 70 | 49 | 23 |
| 63/Male | Supraglottic larynx | IMRT | 70 | n.a.[a] | 171 |
| 63/Male | Lip | IMRT | 54 | 45 | 11 |
| 67/Male | Soft palate | IMRT | 70 | 28 | 44 |
| 68/Female | Tonsil | IMRT | 70 | 23 | 24 |
| 76/Female | Base of tongue | IMRT | 70 | 36 | 31 |
| 68/Male | Pharyngeal arch | IMRT | 60 | 4 | 6 |
| 61/Female | Oral tongue | IMRT | 70 | n.a.[a] | 88 |
| 71/Male | Oropharynx | IMRT | 70 | 36 | 30 |
| 74/Male | Tonsil | IMRT | 70 | 41 | 70 |
| 62/Male | Submandibular gland | IMRT | 56 | 62 | 10 |
| 58/Male | Supraglottic larynx | IMRT | 70 | 18 | 28 |
| 62/Male | Base of tongue | 3D-CRT | 62,5 | 50 | 197 |
| 56/Male | Hypopharynx | IMRT | 70 | 17 | 17 |
| 61/Female | Base of tongue | IMRT | 70 | 24 | 122 |
| 58/Female | Oral tongue | IMRT | 66 | 59 | 23 |

Abbreviations: 3D-CRT, 3-dimensional conformal radiotherapy; IMRT, intensity-modulated radiotherapy; n.a. not available

[a] From 2 patients radiotherapy treatment plans could not be retrieved.

Table 2. Vascular measurements of irradiated patients versus non-irradiated (control) patients.

| **Vascular measurement** | **Irradiated group (n=20) Median (IQR)** | **Control group (n=24) Median (IQR)** | **p[a]** |
|---|---|---|---|
| VD (No.x$10^2$/$mm^2$) | 1.04 (0.83) | 1.77 (0.71) | 0.002** |
| VAF (%) | 1.84 (2.22) | 6.08 (7.14) | 0.001** |
| Mean vessel lumen ($\mu m^2$) | 120.53 (260.32) | 284.87 (313.67) | 0.066 |
| Mean perimeter (μm) | 20.71 (18.29) | 30.43 (17.96) | 0.063 |
| Mean diameter (μm) | 2.42 (1.26) | 3.15 (1.52) | 0.187 |
| Lumen <400 μm (%) | 95.4 (6.2) | 92.6 (5.6) | 0.175 |

Abbreviations: IQR, interquartile range; VD, vascular density; VAF, vascular area fraction.

[a] Mann Whitney U test p-value.

Table 3. Correlations of local radiation dose and vascular measurements (n=18).

| Vascular measurement irradiated patients (n=18) | Spearman's rho Correlation coefficient[a] | p[b] |
|---|---|---|
| VD (No.x102/mm2) | -0.122 | 0.630 |
| VAF (%) | 0.110 | 0.663 |
| Mean vessel lumen (μm2) | 0.219 | 0.383 |
| Mean perimeter (μm) | 0.518 | 0.028* |
| Mean diameter (μm) | 0.407 | 0.094 |
| Lumen <400um (%) | -0.364 | 0.137 |

Abbreviations: VD, vascular density; VAF, vascular area fraction.

[a] Correlation with local radiation dose at biopsy site

[b] Spearman's Rho correlation p-value

Table 4. Comparison of vascular measurements at sites with a local radiation dose of <50 Gy versus a local radiation dose of ≥50 Gy.

| Vascular measurements | Local dose <50 Gy (n=13) Median | Local dose ≥50 Gy (n=5) Median | p[a] |
|---|---|---|---|
| VD (No.x$10^2$/$mm^2$) | 1.39 | 0.85 | 0.075 |
| VAF (%) | 1.64 | 3.95 | 0.503 |
| Mean vessel lumen ($\mu m^2$) | 105.19 | 429.98 | 0.143 |
| Mean perimeter (μm) | 19.91 | 45.25 | 0.026* |
| Mean diameter (μm) | 2.42 | 5.8 | 0.019* |
| Lumen <400um (%) | 96 | 84.7 | 0.035* |

Abbreviations: VD, vascular density; VAF, vascular area fraction.

[a] Mann Whitney U test p-value.

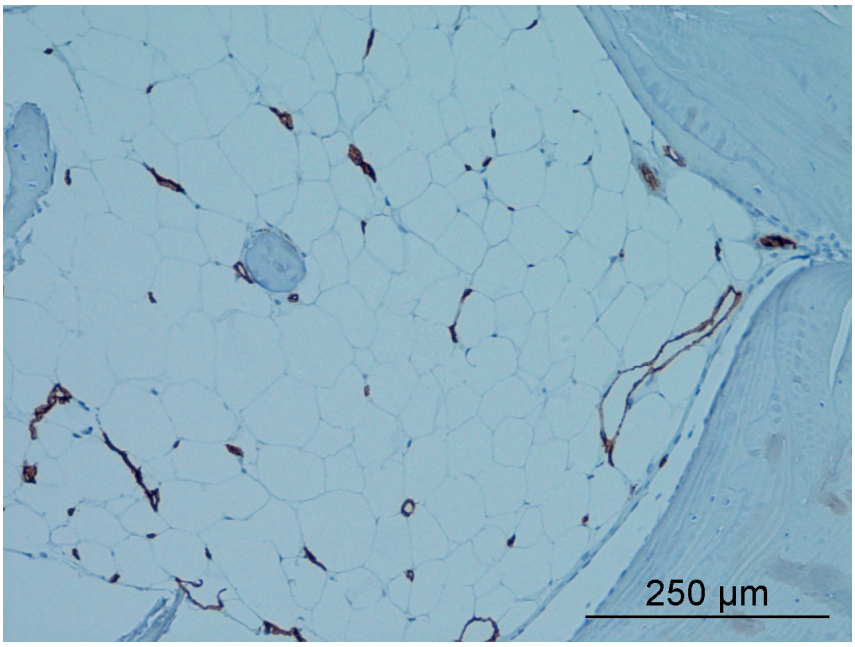


Figure 1. CD34-positive endothelial lined blood vessels in non-irradiated mandibular trabecular bone.

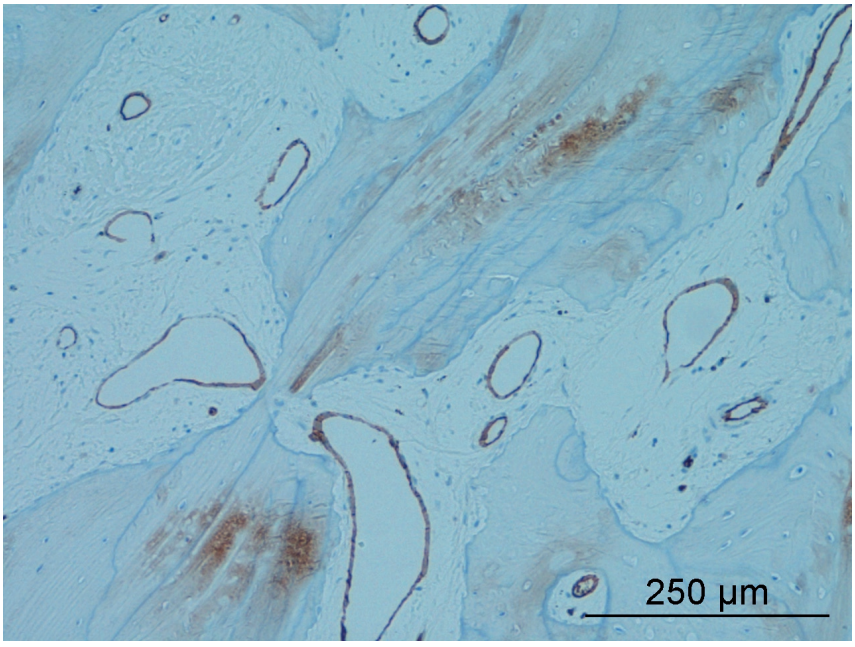


Figure 2. CD34-positive endothelial lined blood vessels in mandibular trabecular bone with a local radiation dose of 59 Gy.

# DISCUSSION

This study showed a significant decrease in vascular area fraction and vascular density in mandibular bone of irradiated patients compared with non-irradiated controls, which indicates that radiation causes hypovascularity. Various human studies have performed histologic evaluation of irradiated mandibles but none has provided a quantitative analysis of bone marrow vascularity. Radiation-induced hypovascularity has been reported in animal studies, using qualitative (ordinal) or descriptive measures.[9-12,15] However, the contribution of these results is limited considering the absence of quantitative data.

Poort et al.[13] measured the lumen of the inferior alveolar artery in irradiated mini-pigs as a measure for mandibular vascularity but did not quantify the vascularity of the mandibular bone marrow. Deshpande et al.[7] performed a quantitative measurement of the vascularity in irradiated rat mandibles. Vessel number, vessel volume fraction, vessel separation and vessel thickness was assessed by contrast enhanced micro-CT. A reduction in vessel volume fraction and vessel number was seen compared to non-irradiated controls, which corresponds with the findings in our study, although the technique used is obviously different given that histological analysis is a 2-dimensional assessment compared to the micro-CT which is a 3-dimensional assessment. Hence, caution must be taken when comparing results from animal studies with human studies.

A limited number of histological studies on irradiated human mandibles is available, although not on a quantitative basis. Bras et al.[16] investigated irradiated human mandibular specimens from patients that underwent surgical resection for either ORN or floor of mouth squamous cell carcinoma. McGregor et al.[19] conducted a study on mandibular specimens from patients, previously irradiated, with recurrent tumor and compared these with non-irradiated mandibular specimens from resections for primary carcinomas serving as controls. In these studies, the inferior alveolar artery and the periosteal vessels were assessed qualitatively as a measure of mandibular vascularity.

Although the main blood supply of the mandible is provided by the inferior alveolar artery and the periosteum, the assessment of these vascular structures does not directly

reflect the vascularity of the trabecular bone. A functioning network of macro- and microvessels is a prerequisite for oxygen and nutrient exchange at tissue level. Therefore, in order to quantify radiation-induced damage to the vascularization of bone, it is vital to quantitatively assess the effect of irradiation on the bone marrow's microvascular network.

Curi et al.[17] analyzed 40 irradiated mandibular specimens from ORN patients and 15 non-irradiated specimens from oncological resections. Vascularity of the mandible was assessed histomorphometrically. Endothelial immunostaining of CD34 was performed and vascular density of the bone marrow was measured using a grid. The vascular density was significantly lower in the irradiated group ($p \leq 0.001$) with a more profound loss of vascular density at 6 months post-irradiation compared to within the first 6 months after irradiation ($p \leq 0.001$).



We did not find a significant correlation between vascular density and vascular area fraction with increased time after radiotherapy, which could be due to the fact that no specimens were taken within 6 months after radiotherapy. We did, however, find a significant negative correlation between time after radiotherapy and percentage of small vessels and a positive correlation between time after radiotherapy with mean vessel perimeter. This may indicate that either the smallest vessels are more affected by irradiation than larger vessels, or that formation of new vessels may be impaired, leading to a more profound hypovascular situation in the later post-irradiation phase. This corresponds with the fibroatrophic theory of Delanian and Lefaix that defines three culminating and irreversible sequences of radiation damage, the last of which is late fibro-atrophy lasting for 5-30 years after radiotherapy, characterized by retractile atrophy and concomitant gradual destruction of the normal tissues in the irradiated volume of bone tissue.[5]

In our study, the specimens in the irradiated group were divided to those with local radiation dose of <50 Gy versus a local radiation dose of ≥50 Gy. Interestingly, no significant differences were found in vascular number or vascular area fraction, but the vascular diameter and vascular perimeter were significantly higher in the ≥50 Gy group whereas the percentage of small vessels was significantly lower ($p = 0.026$, $p = 0.019$

and p = 0.035 respectively). This indicates that a local radiation dose exceeding 50 Gy affects the smaller blood vessels more than the larger, either by a direct effect on the smaller vessels or inhibition of new vessel formation. An important risk factor for the development of ORN is the radiation dose. ORN is rarely seen in patients irradiated with a dose of <50 Gy and it usually develops in patients irradiated with a dose of >66 Gy.[1] In the literature, a cutoff point of 50 Gy local radiation dose is commonly accepted to identify patients at risk for developing ORN.[20,21]

Although interesting significant results were found in the present study, the study did have some potential bias that should be considered. In our institution, previously irradiated patients requiring surgical intervention in an area of the maxilla or mandible, that has been administered a local dose of >50 Gy, receive a prophylactic treatment with hyperbaric oxygen therapy (HBO) according to the Marx treatment protocol.[3] Hyperbaric oxygen is thought to induce angiogenesis, improve oxygen tension in irradiated tissues and increase microvasculature.[22-25] The effect of hyperbaric oxygen treatment in our results is unknown, possibly without HBO the differences in vascularity between patients with a local radiation dose of <50 Gy versus a local radiation dose of ≥50 Gy are more profound. The study group of 20 patients is relatively small and the investigated bone samples are small in dimension. In addition there was considerable heterogeneity in the study group for the local radiation dose and the interval between radiotherapy and biopsy. A consideration is also that the technique of planar histology has the possible disadvantage of double counting in the case of vessels deviating back and forth in their trajectory that could create bias. Despite these study limitations, a major advantage is that it provides quantitative information on irradiated human mandibular tissue which is currently scarce. The material in our study is unique, owing to the fact that no concomitant pathology such as recurrent tumor or ORN was present. More quantitative research on bone marrow vascularity after radiotherapy is needed to verify and further explore the findings in the present study as well as their relevance in the pathogenesis of ORN.

## CONCLUSIONS

Radiotherapy causes a decrease in the number and density of blood vessels in mandibular bone marrow. Radiation doses higher than 50 Gy seem to mainly affect the smaller vessels. With increased time after irradiation, the share of smaller vessels in the mandibular bone marrow seems to decrease. In search of the exact mechanisms of irradiation damage and the pathogenesis of osteoradionecrosis of the mandible, the role of the microvascular system in the mandibular bone marrow warrants further exploration.



## ACKNOWLEDGEMENTS

The authors are grateful to Erik Phernambucq and Gerrit-Jan Blom, radiotherapists, for the radiation dose calculation.

# REFERENCES


1. Chrcanovic BR, Reher P, Sousa AA, Harris M. Osteoradionecrosis of the jaws--a current overview--part 1: Physiopathology and risk and predisposing factors. Oral Maxillofac Surg 2010;14(1):3-16. DOI: 10.1007/s10006-009-0198-9.
2. Moon DH, Moon SH, Wang K, et al. Incidence of, and risk factors for, mandibular osteoradionecrosis in patients with oral cavity and oropharynx cancers. Oral Oncol 2017;72:98-103. DOI: 10.1016/j.oraloncology.2017.07.014.
3. Marx RE. Osteoradionecrosis: a new concept of its pathophysiology. J Oral Maxillofac Surg 1983;41(5):283-8. (https://www.ncbi.nlm.nih.gov/pubmed/6572704).
4. Jegoux F, Malard O, Goyenvalle E, Aguado E, Daculsi G. Radiation effects on bone healing and reconstruction: interpretation of the literature. Oral Surg Oral Med Oral Pathol Oral Radiol Endod 2010;109(2):173-84. DOI: 10.1016/j.tripleo.2009.10.001.
5. Delanian S, Lefaix JL. The radiation-induced fibroatrophic process: therapeutic perspective via the antioxidant pathway. Radiother Oncol 2004;73(2):119-31. DOI: 10.1016/j.radonc.2004.08.021.
6. Asikainen PJ, Dekker H, Sirvio E, et al. Radiation-induced changes in the microstructure of epithelial cells of the oral mucosa: A comparative light and electron microscopic study. J Oral Pathol Med 2017;46(10):1004-1010. DOI: 10.1111/jop.12639.
7. Deshpande SS, Donneys A, Farberg AS, Tchanque-Fossuo CN, Felice PA, Buchman SR. Quantification and characterization of radiation-induced changes to mandibular vascularity using micro-computed tomography. Ann Plast Surg 2014;72(1):100-3. DOI: 10.1097/SAP.0b013e318255a57d.
8. Deshpande SS, Donneys A, Kang SY, et al. Vascular analysis as a proxy for mechanostransduction response in an isogenic, irradiated murine model of mandibular distraction osteogenesis. Microvasc Res 2014;95:143-8. DOI: 10.1016/j.mvr.2014.08.005.
9. Fenner M, Park J, Schulz N, et al. Validation of histologic changes induced by external irradiation in mandibular bone. An experimental animal model. J Craniomaxillofac Surg 2010;38(1):47-53. DOI: 10.1016/j.jcms.2009.07.011.
10. Xu J, Zheng Z, Fang D, et al. Early-stage pathogenic sequence of jaw osteoradionecrosis in vivo. J Dent Res 2012;91(7):702-8. DOI: 10.1177/0022034512448661.
11. Yachouh J, Breton P, Roux JP, Goudot P. Osteogenic capacity of vascularised periosteum: an experimental study on mandibular irradiated bone in rabbits. J Plast Reconstr Aesthet Surg 2010;63(12):2160-7. DOI: 10.1016/j.bjps.2010.01.015.
12. Sonstevold T, Johannessen AC, Stuhr L. A rat model of radiation injury in the mandibular area. Radiat Oncol 2015;10:129. DOI: 10.1186/s13014-015-0432-6.
13. Poort LJ, Ludlage JHB, Lie N, et al. The histological and histomorphometric changes in the mandible after radiotherapy: An animal model. J Craniomaxillofac Surg 2017;45(5):716-721. DOI: 10.1016/j.jcms.2017.02.014.
14. Bodard AG, Debbache S, Langonnet S, Laffay F, Fleury B. A model of mandibular irradiation in the rabbit: preliminary results. Bull Group Int Rech Sci Stomatol Odontol 2013;52(1):e17-22. (https://www.ncbi.nlm.nih.gov/pubmed/25461444).
15. Blery P, Espitalier F, Hays A, et al. Development of mandibular osteoradionecrosis in rats: Importance of dental extraction. J Craniomaxillofac Surg 2015;43(9):1829-36. DOI: 10.1016/j.jcms.2015.08.016.
16. Bras J, de Jonge HK, van Merkesteyn JP. Osteoradionecrosis of the mandible: pathogenesis. Am J Otolaryngol 1990;11(4):244-50. (https://www.ncbi.nlm.nih.gov/pubmed/2240412).
17. Curi MM, Cardoso CL, de Lima HG, Kowalski LP, Martins MD. Histopathologic and Histomorphometric Analysis of Irradiation Injury in Bone and the Surrounding Soft Tissues of the Jaws. J Oral Maxillofac Surg 2016;74(1):190-9. DOI: 10.1016/j.joms.2015.07.009.

**18.** Marx RE, Tursun R. Suppurative osteomyelitis, bisphosphonate induced osteonecrosis, osteoradionecrosis: a blinded histopathologic comparison and its implications for the mechanism of each disease. Int J Oral Maxillofac Surg 2012;41(3):283-9. DOI: 10.1016/j.ijom.2011.12.016.

**19.** McGregor AD, MacDonald DG. Post-irradiation changes in the blood vessels of the adult human mandible. Br J Oral Maxillofac Surg 1995;33(1):15-8. (https://www.ncbi.nlm.nih.gov/pubmed/7536468).

**20.** Tsai CJ, Hofstede TM, Sturgis EM, et al. Osteoradionecrosis and radiation dose to the mandible in patients with oropharyngeal cancer. Int J Radiat Oncol Biol Phys 2013;85(2):415-20. DOI: 10.1016/j.ijrobp.2012.05.032.

**21.** Tatum SA, Theler JM. Principles and practice of craniofacial bone healing. In: Sataloff RT, Sclafani AP, eds. Sataloff's Comprehensive Textbook of Otolaryngology: Head & Neck Surgery: Facial Plastic and Reconstructive Surgery 1ed. New Delhi: Jaypee Brothers,Medical Publishers Pvt. Limited; 2016:913-928.

**22.** Store G, Smith HJ, Larheim TA. Dynamic MR imaging of mandibular osteoradionecrosis. Acta Radiol 2000;41(1):31-7. (https://www.ncbi.nlm.nih.gov/pubmed/10665867).

**23.** Shaw RJ, Butterworth C. Hyperbaric oxygen in the management of late radiation injury to the head and neck. Part II: prevention. Br J Oral Maxillofac Surg 2011;49(1):9-13. DOI: 10.1016/j.bjoms.2009.11.016.

**24.** Shaw RJ, Dhanda J. Hyperbaric oxygen in the management of late radiation injury to the head and neck. Part I: treatment. Br J Oral Maxillofac Surg 2011;49(1):2-8. DOI: 10.1016/j.bjoms.2009.10.036.

**25.** Svalestad J, Hellem S, Thorsen E, Johannessen AC. Effect of hyperbaric oxygen treatment on irradiated oral mucosa: microvessel density. Int J Oral Maxillofac Surg 2015;44(3):301-7. DOI: 10.1016/j.ijom.2014.12.012.

# 5

# Bone microarchitecture and turnover in the irradiated human mandible

Hannah Dekker, Engelbert A.J.M. Schulten, Leo van Ruijven, Huib W. van Essen, Gerrit J. Blom, Elisabeth Bloemena, Christiaan M. ten Bruggenkate, Arja M. Kullaa, Nathalie Bravenboer

**Published in:** Journal of Cranio-Maxillofacial Surgery 2020; 48: 733-740

## ABSTRACT

Objectives: The aim of this study was to assess the microarchitecture and turnover in irradiated cancellous mandibular bone and the relation with radiation dose, to elucidate the effects of radiotherapy on the mandible.

Patients and methods: Mandibular cancellous bone biopsies were taken from irradiated patients and controls. Micro-CT scanning was performed to analyze microstructural bone parameters. Bone turnover was assessed by histomorphometry. Local radiation dose at the biopsy site (Dmax) was estimated from radiotherapy plans.

Results: Twenty-seven irradiated patients and 35 controls were included. Osteoid volume (Osteoid Volume/Bone Volume, OV/BV) [0.066/0.168 (median/interquartile range (IQR), OV/BV; %), $p < 0.001$], osteoid surface (Osteoid Surface/Bone Surface, OS/BS) [0.772/2.17 (median/IQR, OS/BS; %), $p < 0.001$] and osteoclasts number (Osteoclasts per millimeter bone surface, Ocl/mmBS; mm2) [0.026/0.123 (median/IQR, Ocl/mmBS; mm2), $p < 0.001$] were decreased; trabecular number (Tb.N) was lower [1.63/0.63 (median/IQR, Tb.N; $1/mm^{-1}$), $p = 0.012$] and trabecular separation (Tb.Sp) [0.626/0.24 (median/IQR, Tb.Sp; mm), $p = 0.038$] was higher in irradiated mandibular bone. With higher Dmax, trabecular number increases (Spearman's correlation $r = 0.470$, $p = 0.018$) and trabecular separation decreases (Spearman's correlation $r = -0.526$, $p = 0.007$). Bone mineral density (BMD, milligrams hydroxyapatite per cubic centimeter, $mgHA/cm^3$) [1016/99 (median/IQR, BMD; $mgHA/cm^3$), $p = 0.03$] and trabecular separation [0.739/0.21 (median/IQR, Tb.Sp; mm), $p = 0.005$] are higher whereas connectivity density (Conn Dens) [3.94/6.71 (median/IQR, Conn Dens), $p = 0.047$] and trabecular number [1.48/0.44 (median/IQR, Tb.N; $1/mm^{-1}$), $p = 0.002$] are lower in Dmax ≤50 Gy compared to controls.

Conclusions: Radiotherapy dramatically impairs bone turnover in the mandible. Deterioration in microarchitecture only affects bone irradiated with a Dmax of <50 Gy. The 50 Gy value seems to be acritical threshold to where the effects of the radiation is more detrimental.

# INTRODUCTION

Osteoradionecrosis (ORN) is a notorious complication of radiotherapy, which currently affects approximately 4-8% of patients irradiated for cancer of the oral cavity and oropharynx.[1] The risk of ORN becomes higher as radiation dose increases. However, the exact pathophysiology of ORN is poorly understood.[2,3] Radiation injury is a dynamic process that is characterized by an early (acute) and late (chronic) phase. The gross changes in bone matrix develop relatively slowly.[4]

ORN is thought to have a multifactorial and complex etiology. Hypovascularity, hypoxia and hypocellularity, destruction of osteocytes, lack of osteoblasts and newly formed osteoid tissue and bone marrow fibrosis are observed in osteoradionecrosis lesions.[5] Two characteristics of ORN have formed the basis of the most widely accepted treatment protocols.



First, the theory of Marx, first published in 1983, states that radiation leads to a sequence of cellular injury leading to the formation of hypoxic-hypocellular and hypovascular tissue. Subsequent tissue breakdown through persistent hypoxia causes a chronic, non-healing wound that ultimately results in ORN. Marx developed a treatment protocol consisting of a combination of hyperbaric oxygen therapy and surgical resection and reconstruction with microvascular flap surgery based on his concepts, that the trias hypovascularity, hypocellularity and hypoxia is the main pathophysiologic event in ORN.

Second, the theory of Delanian and Lefaix states that radiation induced damage to the endothelial cells stimulates cytokine production that activates myofibroblasts, which deposit abnormal fibrotic material in the extracellular matrix which ultimately leads to paucicellular, fibrotic tissue that, in presence of trauma, could lead to ORN.[6] This theory where radiation-induced fibrosis is thought to be the main pathophysiologic event in ORN, has led to the pentoxifylline-tocopherol combination treatment, which is thought to decrease the superficial fibrosis induced by radiotherapy.

More recent studies addressed the problem of impaired bone regeneration in irradiated bone and osteoradionecrosis. The altered expression of specific growth factors involved in fibrosis and osseo-induction such as transforming growth factor (TGF)-β1 and bone morphogenetic proteins (BMPs) are thought to compromise bone healing after irradiation.[7-9] Several studies suggest that administration of exogenous BMP can improve radiation induced impaired bone regeneration in rats.[10,11] The administration of stem cells is thought to improve regenerative potential of irradiated mandibular bone and is associated with increased bone formation in animal models.[12-14]

Most research on irradiation damage and osteoradionecrosis of the mandible is performed in animal models. These models are a valuable tool as they allow for creating standardized protocols to study the effects of radiation and potential treatments. However, studies on human material are scarce and the available data are derived from excised mandibular bone from ORN lesions or tumor resection specimens.[15-21] Evidently, there is a need to study mandibular bone specimens from irradiated patients with no other pathology.

The aim of the present study was to investigate the effect of radiotherapy on bone turnover and microarchitecture in the human mandible, and explore the relation with radiation dose.

## PATIENTS AND METHODS

*Patients*

Patients with a history of radiotherapy for head and neck malignancy who underwent dental rehabilitation with dental implants in the mandible between August 1, 2012 and April 1, 2016 were included in the irradiated group. Patients with radiation fields that did not include the mandible and patients who had undergone mandibular reconstruction with bone grafts were excluded from this study.

Edentulous patients who underwent dental implant surgery between August 1, 2012 and December 31, 2014 in the Alrijne Hospital in Leiderdorp, the Netherlands were included in the control group.

Exclusion criteria were a history of bisphosphonate medication, impaired bone metabolism (e.g. hyperparathyroidism, osteomalacia) or systemic immunosuppressive medication up to three months prior to the dental implant surgery. All participants had blood calcium, phosphate, parathyroid hormone and HbA1c levels within the normal range.

All patients were fully informed and signed a written consent form for study participation. Prior to the study, approval for the research was provided by the Medical Ethical Committee of the Amsterdam University Medical Centers (location VUmc), Amsterdam, The Netherlands (registration number 2011/220). All methods were performed in accordance with the relevant guidelines and regulations. The study design is a retrospective study with prospective data collection.

*Hyperbaric oxygen therapy*

Hyperbaric oxygen (HBO) therapy is the standard procedure in our department and is administered to patients who undergo surgical procedures in the area of the maxilla or mandible that have been irradiated with 50 Gy or more. For all irradiated patients the radiotherapist was consulted pre-operatively to estimate the maximum radiation dose in the anterior mandible. Patients who had received an estimated dose of 50 Gy or higher on the anterior mandible, were treated with 20 sessions HBO therapy preoperatively and 10 sessions postoperatively (Marx-protocol).[5]

*Dental implant surgery and bone biopsy retrieval*

Dental rehabilitation of all patients from the irradiated group was performed in the Amsterdam University Medical Centers (location VUmc) by one oral and maxillofacial surgeon (ES). Patients in this study group were treated under general anesthesia, no local anesthesia was administered during the surgical procedure. Patients were given antibiotic prophylaxis following the ORN-protocol (amoxicillin/clavulanic acid 500/125 mg 3 times daily, starting 24 hours prior to surgery and continuing until 10 days after surgery). In the study group patients, four dental implants were placed in the interforaminal region of the edentulous mandible, equally distributed on positions 44-42-32-34.

Patients from the control group were treated in the Alrijne Hospital in Leiderdorp by a single oral and maxillofacial surgeon (CB). Patients were given a single dose antibiotic prophylaxis (amoxicillin 3 g orally) prior to dental implant surgery. The surgical procedure was performed under local anesthesia. Patients in the control group received two dental implants in the edentulous mandible, in the left and right canine position.

The dental implant surgical procedure was the same in both groups. The biopsy specimens were harvested as the first step in the sequence of implant placement. A crestal incision was made in the interforaminal region of the mandible with a mid-line buccal release incision. A full thickness mucoperiosteal flap was raised to expose the alveolar ridge and, if necessary, levelled by vertical alveolotomy. Implant preparations were made with a 3.5 mm trephine burr (2.5 mm inner diameter) (Straumann® Dental Implant System, Straumann Holding AG, Basel, Switzerland) to a depth of 10 or 12 mm**,** under copious irrigation with sterile saline. An ejector pin was used to carefully remove the bone cylinder from the trephine drill. One bone cylinder (biopsy specimen) per patient was selected and prepared for further analysis.

*Processing of the bone biopsies*

Bone cylinders were immediately fixed by immersion in 4% phosphate-buffered formaldehyde, dehydrated in ascending series of ethanols, and embedded in 83% methylmethacrylate (BDH Chemicals**,** Poole, England) supplemented with 17% dibuthylphtalate (Merck, Darmstadt, Germany), 8 g/L lucidol CH-50L (Akzo Nobel, Amersfoort, the Netherlands) and 22 μl/10 ml N,Ndimethyl-p-toluidine (Merck Darmstadt, Germany).

*Micro-CT analysis*

Micro-CT analysis was performed to determine parameters of bone microarchitecture. Embedded samples were scanned with a micro-computed tomography system (μCT 40; Scanco Medical AG, Brüttisellen, Switzerland) using 55 kV, 145 μA, 600 ms integration time, and a resolution of 8 μm. The polychromatic source and cone-shaped beam of the scanner was filtered with a 0.5 mm aluminum filter. The beam hardening effect was further reduced by applying a correction algorithm developed by the

manufacturer. The system was calibrated weekly with a reference phantom (QRM GmbH, Mohrendorf, Germany).

Grey values were considered to be proportional to the local bone mineral density, equivalent to the concentration of hydroxyapatite (HA).[22,23] Imaging processing included Gaussian filtering and segmentation with sigma 0.3, support 1, threshold 560 mg HA/$cm^3$. This threshold was used for each measurement. Volumes of interest (VOI) of trabecular regions were chosen by visual inspection. In all VOI's bone volume fraction (BV/TV; %), bone mineral density (BMD; mg HA $cm^{-3}$), trabecular number (Tb.N; 1/$mm^{-1}$), separation (Tb.Sp; μm), thickness (Tb.Th; μm) and trabecular connectivity density were determined. The manufacturer's morphometric software uct_evaluation v6.5-3 (Scanco Medical AG, Brüttisellen, Switzerland) was used for this analysis.



*Histological procedure*

Following the scanning procedure, undecalcified biopsies were cut into five micrometer thick sections with Polycut 2500 S Microtome (Reichert-Jung, Nussloch, Germany). Per biopsy, on three evenly spaced sections a Goldner trichrome staining[24] and a Tartrate Resistant Acid Phosphatase (TRAP) reaction was performed.[25] Goldner's trichrome staining colors osteoid and demineralized bone matrix red, mineralized bone matrix blue and nuclei dark blue. The TRAP activity reaction identifies osteoclasts by staining TRAP positive cells red while mineralized bone matrix and connective tissue was counterstained by light green.

*Histomorphometrical analysis*

Bone samples were blinded by encoding. Histomorphometry was used to determine parameters of bone turnover. Histomorphometry measurements were performed automatically using NIS-Elements AR 4.10.01 (Nikon GmbH, Düsseldorf, Germany) at 40x magnification, according to the ASBMR nomenclature.[26,27] Osteoid volume (osteoid volume/bone volume OV/BV; %) and osteoid surface (osteoid surface/bone surface OS/BS; %) were measured as parameters associated with bone formation. Bone resorption was assessed as osteoclast number per millimeter bone surface (n.Ocl/BS; /mm), which was measured manually, using the digital ROI's as reference. All

measurements were performed by a single investigator (HD). Ten random samples were analyzed by two independent observers (HvE, HD). Interobserver variance was less than 5%.

*Estimation of local radiation dose*

To estimate the local radiation dose at the site of the dental implant (Dmax) in patients treated with intensity modulated radiotherapy (IMRT), the radiotherapy treatment planning CT image was merged with a postoperative cone-beam CT (CBCT) image. In this way the point dose (Dmax) administered at the site of the implant (corresponding with the site of the biopsy) was estimated. In patients who were treated with conventional conformal 3D radiotherapy, the radiotherapist estimated the dose based on the treatment plans. Two patients were treated with radiotherapy in hospitals outside the Amsterdam University Medical Centers. The total radiation dose administered was recorded in their charts. Despite efforts to contact these hospitals to gather detailed treatment plans (and planning CT scans), this information could not be retrieved. Therefore, in these two patients, the Dmax could not be estimated.

*Statistical analysis*

Correlations between micro-CT, histomorphometrical parameters and clinical data were analyzed with correlation coefficients and non-parametric tests. Mann Whitney non-parametric test were used to compare the median of the parameters against the hypothetical value 1.0 (no difference in parameter between two groups; irradiated/non-irradiated, $<50$ Gy and $\geq 50$ Gy). Spearman's correlation coefficient was used to analyze relations between the bone turnover and microarchitectural parameters with radiation dose and time interval between last radiation dose and biopsy. All statistical analyses were performed using SPSS software (version 22). A p-value of $<0.05$ was considered statistically significant.

## RESULTS

The irradiated group consisted of 27 edentulous patients (18 males and 9 females; age range 52-81 years, mean age 65 years). The control group consisted of 35 edentulous patients (18 males and 17 females; age range 34-79 years, mean age 65 years). Patient

and treatment characteristics of the irradiated group are summarized in Table 1. The mean total radiation dose (n=27) was 66 Gy (range 54-70 Gy) and the mean Dmax (n=25) was 41 Gy (range 3-70 Gy). The mean interval between radiotherapy and biopsy was 47 months (range 10-199 months). The irradiated group was subdivided in a group with Dmax <50 Gy and ≥50 Gy. In Table 2 the patient characteristics of the four (sub) groups are summarized.

The histological measurements of the irradiated patients versus non-irradiated (control) patients are summarized in Table 3. Interobserver variance for the histological measurements was less than 5%. A significant decrease was seen in all parameters in the irradiated group (Figures 1a-c). No correlations with Dmax or interval between radiotherapy and biopsy were observed.

The micro-CT measurements of the irradiated patients versus non-irradiated (control) patients are summarized in Table 4. Trabecular separation was higher and trabecular number was lower in the irradiated group. A higher Dmax was associated positively with trabecular thickness (Spearman correlation r = 0.470, p = 0.018) and negatively with trabecular separation (Spearman correlation r = -0.526, p =0 .007) (Figures 2A and B). No correlation between interval between radiotherapy and any of the measured parameters was observed.

Because the radiation dose influenced the bone structural outcomes, micro-CT data were divided among a group irradiated with Dmax <50 Gy and a group irradiated with Dmax ≥50 Gy next to bone samples from the control group, (Figures 3A-F). The group irradiated with <50 Gy had higher bone mineral density, lower connectivity density, lower trabecular number and higher trabecular separation compared to non-irradiated controls. The group irradiated with <50 Gy had lower bone volume, lower trabecular number and higher trabecular separation compared to and the group irradiated with ≥50 Gy. No significant differences were observed between the control group and the group irradiated with ≥50 Gy.

Table 1. Patient and treatment characteristics of the irradiated group (N=27).

| Age/gender | Tumor site | RT-technique | RT dose total (Gy) | RT Dmax (Gy) | Interval RT – biopsy (months) |
|---|---|---|---|---|---|
| 64/Female | Floor of mouth | IMRT | 70 | 70 | 16 |
| 69/Male | Nasopharynx | IMRT | 70 | 15 | 72 |
| 51/Male | Floor of mouth | IMRT | 56 | 56 | 13 |
| 74/Male | Floor of mouth | 3D-CRT | 55 | 55 | 199 |
| 73/Female | Base of tongue | IMRT | 70 | 35 | 21 |
| 63/Female | Floor of mouth | IMRT | 56 | 58 | 18 |
| 61/female | Uvula | IMRT | 70 | 32 | 16 |
| 54/Male | Oral tongue | IMRT | 70 | 66 | 85 |
| 64/Male | Soft palate | IMRT | 70 | 32 | 23 |
| 63/Male | Supraglottic larynx | IMRT | 70 | n.a.[a] | 171 |
| 63/Male | Lip | IMRT | 54 | 53 | 11 |
| 81/Female | Floor of mouth | IMRT | 66 | 62 | 10 |
| 67/Male | Soft palate | IMRT | 70 | 18 | 44 |
| 68/Female | Tonsil | IMRT | 70 | 31 | 24 |
| 67/Female | Retromolar trigone | IMRT | 66 | 57 | 10 |
| 76/Male | Base of tongue | IMRT | 70 | 39 | 31 |
| 58/Male | Tonsil | IMRT | 70 | 34 | 13 |
| 70/Male | Floor of mouth | IMRT | 66 | 51 | 17 |
| 68/Male | Pharyngeal arch | IMRT | 60 | 3 | 13 |
| 61/Female | Oral tongue | IMRT | 70 | n.a.[a] | 88 |
| 71/Male | Oropharynx | IMRT | 70 | 25 | 30 |
| 74/Male | Tonsil | IMRT | 70 | 41 | 70 |
| 69/Male | Submandibular gland | IMRT | 56 | 63 | 10 |
| 58/Male | Supraglottic larynx | IMRT | 70 | 13 | 28 |

Table 1. Patient and treatment characteristics of the irradiated group (N=27). *(Continued)*

| Age/gender | Tumor site | RT-technique | RT dose total (Gy) | RT Dmax (Gy) | Interval RT – biopsy (months) |
|---|---|---|---|---|---|
| 62/Male | Base of tongue | 3D-CRT | 62,5 | 50 | 197 |
| 56/Male | Hypopharynx | IMRT | 70 | 18 | 17 |
| 58/Female | Oral tongue | IMRT | 66 | 57 | 23 |

Abbreviations: 3D-CRT, 3-dimensional conformal radiotherapy; IMRT, intensity-modulated radiotherapy; n.a. not available; Dmax, maximum radiation dose at biopsy site

[a] From 2 patients radiotherapy treatment plans could not be retrieved.

Table 2. Patient characteristics of control group and irradiated groups.

| | Control (n=35) | Irradiated (n=27) | Irradiated <50 Gy (n=13) | Irradiated ≥50 Gy (n=12) |
|---|---|---|---|---|
| Gender *m:f* | 18:17 | 18:9 | 10:3 | 7:5 |
| Age, in years (median; *min-max*) | 65; *34-79* | 65; *51-81* | 68; *56-76* | 64; *51-81* |
| Time interval last RT and biopsy, in months (median; *min-max*) | n.a. | 23; *10-199* | 24; *13-72* | 17; *10-199* |

Abbreviations: RT, radiotherapy; n.a., not applicable

Table 3. Histomorphometry measurements of non-irradiated versus irradiated mandibular trabecular bone.

| Histomorphometry measurement | Unit | Control (n=35) Median (IQR) | Irradiated (n=27) Median (IQR) | p[a] |
|---|---|---|---|---|
| Osteoid Surface | **OS/BS (%)** | 16.51 (32.4) | 0.772 (2.17) | <0.0001 |
| Osteoid Volume | **OV/BV (%)** | 1.36 (5.71) | 0.066 (0.168) | <0.0001 |
| Osteoclast Number | **NOc/BS (/mm$^2$)** | 0.298 (0.562) | 0.026 (0.123) | <0.0001 |

Abbreviations: IQR, interquartile range.

a Mann Whitney U test P-value

* significant at <0.05 level

Table 4. Micro-CT measurements of non-irradiated versus irradiated mandibular trabecular bone.

| Micro-CT measurement | Unit | Control group (n=35) Median (IQR) | Irradiated group (n=27) Median (IQR) | p[a] |
|---|---|---|---|---|
| Bone volume fraction | **BV/TV (%)** | 33 (14.8) | 30 (19.1) | 0.634 |
| Bone mineral density | **BMD (mg HA/cm$^3$)** | 945 (106) | 952 (98) | 0.073 |
| Connectivity density | **Conn. Dens** | 6.27 (8.50) | 5.08 (6.85) | 0.158 |
| Trabecular number | **Tb.N (1/mm$^{-1}$)** | 1.94 (.67) | 1.63 (0.63) | 0.012* |
| Trabecular thickness | **Tb.Th (µm)** | 0.251 (0.06) | 0.240 (0.10) | 0.848 |
| Trabecular separation | **Tb.Sp (µm)** | 0.543 (0.18) | 0.626 (0.24) | 0.038* |

Abbreviations: IQR, interquartile range.

[a] Mann Whitney U test P-value

* significant at <0.05 level

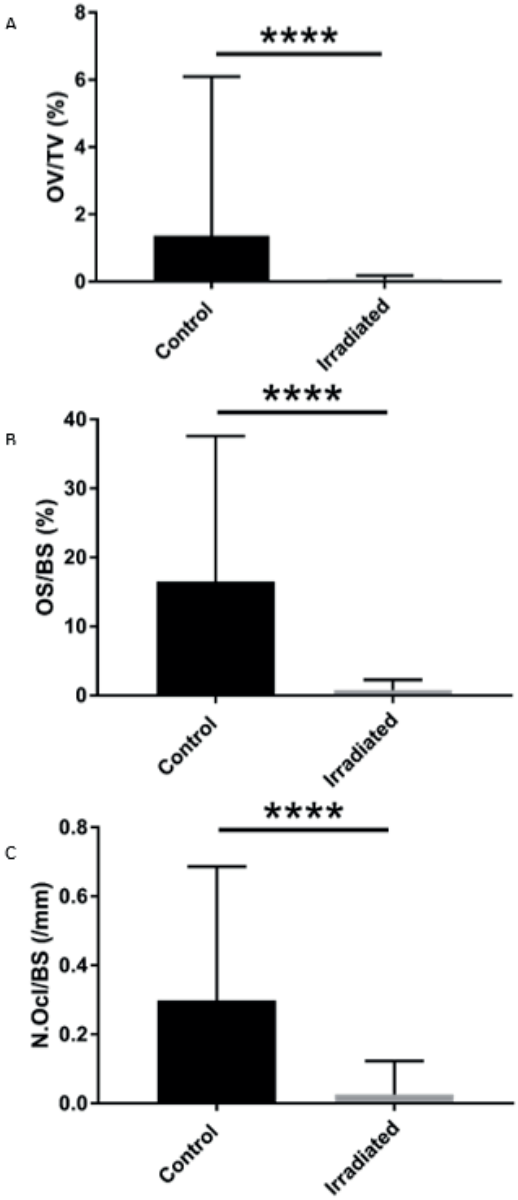


Figure 1.

A. Osteoid volume fraction (OV/TV) in control and irradiated group (Mann Whitney *U* test; P<0,001).

B. Osteoid surface fraction (OS/BS) in control and irradiated group (Mann Whitney *U* test; P<0,001).

C. Osteoclasts per millimeter bone surface (N.Ocl/BS) in control and irradiated group (Mann Whitney *U* test; P<0,001).

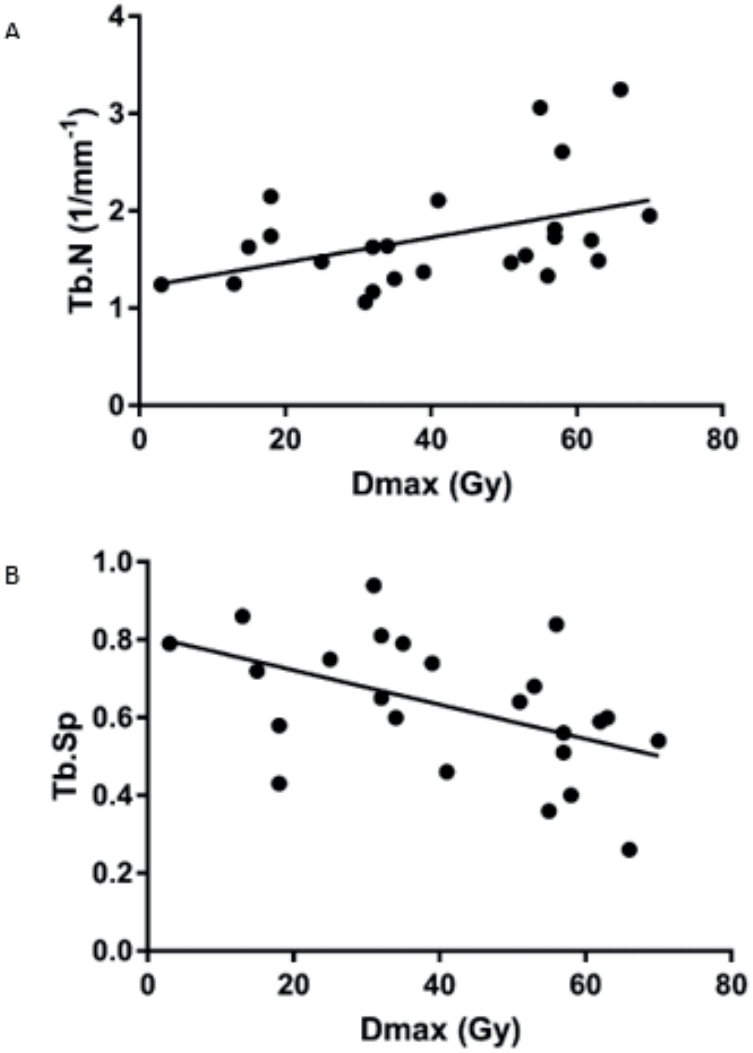


Figure 2.

A. Correlation between radiation dose at biopsy site (Dmax, in Gray) and trabecular number (Tb.N) (Spearman's correlation R=0.470, P=0.018).

B. Correlation between radiation dose at biopsy site (Dmax, in Gray) and trabecular separation (Tb.Sp) (Spearman's correlation R=-0.526, P=0.007).

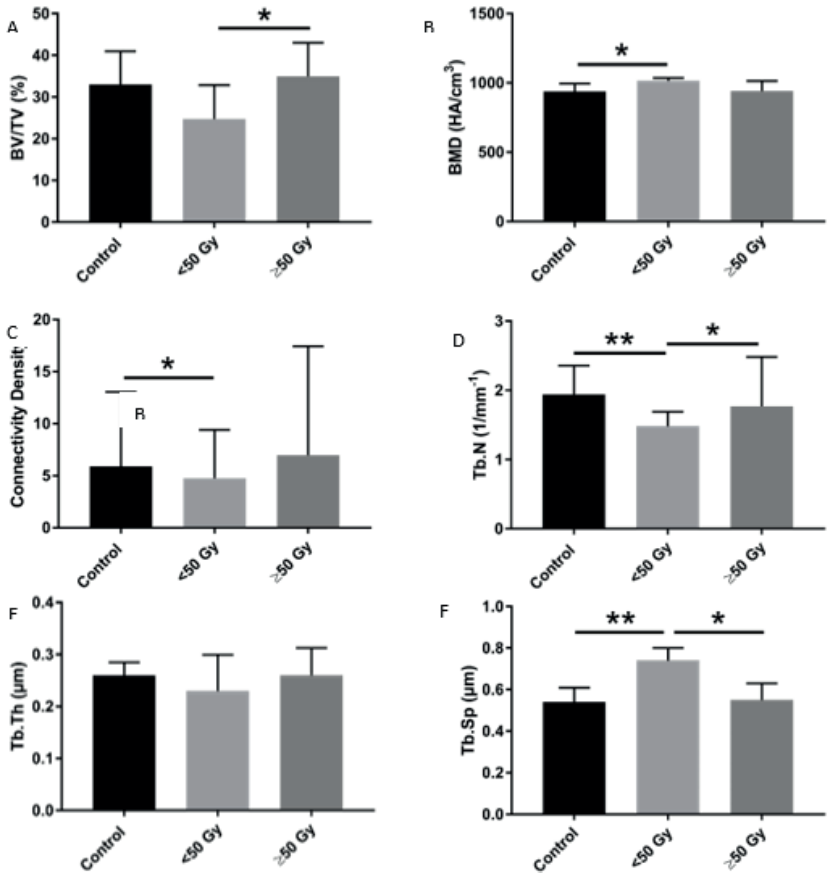


Figure 3.

A. Bone volume in the control group and groups with Dmax <50 Gy and ≥50 Gy. A significant difference is seen between groups Dmax <50 Gy and ≥50 Gy (Mann Whitney *U* Test, p = 0.014).

B. Bone mineral density in the control group and groups Dmax <50 Gy and ≥50Gy. A significant difference is seen between the control group and groups Dmax <50 Gy (Mann Whitney *U* Test, p = 0.03).

C. Connectivity density in the control group and groups Dmax <50 Gy and ≥50 Gy. A significant difference is seen between the control group and groups Dmax <50 Gy (Mann Whitney *U* Test, p = 0.047).

D. Trabecular number in the control group and groups with Dmax <50 Gy and ≥50 Gy. A significant difference is seen between the control group and the groups with Dmax <50 Gy (Mann Whitney *U* Test, p = 0.002) and between the groups with Dmax <50 Gy and ≥50 Gy (Mann Whitney *U* Test, p = 0.035).

E. Trabecular Thickness in the control group and groups with Dmax <50 Gy and ≥50 Gy. No significant differences are observed between the groups.

F. Trabecular separation in the control group and groups Dmax <50 Gy and ≥50 Gy. A significant difference is seen between the control group and the groups with Dmax <50 Gy (Mann Whitney *U* Test, p = 0.005) and between the groups with Dmax <50 Gy and ≥50 Gy (Mann Whitney *U* Test, p = 0.014).

# DISCUSSION

This study showed that radiotherapy dramatically reduces bone turnover, which results in deterioration of trabecular microarchitecture, only in bone irradiated with a Dmax <50 Gy. All irradiated specimens showed a dramatic decrease in bone turnover with no apparent relationship with Dmax or time after radiotherapy.

Our findings on the effects of irradiation on mandibular bone structure and turnover have also been investigated in animal studies, in which mandibular ORN was induced by a mandibular defect caused by a dental extraction or surgical trauma shortly after irradiation.[28-32] In these models micro-CT and histological analysis show impaired bone formation with low bone volumes at mandibular defect sites with increased osteoclastic activity. The single dose regimens and trauma applied shortly after irradiation do not translate well to the head and neck cancer radiation treatment as applied to participants in our study, which uses fractionated dosing schedules and avoids dental extractions and oral surgery during or shortly after irradiation therapy. Furthermore, the animal models focus on bone regeneration after bone defects in irradiated sites rather than bone turnover of non-injured irradiated bone, the latter being the clinical starting point in the development of ORN in most patients.

In this study a low number of osteoclasts was observed in the irradiated patients, which indicates bone resorption is decreased by irradiation. This is in contrast to studies in rodent models where ionizing radiation (IR) induced bone loss.[33] In these studies usually the limbs are investigated. IR induced bone loss is thought to be caused by increased osteoclastogenesis in response to radiation induced osteocyte death. However, in vitro studies have shown that osteoclastogenesis was accelerated at relatively low-dose, but inhibited at higher doses of irradiation.[34,35]

Our study showed a significant difference with a threshold value of 50 Gy radiation dose in trabecular number and trabecular separation. In specimens with Dmax <50 Gy trabecular number was lower and trabecular separation was higher than in specimens with Dmax ≥50 Gy and non-irradiated controls. Radiotherapy disrupts the balance of bone remodeling by affecting the different bone cells, which vary in radiosensitivity. As

a possible interpretation of our findings, it could be speculated that a decreased bone resorption could protect against deterioration of microarchitecture in micro-CT measurements. When – above a certain radiation dose – turnover is decreased to an extent that the net resorption and apposition of bone is insufficient to alter the microarchitecture of the bone, this bone will not significantly differ from non-irradiated bone in micro-CT measurements. However, this bone is pathological in the sense, that it has no capacity to remodel and renew itself and could play a role in the pathogenesis of ORN when areas of this bone become void of osteocytes and essentially non-vital due to radiation induced osteocyte death, ageing or local injury. In the literature, a cutoff point of 50 Gy local radiation dose is commonly accepted to identify patients at risk for developing ORN.[36,37] During the planning of the radiotherapy, especially in intensity modulated radiotherapy, this 50 Gy threshold could be of relevance and, if possible, an effort to keep the doses on the mandible below this value should be pursued.



Patients in our study that received more than 50 Gy on the anterior mandible prior to dental implant placement have been administered HBO therapy as a prophylactic measure for ORN, because a radiation dose of 50 Gy or more is a known risk factor for developing ORN. However, in the present study HBO could act as a confounder. Literature on the effect of HBO on bone turnover and micro-architecture in irradiated mandibles is scarce though, and solely reported from animal studies. Spiegelberg et al.[38] demonstrated that HBO therapy positively influenced the micro-architectural parameters of irradiated mandibular trabecular bone in mice. HBO completely normalized values for BV/TV, trabecular separation, trabecular thickness and porosity in irradiated bone, but trabecular number remained significantly increased in irradiated bone. Bone histology showed a lower number of empty lacunae and a decrease in osteoclast number in the HBO group compared to the non-HBO group. Radiotherapy increased the osteoclast number compared to controls, which does not correspond with our findings, which showed a near absence of osteoclasts in all irradiated specimens. This animal model, however, studied acute response after a single dose, biologically equivalent to a cumulative dose of 32 Gy. Hence, caution must be taken when comparing results from animal studies with human studies.

Few studies on irradiated mandibular bone in humans have been reported. Several authors have made an attempt to differentiate between ORN, MRONJ and osteomyelitis histologically,[18,20,21] but with conflicting results on the presence of osteoclasts. Shuster and Marx found a complete absence of osteoclasts in ORN whereas De Antoni did find osteoclasts in ORN lesions. Støre et al. studied the number of resorption areas and regeneration areas in microradiographs from cortical bone from mandibular ORN lesions, irradiated non-ORN mandibles and non-irradiated mandibles.[17] Irradiated and non-irradiated mandibular cortical bone showed no resorption and regeneration areas whereas ORN cortical bone showed increased resorption and regeneration areas which further increased in ORN specimens subjected to HBO.

The absence of an association between dose and bone turnover parameters whilst the microarchitecture parameters do reflect clear relation with radiation dose is a paradoxical finding. Micro-CT data reflect the result of remodeling over a longer period of time, whereas histomorphometric bone turnover indices are a snapshot of the continuous process of bone apposition and resorption. Bone turnover is dramatically decreased in irradiated bone samples. Subtle trends in the very low and frequently absent osteoid volumes and osteoclast numbers may be missed due to the small bone surface measures and the relatively small sample size of the study group.

Radiation damage to mandibular bone tissue is a dynamic and multifactorial process, which makes it difficult to investigate this process, especially in humans. Most studies on radiation damage to (mandibular) bone have been performed in animal models, with standardized conditions, such as similar radiation doses, methods of administration and time interval between radiotherapy and sacrifice. Obviously, such a design is not possible in humans which means there are limitations to this study that need to be addressed. Dental implant placement in irradiated patients in our department is performed following specific treatment protocols that for ethical reasons cannot be applied to healthy individuals. The protocollar administration of HBO is only indicated for patients with a dose of ≥50 Gy on the anterior mandible, patients with lower doses could therefore not be treated in this protocol.

The control group consists of healthy edentulous individuals and the irradiated group consists of patients with a history of head and neck cancer. Since head and neck cancer is known to have a strong association with alcohol and tobacco use, these two groups may not be comparable with regard to smoking and drinking habits.

The implant treatment in irradiated patients is different from the control group with regard to the antibiotic prophylactic treatment in the irradiated group, the placement of four instead of two implants and the surgical procedure under general anesthesia versus local anesthesia. In the irradiated group, there is a heterogeneity in tumor localization, radiation dose and time interval between radiotherapy and biopsy.

As mentioned before, HBO was administered in the group irradiated with ≥50 Gy which may impair the comparability of the patients irradiated with Dmax of ≥50 Gy and Dmax of <50 Gy . Although a recent review showed there was no consistent evidence for support of HBO in prevention or management of ORN, we cannot exclude HBO was a confounder in our analysis.[39]



A methodological limitation is the weekly calibration with a phantom instead of scanning all samples with a phantom. However the micro-CT calibration with 800 en 2600 mg HA/cm3 phantoms consistently show these densities over time. We therefore believe our quantitative measurements are reliable.

To better understand the mechanisms of irradiation damage to bone and ORN, the contribution of bone microarchitecture and turnover should be further explored. Studies investigating the role of bone remodeling in the pathophysiology of ORN at a cellular level are underrepresented in the literature. Future research should further focus on this topic. In order to unravel the direct effect of irradiation on cells of the bone remodeling system and the consequential effect on bone microarchitecture in the mandible, preclinical studies focusing on these mechanisms should be performed.

## CONCLUSIONS

Radiotherapy dramatically decreases bone turnover in human mandibles, which leads to deterioration of trabecular microarchitecture in bone with a Dmax of <50 Gy. The effect of variety in radiosensitivity of the different bone cells on intercellular processes may disrupt bone turnover in different ways with increasing radiation dose. The 50 Gy value seems to be a critical threshold to where the effects of the radiation are more detrimental.

## ACKNOWLEDGEMENTS

The authors are grateful to Erik Phernambucq and Derek Rietveld, radiotherapists in Amsterdam UMC, location VUmc, for the radiation dose estimation and to Astrid Vreke for her valuable laboratory work and input in this study.

# REFERENCES


1. Moon DH, Moon SH, Wang K, et al. Incidence of, and risk factors for, mandibular osteoradionecrosis in patients with oral cavity and oropharynx cancers. Oral Oncol 2017;72:98-103. DOI: 10.1016/j.oraloncology.2017.07.014.
2. Chrcanovic BR, Reher P, Sousa AA, Harris M. Osteoradionecrosis of the jaws--a current overview--part 1: Physiopathology and risk and predisposing factors. Oral Maxillofac Surg 2010;14(1):3-16. DOI: 10.1007/s10006-009-0198-9.
3. De Felice F, Musio D, Tombolini V. Osteoradionecrosis and intensity modulated radiation therapy: An overview. Crit Rev Oncol Hematol 2016;107:39-43. DOI: 10.1016/j.critrevonc.2016.08.017.
4. Vissink A, Jansma J, Spijkervet FK, Burlage FR, Coppes RP. Oral sequelae of head and neck radiotherapy. Crit Rev Oral Biol Med 2003;14(3):199-212. (https://www.ncbi.nlm.nih.gov/pubmed/12799323).
5. Marx RE. Osteoradionecrosis: a new concept of its pathophysiology. J Oral Maxillofac Surg 1983;41(5):283-8. (https://www.ncbi.nlm.nih.gov/pubmed/6572704).
6. Delanian S, Lefaix JL. The radiation-induced fibroatrophic process: therapeutic perspective via the antioxidant pathway. Radiother Oncol 2004;73(2):119-31. DOI: 10.1016/j.radonc.2004.08.021.
7. Schultze-Mosgau S, Lehner B, Rodel F, et al. Expression of bone morphogenic protein 2/4, transforming growth factor-beta1, and bone matrix protein expression in healing area between vascular tibia grafts and irradiated bone-experimental model of osteonecrosis. Int J Radiat Oncol Biol Phys 2005;61(4):1189-96. DOI: 10.1016/j.ijrobp.2004.12.008.
8. Fenner M, Park J, Schulz N, et al. Validation of histologic changes induced by external irradiation in mandibular bone. An experimental animal model. J Craniomaxillofac Surg 2010;38(1):47-53. DOI: 10.1016/j.jcms.2009.07.011.
9. Zhang WB, Zheng LW, Chua DT, Cheung LK. Expression of bone morphogenetic protein, vascular endothelial growth factor, and basic fibroblast growth factor in irradiated mandibles during distraction osteogenesis. J Oral Maxillofac Surg 2011;69(11):2860-71. DOI: 10.1016/j.joms.2010.12.037.
10. Wurzler KK, DeWeese TL, Sebald W, Reddi AH. Radiation-induced impairment of bone healing can be overcome by recombinant human bone morphogenetic protein-2. J Craniofac Surg 1998;9(2):131-7. DOI: 10.1097/00001665-199803000-00009.
11. Springer IN, Niehoff P, Acil Y, et al. BMP-2 and bFGF in an irradiated bone model. J Craniomaxillofac Surg 2008;36(4):210-7. DOI: 10.1016/j.jcms.2007.09.001.
12. Zhang WB, Zheng LW, Chua DT, Cheung LK. Treatment of irradiated mandibles with mesenchymal stem cells transfected with bone morphogenetic protein 2/7. J Oral Maxillofac Surg 2012;70(7):1711-6. DOI: 10.1016/j.joms.2012.01.022.
13. Jin IG, Kim JH, Wu HG, Kim SK, Park Y, Hwang SJ. Effect of bone marrow-derived stem cells and bone morphogenetic protein-2 on treatment of osteoradionecrosis in a rat model. J Craniomaxillofac Surg 2015;43(8):1478-86. DOI: 10.1016/j.jcms.2015.06.035.
14. Janus JR, Jackson RS, Lees KA, et al. Human Adipose-Derived Mesenchymal Stem Cells for Osseous Rehabilitation of Induced Osteoradionecrosis: A Rodent Model. Otolaryngol Head Neck Surg 2017;156(4):616-621. DOI: 10.1177/0194599816688647.
15. Bras J, de Jonge HK, van Merkesteyn JP. Osteoradionecrosis of the mandible: pathogenesis. Am J Otolaryngol 1990;11(4):244-50. (https://www.ncbi.nlm.nih.gov/pubmed/2240412).
16. McGregor AD, MacDonald DG. Post-irradiation changes in the blood vessels of the adult human mandible. Br J Oral Maxillofac Surg 1995;33(1):15-8. (https://www.ncbi.nlm.nih.gov/pubmed/7536468).
17. Store G, Granstrom G. Osteoradionecrosis of the mandible: a microradiographic study of cortical bone. Scand J Plast Reconstr Surg Hand Surg 1999;33(3):307-14. (https://www.ncbi.nlm.nih.gov/pubmed/10505444).

**18.** Marx RE, Tursun R. Suppurative osteomyelitis, bisphosphonate induced osteonecrosis, osteoradionecrosis: a blinded histopathologic comparison and its implications for the mechanism of each disease. Int J Oral Maxillofac Surg 2012;41(3):283-9. DOI: 10.1016/j.ijom.2011.12.016.

**19.** Curi MM, Cardoso CL, de Lima HG, Kowalski LP, Martins MD. Histopathologic and Histomorphometric Analysis of Irradiation Injury in Bone and the Surrounding Soft Tissues of the Jaws. J Oral Maxillofac Surg 2016;74(1):190-9. DOI: 10.1016/j.joms.2015.07.009.

**20.** De Antoni CC, Matsumoto MA, Silva AAD, et al. Medication-related osteonecrosis of the jaw, osteoradionecrosis, and osteomyelitis: A comparative histopathological study. Braz Oral Res 2018;32:e23. DOI: 10.1590/1807-3107bor-2018.vol32.0023.

**21.** Shuster A, Reiser V, Trejo L, Ianculovici C, Kleinman S, Kaplan I. Comparison of the histopathological characteristics of osteomyelitis, medication-related osteonecrosis of the jaw, and osteoradionecrosis. Int J Oral Maxillofac Surg 2018. DOI: 10.1016/j.ijom.2018.07.002.

**22.** Nuzzo S, Peyrin F, Cloetens P, Baruchel J, Boivin G. Quantification of the degree of mineralization of bone in three dimensions using synchrotron radiation microtomography. Med Phys 2002;29(11):2672-81. DOI: 10.1118/1.1513161.

**23.** Mulder L, Koolstra JH, Van Eijden TM. Accuracy of microCT in the quantitative determination of the degree and distribution of mineralization in developing bone. Acta Radiol 2004;45(7):769-77. (https://www.ncbi.nlm.nih.gov/pubmed/15624521).

**24.** Goldner J. A modification of the masson trichrome technique for routine laboratory purposes. Am J Pathol 1938;14(2):237-43. (https://www.ncbi.nlm.nih.gov/pubmed/19970387).

**25.** van de Wijngaert FP, Burger EH. Demonstration of tartrate-resistant acid phosphatase in un-decalcified, glycolmethacrylate-embedded mouse bone: a possible marker for (pre)osteoclast identification. J Histochem Cytochem 1986;34(10):1317-23. DOI: 10.1177/34.10.3745910.

**26.** Parfitt AM, Drezner MK, Glorieux FH, et al. Bone histomorphometry: standardization of nomenclature, symbols, and units. Report of the ASBMR Histomorphometry Nomenclature Committee. J Bone Miner Res 1987;2(6):595-610. DOI: 10.1002/jbmr.5650020617.

**27.** Dempster DW, Compston JE, Drezner MK, et al. Standardized nomenclature, symbols, and units for bone histomorphometry: a 2012 update of the report of the ASBMR Histomorphometry Nomenclature Committee. J Bone Miner Res 2013;28(1):2-17. DOI: 10.1002/jbmr.1805.

**28.** Cohen M, Nishimura I, Tamplen M, et al. Animal model of radiogenic bone damage to study mandibular osteoradionecrosis. Am J Otolaryngol 2011;32(4):291-300. DOI: 10.1016/j.amjoto.2010.06.001.

**29.** Tamplen M, Trapp K, Nishimura I, et al. Standardized analysis of mandibular osteoradionecrosis in a rat model. Otolaryngol Head Neck Surg 2011;145(3):404-10. DOI: 10.1177/0194599811400576.

**30.** Xu J, Zheng Z, Fang D, et al. Early-stage pathogenic sequence of jaw osteoradionecrosis in vivo. J Dent Res 2012;91(7):702-8. DOI: 10.1177/0022034512448661.

**31.** Damek-Poprawa M, Both S, Wright AC, Maity A, Akintoye SO. Onset of mandible and tibia osteoradionecrosis: a comparative pilot study in the rat. Oral Surg Oral Med Oral Pathol Oral Radiol 2013;115(2):201-11. DOI: 10.1016/j.oooo.2012.09.008.

**32.** Jackson RS, Voss SG, Wilson ZC, et al. An Athymic Rat Model for Mandibular Osteoradionecrosis Allowing for Direct Translation of Regenerative Treatments. Otolaryngol Head Neck Surg 2015;153(4):526-31. DOI: 10.1177/0194599815593278.

**33.** Zhang J, Qiu X, Xi K, et al. Therapeutic ionizing radiation induced bone loss: a review of in vivo and in vitro findings. Connect Tissue Res 2018;59(6):509-522. DOI: 10.1080/03008207.2018.1439482.

**34.** Zhang J, Wang Z, Wu A, et al. Differences in responses to X-ray exposure between osteoclast and osteoblast cells. J Radiat Res 2017;58(6):791-802. DOI: 10.1093/jrr/rrx026.

**35.** Zhai J, He F, Wang J, Chen J, Tong L, Zhu G. Influence of radiation exposure pattern on the bone injury and osteoclastogenesis in a rat model. Int J Mol Med 2019;44(6):2265-2275. DOI: 10.3892/ijmm.2019.4369.

**36.** Tsai CJ, Hofstede TM, Sturgis EM, et al. Osteoradionecrosis and radiation dose to the mandible in patients with oropharyngeal cancer. Int J Radiat Oncol Biol Phys 2013;85(2):415-20. DOI: 10.1016/j.ijrobp.2012.05.032.

**37.** Tatum SA, Theler JM. Principles and practice of craniofacial bone healing. In: Sataloff RT, Sclafani AP, eds. Sataloff's Comprehensive Textbook of Otolaryngology: Head & Neck Surgery: Facial Plastic and Reconstructive Surgery 1ed. New Delhi: Jaypee Brothers,Medical Publishers Pvt. Limited; 2016:913-928.

**38.** Spiegelberg L, Braks JA, Groeneveldt LC, Djasim UM, van der Wal KG, Wolvius EB. Hyperbaric oxygen therapy as a prevention modality for radiation damage in the mandibles of mice. J Craniomaxillofac Surg 2015;43(2):214-9. DOI: 10.1016/j.jcms.2014.11.008.

**39.** Sultan A, Hanna GJ, Margalit DN, et al. The Use of Hyperbaric Oxygen for the Prevention and Management of Osteoradionecrosis of the Jaw: A Dana-Farber/Brigham and Women's Cancer Center Multidisciplinary Guideline. Oncologist 2017;22(11):1413. DOI: 10.1634/theoncologist.2016-0298erratum.

# 6

# Osteocyte apoptosis, bone marrow adiposity and fibrosis in the irradiated human mandible

Hannah Dekker, Engelbert A.J.M. Schulten, Inez Lichters, Leo van Ruijven, Huib W. van Essen, Gerrit J. Blom, Elisabeth Bloemena, Christiaan M. ten Bruggenkate, Arja M. Kullaa, Nathalie Bravenboer

**Published in:** Advances in Radiation Oncology 2022; 7: 10096

# ABSTRACT

To assess the effect of radiotherapy on osteocyte apoptosis, osteocyte death and bone marrow adipocytes in the human mandible and its contribution to the pathophysiology of radiation damage to the mandibular bone.

Mandibular trabecular bone biopsies were taken from irradiated patients and non-irradiated controls. Immunohistochemical detection of cleaved caspase-3 was performed to visualize apoptotic osteocytes. The number of apoptotic osteocytes per bone area (N.Pos.Ot/B.Ar; /mm²) and per total amount of osteocytes (N.Pos.Ot/N.Tt.Ost; %), osteocytes per bone area (N.Ot/B.Ar; /mm²) and empty lacunae per bone area (N.e.Lc/B.Ar; /mm²) were counted manually. The percentage fibrotic tissue and adipose tissue per bone marrow area (Fb.T.Ar/Ma.Ar; %, Ad.T.Ar/Ma.Ar; %), the percentage bone marrow of total area (Ma.Ar/Tt.Ar; %) and the mean adipocyte diameter (μm) was determined digitally from adjacent Goldner stained sections.

Biopsies of 15 irradiated patients (12 males and 3 females) and 7 non-irradiated controls (5 males and 2 females) were assessed. In the study group a significant increase was seen in the number of empty lacunae, the percentage of adipose tissue of bone marrow area and the adipocyte diameter. There was no significant difference in bone marrow fibrosis nor apoptotic osteocytes between the irradiated group and the controls.

Irradiation alone does not seem to induce excessive bone marrow fibrosis. The damage to bone mesenchymal stem cells leads to increased marrow adipogenesis and decreased osteoblastogenic potential. Early osteocyte death resulting in avital persisting bone matrix with severely impaired regenerative potential may contribute to the vulnerability of irradiated bone to infection and necrosis.

# INTRODUCTION

Osteoradionecrosis (ORN) of the jaw is a serious complication of radiotherapy in head and neck cancer patients. To date, the events leading up to radiation-induced bone damage and ORN have not been fully elucidated.[1] The primary findings of radiation damage to bone is local tissue atrophy, loss of functional osteoblasts, marrow adiposity and microvascular impairments.[2] The resulting effect of these independent findings on bone homeostasis and regeneration capacity is not clear.

Many theories on the pathophysiology of ORN of the jaw have been proposed. In 1983, Marx proposed the well-known hypothesis which states that irradiation leads to a sequence of hypoxic-hypocellular-hypovascular tissue, tissue breakdown and chronic non-healing wound.[3] Marx found progressive loss of capillaries and fibrosis of marrow spaces in irradiated mandibular bone. His theory formed the cornerstone for the hyperbaric oxygen treatment, although its clinical efficacy is controversial.[4,5] Delanian and Lefaix postulated another well-established theory in 2011, stating that ORN occurs because of a radiation-induced fibro-atrophic mechanism, including free radical formation, endothelial dysfunction, inflammation, microvascular thrombosis, fibrosis and remodeling, and finally bone and tissue necrosis.[6] A possible role for osteoclast deficiency as crucial mechanism in the pathophysiology of ORN has been proposed by several authors, arising from the resemblance with medication-related osteonecrosis of the jaw (MRONJ) that is typically caused by drugs that inhibit osteoclast function.[7,8]

In the past decades, the view on the role of osteocytes and bone marrow adipocytes have changed from silent bystander to having their own important role in bone metabolism. Osteocytes are formed during bone formation when osteoblasts are encapsulated in the bone matrix and play a critical role in regulating bone turnover.[9] A canicular network in the bone matrix enables communication between osteocytes and the cells on the bone surface, which is essential for the regulation of osteoblasts and osteoclasts.[10] The adaptation of bone in relation to mechanical forces has been largely investigated and osteocytes are thought to have a function as mechanosensors.[11] Osteocytes produce receptor activator of nuclear factor-κB ligand (RANKL) that stimulates differentiation of osteoclasts.[10,12,13] Apoptotic death of osteocytes is thought

to be a critical event in the recruitment of osteoclasts to sites where bone resorption is needed, such as areas of fatigue damage, estrogen deficiency, skeletal unloading and possibly other states that necessitate bone to be removed.[14]

Marrow adipocytes originate from the mesenchymal stem cells, alike osteoblasts. Studies have shown that increased bone marrow adiposity is associated with diseases such as osteoporosis, obesity and diabetes and is often associated with a deterioration of bone mass.[15] An unbalanced shift to adipogenesis in the bone marrow is thought to have detrimental effects on bone through the release of different factors that can promote apoptosis, osteoclastogenesis, alter osteoblastogenesis and favor adipogenesis and release of saturated fatty acids that impair osteoblast function and survival.[16] Irradiation is known to induce bone marrow adipogenesis in postcranial skeletal sites[17] but little is known about this effect in the mandible.

Radiation therapy affects all cells in the targeted area and, therefore, ORN is a multifactorial disease. As the exact pathophysiology of ORN remains unclear, studies targeting on the effect of irradiation on mandibular bone homeostasis and bone marrow composition could provide better insight in the process leading up to ORN. We hypothesize that irradiation alters bone marrow composition and disrupts bone homeostasis on different levels making the bone vulnerable and potentially susceptible for ORN. The present study seeks to evaluate two aspects in the field of bone metabolism that are underrepresented in current literature on mandibular bone radiation damage: osteocyte death and bone marrow adiposity.

## PATIENTS AND METHODS

### *Patients*

Fifteen patients with a history of radiotherapy for head and neck malignancy were compared to seven edentulous patients with no history of oral cancer or radiotherapy. All irradiated patients were edentulous with an indication for oral rehabilitation with mandibular dental implants and were treated between August 1, 2012 and April 1, 2016. Patients without radiation dose on the mandible and patients who had undergone mandibular reconstruction with bone grafts were excluded from this study. Patients in

the control group were treated with dental implants in the mandible between August 1, 2012 and December 31, 2014.

Exclusion criteria were a history of bisphosphonate medication, impaired bone metabolism (e.g. hyperparathyroidism, osteomalacia) or systemic immunosuppressive medication up to three months prior to dental implant surgery. All participants had blood calcium, phosphate, parathyroid hormone and HbA1c levels within the normal range.

All patients were fully informed and signed a written consent form for study participation. Prior to the study, approval for the research was provided by the Medical Ethical Committee of the Amsterdam University Medical Center, location VUmc (registration number 2011/220). All methods were performed in accordance with the relevant guidelines and regulations.

*Hyperbaric oxygen therapy*

In accordance with the department´s protocol, hyperbaric oxygen (HBO) therapy is administered to patients who undergo surgical procedures in the area of the maxilla or mandible that have been irradiated with 50 Gy or more. Edentulous patients typically are treated with two or four dental implants in the interforaminal region of the anterior mandible, to accommodate retention of an overdenture. Therefore, for all irradiated patients the radiotherapist was preoperatively consulted to estimate the maximum radiation dose in the anterior mandible. Patients who had received an estimated dose of 50 Gy or more on the anterior mandible, were treated with 20 sessions HBO therapy preoperatively and 10 sessions postoperatively, according to the 'Marx-protocol'.[3] Thirty HBO sessions were administered on consecutive days excluding the weekends, that is, for a total duration of 6 weeks. Sessions consisted of administration of a total of 80 minutes of 100 per cent oxygen at 243–253 kPa.

*Dental implant surgery and bone biopsy retrieval*

Dental rehabilitation of all patients from the irradiated group was performed in the Amsterdam University Medical Centers, location VUmc, by a single oral and maxillofacial surgeon (ES). Patients in the control group were treated in the Alrijne hospital,

Leiderdorp by a single oral and maxillofacial surgeon (CtB). Dental implants were placed in the interforaminal region of the anterior mandible.

The dental implant surgical procedure was the same in both groups. Implant preparations were made under copious irrigation with a 3.5 mm trephine burr (2.5 mm inner diameter) (Straumann® Dental Implant System, Straumann Holding AG, Basel, Switzerland) to a depth of 10 or 12 mm. An ejector pin was used to carefully remove the bone cylinder from the trephine drill. One bone cylinder (biopsy specimen) per patient was selected and prepared for further analysis.

*Determination of radiation dose*

All 15 patients were treated with intensity modulated radiotherapy (IMRT). To determine the Dmax at the site of the dental implant, the radiotherapy treatment planning CT image was merged with a postoperative cone-beam CT image. In this way the dose administered at the site of the implant (corresponding with the site of the biopsy) was estimated.

Two patients were treated with radiotherapy in clinics outside the Amsterdam University Medical Centers. The total radiation dose was known for these patients. However, despite efforts to contact these clinics to gather the IMRT treatment plans, this information could not be retrieved. Therefore, in these two patients, the Dmax at biopsy site could not be determined. These two patients were only included in comparisons between irradiated and non-irradiated groups but not in the dosimetry statistics.

*Processing and measurements of the bone biopsies*

Bone cylinders were immediately fixed by immersion in 4% phosphate-buffered formaldehyde, dehydrated in ascending series of ethanols, and embedded in 83% methylmethacrylate (BDH Chemicals) supplemented with 17% dibuthylphtalate (Merck), 8 g/L lucidol CH-50L (Akzo Nobel) and 22 µl/10 ml N,Ndimethyl-p-toluidine (Merck). Undecalcified biopsies were cut into sections of 5 µm with a microtome (Polycut 2500 S, Reichert-Jung). Immunohistochemical detection of cleaved caspase-3 was performed to visualize apoptotic osteocytes on two sections per biopsy, spaced by

50 μm. Sections were transferred to poly-l-lysine-coated slides and stained according to the following method:

The sections were deplastificated, rehydrated and decalcified in 1% acidic acid for 10 minutes. Sections were incubated with Saponin (0,05%) in phosphate-buffered saline (PBS) incubation for 30 minutes and 10 minutes with DNAse (3.5 μg/mL DNAse II (Sigma) in 25 mM Tris + 10 mM MgSO4) for antigen retrieval. Endogenous peroxidase was blocked with 3% H2O2 in methanol for 15 minutes. Primary antibody incubation was performed for 3 hours with 1/300 rabbit-anti-cleaved-caspase-3 antibody (Cell Signaling Technology, Beverly, MA) in PBS + 0.05% Tween. Sections were incubated with EnVision-rabbit (Agilent Dako products, Santa Clara, CA) for 1 hour. Staining was performed for 10 minutes with the Nova Red kit (Vector Labs, Burlingame, CA). The sections were counterstained with 10% Toluidine blue in ethanol 60%. Sections were then dehydrated and sealed in DEPEX mounting medium (BDH Chemicals). An adjacent (undecalcified) section was selected for each section, with a maximum distance of 3 sections, and Goldner trichrome staining was performed.[18]

*Histomorphometrical analysis*

Bone samples were analyzed blinded. Bone volume, the number of adipocytes, the total adipose area, the total fibrotic marrow area, the total bone marrow area and the total area of the section was measured in the Goldner section. A Nikon eclipse E800 microscope with 40x magnification and NIS-Elements AR 4.10.01 (Nikon GmbH) to photograph and analyze the sections. From these measurements, the percentage fibrotic tissue of bone marrow area (Fb.T.Ar/Tt.Ar; %) the percentage adipose tissue of bone marrow area (Ad.T.Ar/Ma.Ar; %), the percentage bone marrow of total area of the section (Ma.Ar/Tt.Ar; %) and the mean adipocyte diameter (μm) were calculated. A magnification of x200 was used to count the total number of osteocytes per bone area (N.Ot/B.Ar; /mm²) and total number of empty lacunae per bone area (N.e.Lc/B.Ar; /mm²) in the Goldner sections, and the number of cleaved caspase-3 positive osteocytes per bone area (N.Pos.Ot/B.Ar; /mm²) and the percentage of positive osteocytes per total amount of osteocytes (N.Pos.Ot/N.Tt.Ost; %) in the cleaved caspase-3 sections (Figure 1A and B).

*Statistical analysis*

All statistical analyses were performed using SPSS software (version 25). $P<0.05$ was considered statistically significant. Mann Whitney non-parametric tests were used to compare the median of the parameters against the hypothetical value 1.0 (no difference in parameter between two groups; irradiated/non-irradiated, <50 Gy and ≥50 Gy). Correlations between histomorphometrical parameters and clinical data were analyzed with correlation coefficients and non-parametric tests. Spearman's correlation coefficient was used to analyze relations between the bone turnover and microarchitectural parameters with radiation dose and time interval between last radiation dose and biopsy.

## RESULTS

The characteristics of the irradiated patients are summarized in Table 1. The irradiated group consisted of 12 males and 3 females with a mean age of 66 years (range 56-76). The mean total radiation dose was 66 Gy (range 54-70) and the median Dmax at biopsy site was 39 Gy (range 3-63). The median interval between radiotherapy and biopsy was 24 months (range 10-197). The control group consisted of 5 males and 2 females, with a mean age of 64 (range 34-73). Smoking and drinking habits of irradiated and controls groups are summarized in Table 2.

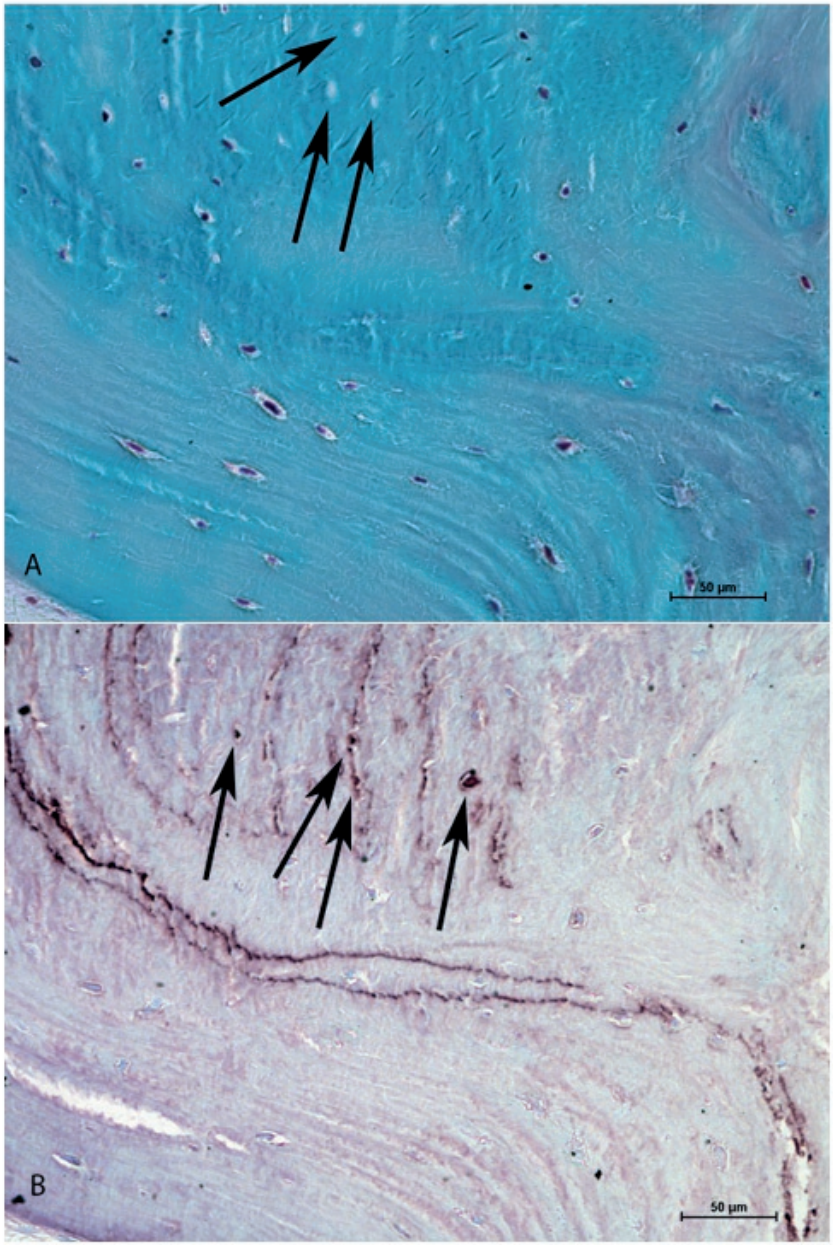


Figure 1. Histological sections (x200 magnification) of irradiated mandibular bone from an irradiated patient (Dmax 34 Gy). A: Goldner trichrome stain. Osteocyte nuclei are stained dark purple. Arrowheads point towards empty lacunae, indicating osteocyte death. B: Cleaved caspase-3 stain. Arrowheads point towards cleaved caspase-3 positive osteocytes, indicating osteocyte apoptosis.

The histological measurements of the irradiated bone versus non-irradiated (control) bone are summarized in Table 3. There was no significant difference in number or percentage of cleaved caspase-3 positive osteocytes between the irradiated group and the controls. The empty lacunae are expressed as number per $mm^2$ bone area. In percentages, this corresponds with a median of 9.7% (range 24.9) of lacunae in the control group and 46.4% (range 48.3) in the irradiated group, which is a significant difference (P=0.007). The percentage of adipose tissue in bone marrow area and the adipocyte diameter were significantly higher in the irradiated group (P=0.007 and P=0.005, respectively) (Figure 2A-C). There was no significant difference in bone marrow fibrosis between irradiated and non-irradiated specimens, although the visual aspect of fibrosis as well as the adipose content in the irradiated samples have a distinct appearance (Figure 3A-D).

No correlations between the histological measurements and Dmax, total radiation dose or time interval between radiotherapy and biopsy were observed. During follow-up, 6 of the irradiated patients died. Of the 9 patients that survived, one was lost to follow-up. The remaining 8 are still in follow-up (years in follow-up mean 5,8; range 4,2-6,7). None of the irradiated patients included in this study developed ORN.

Table 1. Patient and treatment characteristics of the irradiated group (N=15)

| Age/sex | Tumor site | Total RT dose (Gy) | RT Dmax (Gy) | Interval RT – biopsy (months) |
|---|---|---|---|---|
| 69/Male | Submandibular gland | 56 | 63 | 10 |
| 68/Male | Oropharynx | 60 | 3 | 13 |
| 58/Male | Supraglottic larynx | 70 | 13 | 28 |
| 56/Male | Hypopharynx | 70 | 18 | 17 |
| 62/Male | Oropharynx | 62,5 | 50 | 197 |
| 68/Female | Oropharynx | 70 | 31 | 24 |
| 63/Male | Lower lip | 54 | 53 | 11 |
| 63/Male | Supraglottic larynx | 70 | n.a.* | 171 |
| 76/Male | Tongue base | 70 | 39 | 31 |
| 71/Male | Oropharynx | 70 | 25 | 30 |
| 74/Male | Tonsil | 70 | 41 | 70 |
| 58/Male | Tonsil | 70 | 34 | 23 |
| 61/Female | Lateral tongue | 70 | n.a.* | 88 |

Table 1. Patient and treatment characteristics of the irradiated group (N=15) *(Continued)*

| Age/sex | Tumor site | Total RT dose (Gy) | RT Dmax (Gy) | Interval RT – biopsy (months) |
|---|---|---|---|---|
| 70/Male | Floor of mouth | 66 | 51 | 17 |
| 67/Female | Retromolar trigone | 66 | 57 | 10 |

Abbreviations: RT: radiotherapy, Dmax: radiation dose at biopsy site, Gy: Gray, n.a.: not available.

Table 2. Smoking and drinking characteristics of control group (n=7) and irradiated group (n=15).

| | **Current smoker** | **Pack years** | **Alcohol units per week** |
|---|---|---|---|
| **Control 1** | No | 0 | 4 |
| **Control 2** | No | 12 | 21 |
| **Control 3** | Yes | 10 | 10 |
| **Control 4** | No | 36 | 14 |
| **Control 5** | No | 35 | 18 |
| **Control 6** | No | 0 | 0 |
| **Control 7** | No | 0 | 3 |
| **Irradiated 1** | Yes | 25 | 0 |
| **Irradiated 2** | No | 40 | 0 |
| **Irradiated 3** | No | 5 | 0 |
| **Irradiated 4** | No | 26 | 35 |
| **Irradiated 5** | Yes | 23 | 28 |
| **Irradiated 6** | No | 30 | 30 |
| **Irradiated 7** | No | 0 | 5 |
| **Irradiated 8** | No | 30 | 0 |
| **Irradiated 9** | Yes | 80 | 0 |
| **Irradiated 10** | Yes | 70 | 20 |
| **Irradiated 11** | No | 0 | 14 |
| **Irradiated 12** | Yes | 41 | 12 |
| **Irradiated 13** | Yes | 50 | 30 |
| **Irradiated 14** | No | 28 | 40 |
| **Irradiated 15** | No | 0 | 21 |

Table 3. Measurements of non-irradiated versus irradiated mandibular trabecular bone biopsies.

| Parameter | Control group (n=7) Median (IQR) | Irradiated group (n=15) Median (IQR) | p |
|---|---|---|---|
| N.Ot/B.Ar (n/mm2) | 134.95 (60.94) | 127.47 (59.15) | 0.837 |
| N.e.Lc/B.Ar (n/mm2) | 13.13 (7.16) | 25.81 (24.93) | 0.007* |
| N.Pos.Ot/B.Ar (n/mm2) | 2.09 (5.64) | 4.84 (8.36) | 0.267 |
| N.Pos.Ot/N.Tt.Ot (%) | .981 (6.42) | 4.08 (8,21) | 0.237 |
| Fb.T.Ar/Ma.Ar (%) | 9.1 (17.25) | 13.7 (9.63) | 0.630 |
| Ad.T.Ar/Ma.Ar (%) | 35.34 (28.93) | 64.38 (27.55) | 0.007* |
| Ma.Ar/Tt.Ar (%) | 45.77 (16.20) | 50.98 (21.34) | 0.447 |
| Adipocyte diameter (μm) | 58.14 (13.69) | 70.88 (9.51) | 0.005* |

Abbreviations: IQR, interquartile range.

a Mann Whitney *U* test p-value

* significant at <0.05 level

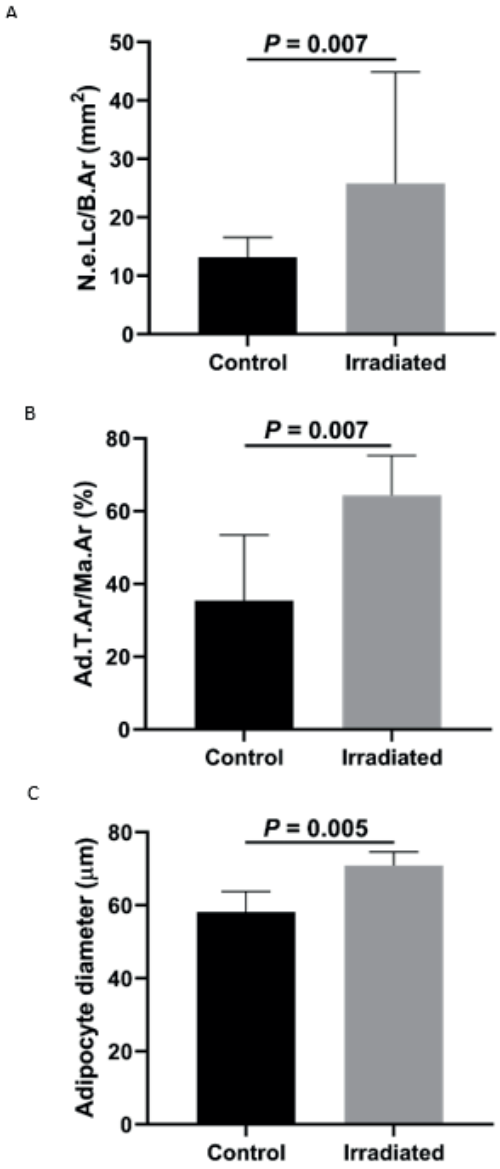


Figure 2.

A. Number of empty lacunae per bone area (N.e.Lc/B.Ar; $mm^2$) in control and irradiated group (Mann Whitney *U* test; p = 0.007).

B. Percentage of adipose tissue of bone marrow area (Ad.T.Ar/Ma.Ar; %) in control and irradiated group (Mann Whitney *U* test; p = 0.007).

C. Adipocyte diameter (µm) in control and irradiated group (Mann Whitney *U* test; p = 0.005).

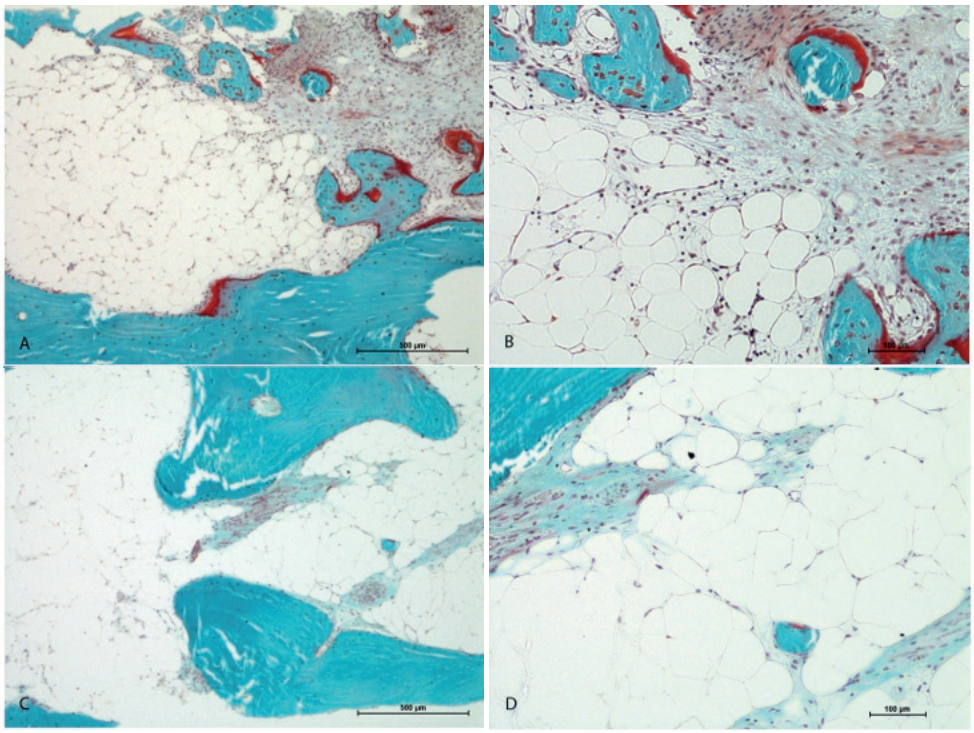


Figure 3. Histological sections, Goldner trichrome stain of mandibular bone from an non-irradiated patient (A: x40, B: x100) and from an irradiated patient, Dmax 53 Gy. (C: x40, D: x100). In both specimens, fibrotic areas as well as adipose tissue is present. The non-irradiated bone marrow has more abundant nuclei and the fibrosis is more localized. The irradiated bone marrow is hypocellular with smaller fibrotic patches scattered throughout the marrow space.

# DISCUSSION

This study shows an increase in empty lacunae in irradiated mandibles which is likely a result of osteocyte death. However, no significant increase in apoptotic osteocytes in the irradiated group was observed. Few studies have investigated irradiation-induced osteocyte apoptosis, and the available literature is based on 'in vitro' experiments. Osteocytes irradiated 'in vitro' are relatively sensitive to radiation-induced apoptosis, which is time and dose dependent, and detected as early as 48 hours after radiation.[19,20] Although the results of these 'in vitro' studies must be interpreted with caution, it is conceivable that osteocyte apoptosis is an early sequence of irradiation and is therefore not increased in our irradiated samples, as in the current study the time interval between the last radiotherapy and biopsy ranged from 10-197 months.

Osteocyte apoptosis is known to increase osteoclastogenesis.[14,19] In animal and in vitro studies, it has been revealed that irradiation causes an initial increase of osteoclast recruitment and activity.[20-25] However, in murine models, this early, transient increase in osteoclasts is followed by long-term osteoclast depletion.[2,25,26] In human irradiated mandibles, a significant reduction as well as an absence of osteoclasts is observed.[27-29] The bone samples in human studies were derived from resections of osteoradionecrotic lesions[28,29] and from trephine biopsies taken during implant surgery in irradiated bone[27], which represents bone harvested months to years after radiotherapy and captures the ´late stage´ radiation injury. As osteocyte apoptosis is thought to recruit osteoclasts to areas in need of bone resorption, perhaps the early radiation-induced apoptotic osteocyte death induces an initial increased osteoclast recruitment. Possibly this effect extinguishes in later stages of radiation damage, when osteocyte apoptosis is no longer increased. Furthermore, as irradiation is known to deplete bone marrow osteoclast precursors, the combination of a lack of osteoclastogenic stimuli and local marrow suppression may cause the absence of osteoclasts in the irradiated human mandible.

Empty lacunae as an indication of earlier osteocyte death have been more commonly investigated in studies on the effects of irradiation on bone. In the present study, a significant increase of empty lacunae was seen in the irradiated group. No correlation between radiation dose and histological findings was observed. Rodent models have

been widely used to investigate dose- and time dependent effects of irradiation on mandibular bone. Irradiation causes an increase in empty lacunae that seem to be dose and time dependent, with most osteocyte death occurring in the first weeks after irradiation and dependent on the administered dose.[30-32]

The literature on osteocyte viability in irradiated human mandibles is scarce. The available studies on human material have been performed on bone specimens from ORN lesions, with empty lacunae mentioned as a qualitative rather than a quantitative outcome.[28,29] The persistent presence of empty lacunae in irradiated bone, even many years after irradiation, could in part be due to the absence of osteoclasts, which leads to the preservation of mineralized matrix that should have been resorbed.[27]

All patients with a Dmax of more than 50 Gy at the dental implant site are treated with HBO therapy in accordance with the department´s protocol. All patients receive 20 sessions before and 10 sessions after dental implant placement. In the current study the patients did not start HBO until the implant surgery was indicated. No dental implant surgery is undertaken in the first 9 months after radiotherapy according to protocol. Since no control group of irradiated patients without HBO treatment was investigated in present study, it is not possible to interpret the effect that HBO therapy could have in the examined specimens.

Spiegelberg et al. found in a study in mice that HBO therapy reduced the number of empty lacunae in irradiated specimens 24 weeks after treatment. No effect was observed on bone marrow adiposity.[22] The mice did, however, start with HBO treatment one day after radiation therapy. No conclusive evidence from double blind randomized controlled trials on the efficacy of HBO on preventing ORN is available to date.[4,5,30-34] Since osteocyte death seems to be an early sequence of radiotherapy rather than a late one, the HBO therapy administered to patients in the present study cannot influence the osteocytes that have already perished.

It should be mentioned that the irradiated group contained more patients with heavier smoking and drinking habits. The amount and duration of smoking and drinking habits as well as the number of years of cessation vary greatly which makes it extremely

difficult to determine and interpret the potential confounding effect. It is known that heavy smoking and drinking is associated with decreased bone volume.[35,36] The specific effect on the mandible is not well known. In a previous study mandibular bone samples from irradiated patients and healthy edentulous patients were compared, and no significant difference in bone volume and bone mineral density was observed between the groups.[27]

Unexpectedly, no significant increase in bone marrow fibrosis is seen in irradiated specimens compared to control biopsies. In edentulous mandibles, fibrosis in the bone marrow is a physiologic finding as a result of alveolar healing.[37] The control biopsies show fibrotic areas in the bone marrow as well, although the visual aspect is different. Bone marrow fibrosis is considered a key event in the theories of Marx as well of Delanian and Lefaix for the pathogenesis of ORN. Marx described progressive fibrosis over time after irradiation in a qualitative assessment of biopsies taken from patients irradiated for oral malignancies. However, the specific sites, technique and circumstances under which the biopsies were taken is not further specified. In the study by Fenner et al. describing histologic changes in an 4x15 Gy fractionated irradiated rat model, progressive fibrosis in the bone marrow cavity in the irradiated site was seen at both 6 and 12 weeks after radiation, while the overlying skin and mucosa were intact.[38] The scarce histomorphometric studies that describe bone marrow fibrosis on human irradiated mandibles are performed on specimens from segmental resections that were performed because of osteoradionecrosis or tumor resection. Bras et al. compared histologic findings in mandibles with manifest osteoradionecrosis, non-osteoradionecrotic irradiated mandibles and non-irradiated mandibles (the latter two from tumor resections).[39] The non-osteoradionecrotic irradiated mandibles exhibited fibrosis of the periosteum and adjacent submucosa, but no fibrosis of the bone marrow. The bone marrow adjacent to ORN lesions was replaced by a dense fibrous, less-vascularized tissue with a gradual decrease of fibrosis toward the periphery. Multiple other histological studies have reported bone marrow fibrosis in human mandibular osteoradionecrosis lesions.[28,40] To the authors' best knowledge, no previous studies quantitatively assessing the extent of fibrosis in irradiated human mandibular bone without other pathology such as recurrent tumor or ORN are available. The present study shows that even in

areas of the mandible that received a high dose of irradiation, abundant marrow fibrosis is not a characteristic finding.

In the present study a marked increase in adipocyte area in the bone marrow as well as adipocyte diameter in the irradiated group was found. No relation with dose or interval between radiation and biopsy was demonstrated. Bone marrow mesenchymal stem cells can differentiate into either osteoblasts or bone marrow adipocytes. Irradiation inhibits proliferation and differentiation of surviving mesenchymal stem cells (MSCs) and osteoprecursor cells into osteoblast cell lineages.[41] Osteogenic differentiation potential of hMSC's is less resistant to irradiation than adipogenic potential.[42] Osteoblastic activity is significantly decreased in irradiated human mandibles.[27]

It is well established that irradiation causes myelosuppression, damage to bone marrow populations and increased marrow fat cellularity.[17,43] This phenomenon is studied extensively in postcranial sites, rather than mandibular bone. Multiple studies in mice have demonstrated that bone marrow adiposity, or fatty substitution triggers bone loss and other skeletal alterations.[44,45] In humans, bone marrow adiposity has been demonstrated in patients after radiotherapy in postcranial sites.[46-48] However, the mandibular bone has distinct features that differ from other skeletal sites, including developmental origin, osteoclastic activity, osteogenic potential of mesenchymal stem cells, the rate of bone turnover and collagen properties.[49-57] Therefore, experimental data on bone from postcranial sites may not translate entirely to the mandibular bone.

Few animal studies have investigated the effect of radiation on bone marrow adipocytes in mandibular bone. Spiegelberg et al.[22] found a significant increase in adipocyte density in bone marrow of irradiated mice mandibles, 10 and 24 weeks after irradiation with 15 Gy. Hyperbaric oxygen therapy that was also included in this study, had no effect on adipocyte density. Marx et al. did observe increased mandibular marrow adiposity and fibrosis in rabbits 6 months after irradiation, also in rabbits treated with HBO, but to a qualitatively lesser extent.[58]

No quantitative data on marrow adipocytes in irradiated human mandibles have been previously reported. Few studies on irradiated human mandibles report data on marrow

adiposity. Marx et al. described histological findings in 45 ORN specimens in a qualitative report and found an absence of fat cells in the bone marrow. Instead, the bone marrow in these specimens was replaced with acellular collagen.[28] Conversely, Curi et al. investigated 40 bone specimens from mandibular ORN and found an increase in marrow fat besides fibrosis. A significant relation was found between the increased amount of marrow fat and increased time after radiation.[40]

In conclusion, the increased adipocytes (shown in this study) and the reduced presence of osteoblastic activity (demonstrated in a previous study[27]) that is observed in irradiated human mandibles together with absent osteocytes (shown in this study) and osteoclasts (demonstrated in a previous study[27]) lead to the hypothesis that irradiation disrupts bone homeostasis at different levels. Radiation causes early death of osteocytes, persistent suppression of osteoclastogenesis by lack of signaling from osteocytes and osteoblasts as well as deprivation of osteoclast precursors, leading to persistence of fragile bone matrix void of osteocytes. The damage to bone mesenchymal stem cells leads to increased adipogenesis in the bone marrow and decreased osteoblastogenic potential. The non-vital persisting bone matrix with severely impaired regenerative and remodeling potential may contribute to the vulnerability of the bone to infection and necrosis, particularly when a 'porte d'entrée' is introduced by disruption to the overlying soft tissue barrier, and could as such be a key event in the pathogenesis of ORN.

# REFERENCES


1. Frankart AJ, Frankart MJ, Cervenka B, Tang AL, Krishnan DG, Takiar V. Osteoradionecrosis: Exposing the Evidence Not the Bone. Int J Radiat Oncol Biol Phys 2021. DOI: 10.1016/j.ijrobp.2020.12.043.
2. Zhang J, Qiu X, Xi K, et al. Therapeutic ionizing radiation induced bone loss: a review of in vivo and in vitro findings. Connect Tissue Res 2018;59(6):509-522. DOI: 10.1080/03008207.2018.1439482.
3. Marx RE. Osteoradionecrosis: a new concept of its pathophysiology. J Oral Maxillofac Surg 1983;41(5):283-8. (https://www.ncbi.nlm.nih.gov/pubmed/6572704).
4. Sultan A, Hanna GJ, Margalit DN, et al. The Use of Hyperbaric Oxygen for the Prevention and Management of Osteoradionecrosis of the Jaw: A Dana-Farber/Brigham and Women's Cancer Center Multidisciplinary Guideline. Oncologist 2017;22(11):1413. DOI: 10.1634/theoncologist.2016-0298erratum.
5. Shaw RJ, Butterworth CJ, Silcocks P, et al. HOPON (Hyperbaric Oxygen for the Prevention of Osteoradionecrosis): A Randomized Controlled Trial of Hyperbaric Oxygen to Prevent Osteoradionecrosis of the Irradiated Mandible After Dentoalveolar Surgery. Int J Radiat Oncol Biol Phys 2019;104(3):530-539. DOI: 10.1016/j.ijrobp.2019.02.044.
6. Delanian S, Lefaix JL. The radiation-induced fibroatrophic process: therapeutic perspective via the antioxidant pathway. Radiother Oncol 2004;73(2):119-31. DOI: 10.1016/j.radonc.2004.08.021.
7. Rivero JA, Shamji O, Kolokythas A. Osteoradionecrosis: a review of pathophysiology, prevention and pharmacologic management using pentoxifylline, alpha-tocopherol, and clodronate. Oral Surg Oral Med Oral Pathol Oral Radiol 2017;124(5):464-471. DOI: 10.1016/j.oooo.2017.08.004.
8. Jacobson AS, Buchbinder D, Hu K, Urken ML. Paradigm shifts in the management of osteoradionecrosis of the mandible. Oral Oncol 2010;46(11):795-801. DOI: 10.1016/j.oraloncology.2010.08.007.
9. Goldring SR. The osteocyte: key player in regulating bone turnover. RMD Open 2015;1(Suppl 1):e000049. DOI: 10.1136/rmdopen-2015-000049.
10. Lee SH, Kim TS, Choi Y, Lorenzo J. Osteoimmunology: cytokines and the skeletal system. BMB Rep 2008;41(7):495-510. DOI: 10.5483/bmbrep.2008.41.7.495.
11. Noble BS, Reeve J. Osteocyte function, osteocyte death and bone fracture resistance. Mol Cell Endocrinol 2000;159(1-2):7-13. DOI: 10.1016/s0303-7207(99)00174-4.
12. Nakashima T, Hayashi M, Fukunaga T, et al. Evidence for osteocyte regulation of bone homeostasis through RANKL expression. Nat Med 2011;17(10):1231-4. DOI: 10.1038/nm.2452.
13. Bellido T. Osteocyte-driven bone remodeling. Calcif Tissue Int 2014;94(1):25-34. DOI: 10.1007/s00223-013-9774-y.
14. Jilka RL, Noble B, Weinstein RS. Osteocyte apoptosis. Bone 2013;54(2):264-71. DOI: 10.1016/j.bone.2012.11.038.
15. Veldhuis-Vlug AG, Rosen CJ. Clinical implications of bone marrow adiposity. J Intern Med 2018;283(2):121-139. DOI: 10.1111/joim.12718.
16. Rharass T, Lucas S. MECHANISMS IN ENDOCRINOLOGY: Bone marrow adiposity and bone, a bad romance? Eur J Endocrinol 2018;179(4):R165-R182. DOI: 10.1530/EJE-18-0182.
17. Costa S, Reagan MR. Therapeutic Irradiation: Consequences for Bone and Bone Marrow Adipose Tissue. Front Endocrinol (Lausanne) 2019;10:587. DOI: 10.3389/fendo.2019.00587.
18. Goldner J. A modification of the masson trichrome technique for routine laboratory purposes. Am J Pathol 1938;14(2):237-43. (https://www.ncbi.nlm.nih.gov/pubmed/19970387).
19. O'Brien CA, Nakashima T, Takayanagi H. Osteocyte control of osteoclastogenesis. Bone 2013;54(2):258-63. DOI: 10.1016/j.bone.2012.08.121.
20. He F, Bai J, Wang J, Zhai J, Tong L, Zhu G. Irradiation-induced osteocyte damage promotes HMGB1-mediated osteoclastogenesis in vitro. J Cell Physiol 2019;234(10):17314-17325. DOI: 10.1002/jcp.28351.
21. Willey JS, Lloyd SA, Robbins ME, et al. Early increase in osteoclast number in mice after whole-body irradiation with 2 Gy X rays. Radiat Res 2008;170(3):388-92. DOI: 10.1667/RR1388.1.

**22.** Spiegelberg L, Braks JA, Groeneveldt LC, Djasim UM, van der Wal KG, Wolvius EB. Hyperbaric oxygen therapy as a prevention modality for radiation damage in the mandibles of mice. J Craniomaxillofac Surg 2015;43(2):214-9. DOI: 10.1016/j.jcms.2014.11.008.

**23.** Wright LE, Buijs JT, Kim HS, et al. Single-Limb Irradiation Induces Local and Systemic Bone Loss in a Murine Model. J Bone Miner Res 2015;30(7):1268-79. DOI: 10.1002/jbmr.2458.

**24.** Damek-Poprawa M, Both S, Wright AC, Maity A, Akintoye SO. Onset of mandible and tibia osteoradionecrosis: a comparative pilot study in the rat. Oral Surg Oral Med Oral Pathol Oral Radiol 2013;115(2):201-11. DOI: 10.1016/j.oooo.2012.09.008.

**25.** Zhai J, He F, Wang J, Chen J, Tong L, Zhu G. Influence of radiation exposure pattern on the bone injury and osteoclastogenesis in a rat model. Int J Mol Med 2019;44(6):2265-2275. DOI: 10.3892/ijmm.2019.4369.

**26.** Oest ME, Franken V, Kuchera T, Strauss J, Damron TA. Long-term loss of osteoclasts and unopposed cortical mineral apposition following limited field irradiation. J Orthop Res 2015;33(3):334-42. DOI: 10.1002/jor.22761.

**27.** Dekker H, Schulten E, van Ruijven L, et al. Bone microarchitecture and turnover in the irradiated human mandible. J Craniomaxillofac Surg 2020. DOI: 10.1016/j.jcms.2020.05.015.

**28.** Marx RE, Tursun R. Suppurative osteomyelitis, bisphosphonate induced osteonecrosis, osteoradionecrosis: a blinded histopathologic comparison and its implications for the mechanism of each disease. Int J Oral Maxillofac Surg 2012;41(3):283-9. DOI: 10.1016/j.ijom.2011.12.016.

**29.** Shuster A, Reiser V, Trejo L, Ianculovici C, Kleinman S, Kaplan I. Comparison of the histopathological characteristics of osteomyelitis, medication-related osteonecrosis of the jaw, and osteoradionecrosis. Int J Oral Maxillofac Surg 2018. DOI: 10.1016/j.ijom.2018.07.002.

**30.** Svalestad J, Hellem S, Thorsen E, Johannessen AC. Effect of hyperbaric oxygen treatment on irradiated oral mucosa: microvessel density. Int J Oral Maxillofac Surg 2015;44(3):301-7. DOI: 10.1016/j.ijom.2014.12.012.

**31.** Heyboer M, 3rd, Wojcik SM, McCabe JB, et al. Hyperbaric oxygen and dental extractions in irradiated patients: short- and long-term outcomes. Undersea Hyperb Med 2013;40(3):283-8. (https://www.ncbi.nlm.nih.gov/pubmed/23789563).

**32.** Bennett MH, Feldmeier J, Hampson N, Smee R, Milross C. Hyperbaric oxygen therapy for late radiation tissue injury. Cochrane Database Syst Rev 2012(5):CD005005. DOI: 10.1002/14651858.CD005005.pub3.

**33.** Hampson NB, Holm JR, Wreford-Brown CE, Feldmeier J. Prospective assessment of outcomes in 411 patients treated with hyperbaric oxygen for chronic radiation tissue injury. Cancer 2012;118(15):3860-8. DOI: 10.1002/cncr.26637.

**34.** Feldmeier JJ. Hyperbaric oxygen therapy and delayed radiation injuries (soft tissue and bony necrosis): 2012 update. Undersea Hyperb Med 2012;39(6):1121-39. (https://www.ncbi.nlm.nih.gov/pubmed/23342770).

**35.** Law MR, Hackshaw AK. A meta-analysis of cigarette smoking, bone mineral density and risk of hip fracture: recognition of a major effect. BMJ 1997;315(7112):841-6. DOI: 10.1136/bmj.315.7112.841.

**36.** Berg KM, Kunins HV, Jackson JL, et al. Association between alcohol consumption and both osteoporotic fracture and bone density. Am J Med 2008;121(5):406-18. DOI: 10.1016/j.amjmed.2007.12.012.

**37.** Brugnami F, Then PR, Moroi H, Leone CW. Histologic evaluation of human extraction sockets treated with demineralized freeze-dried bone allograft (DFDBA) and cell occlusive membrane. J Periodontol 1996;67(8):821-5. DOI: 10.1902/jop.1996.67.8.821.

**38.** Fenner M, Park J, Schulz N, et al. Validation of histologic changes induced by external irradiation in mandibular bone. An experimental animal model. J Craniomaxillofac Surg 2010;38(1):47-53. DOI: 10.1016/j.jcms.2009.07.011.

**39.** Bras J, de Jonge HK, van Merkesteyn JP. Osteoradionecrosis of the mandible: pathogenesis. Am J Otolaryngol 1990;11(4):244-50. (https://www.ncbi.nlm.nih.gov/pubmed/2240412).

**40.** Curi MM, Cardoso CL, de Lima HG, Kowalski LP, Martins MD. Histopathologic and Histomorphometric Analysis of Irradiation Injury in Bone and the Surrounding Soft Tissues of the Jaws. J Oral Maxillofac Surg 2016;74(1):190-9. DOI: 10.1016/j.joms.2015.07.009.

**41.** Han B, Yang Z, Nimni M. Effects of gamma irradiation on osteoinduction associated with demineralized bone matrix. J Orthop Res 2008;26(1):75-82. DOI: 10.1002/jor.20478.

**42.** Georgiou KR, Hui SK, Xian CJ. Regulatory pathways associated with bone loss and bone marrow adiposity caused by aging, chemotherapy, glucocorticoid therapy and radiotherapy. Am J Stem Cells 2012;1(3):205-24. (https://www.ncbi.nlm.nih.gov/pubmed/23671809).

**43.** Naveiras O, Nardi V, Wenzel PL, Hauschka PV, Fahey F, Daley GQ. Bone-marrow adipocytes as negative regulators of the haematopoietic microenvironment. Nature 2009;460(7252):259-63. DOI: 10.1038/nature08099.

**44.** Hui SK, Sharkey L, Kidder LS, et al. The influence of therapeutic radiation on the patterns of bone marrow in ovary-intact and ovariectomized mice. PLoS One 2012;7(8):e42668. DOI: 10.1371/journal.pone.0042668.

**45.** Green DE, Adler BJ, Chan ME, et al. Altered composition of bone as triggered by irradiation facilitates the rapid erosion of the matrix by both cellular and physicochemical processes. PLoS One 2013;8(5):e64952. DOI: 10.1371/journal.pone.0064952.

**46.** Mostoufi-Moab S, Magland J, Isaacoff EJ, et al. Adverse Fat Depots and Marrow Adiposity Are Associated With Skeletal Deficits and Insulin Resistance in Long-Term Survivors of Pediatric Hematopoietic Stem Cell Transplantation. J Bone Miner Res 2015;30(9):1657-66. DOI: 10.1002/jbmr.2512.

**47.** Casamassima F, Ruggiero C, Caramella D, Tinacci E, Villari N, Ruggiero M. Hematopoietic bone marrow recovery after radiation therapy: MRI evaluation. Blood 1989;73(6):1677-81. (https://www.ncbi.nlm.nih.gov/pubmed/2713500).

**48.** Carmona R, Pritz J, Bydder M, et al. Fat composition changes in bone marrow during chemotherapy and radiation therapy. Int J Radiat Oncol Biol Phys 2014;90(1):155-63. DOI: 10.1016/j.ijrobp.2014.05.041.

**49.** Matsubara T, Suardita K, Ishii M, et al. Alveolar bone marrow as a cell source for regenerative medicine: differences between alveolar and iliac bone marrow stromal cells. J Bone Miner Res 2005;20(3):399-409. DOI: 10.1359/JBMR.041117.

**50.** Huja SS, Fernandez SA, Hill KJ, Li Y. Remodeling dynamics in the alveolar process in skeletally mature dogs. Anat Rec A Discov Mol Cell Evol Biol 2006;288(12):1243-9. DOI: 10.1002/ar.a.20396.

**51.** Chai Y, Maxson RE, Jr. Recent advances in craniofacial morphogenesis. Dev Dyn 2006;235(9):2353-75. DOI: 10.1002/dvdy.20833.

**52.** Akintoye SO, Lam T, Shi S, Brahim J, Collins MT, Robey PG. Skeletal site-specific characterization of orofacial and iliac crest human bone marrow stromal cells in same individuals. Bone 2006;38(6):758-68. DOI: 10.1016/j.bone.2005.10.027.

**53.** Aghaloo TL, Chaichanasakul T, Bezouglaia O, et al. Osteogenic potential of mandibular vs. long-bone marrow stromal cells. J Dent Res 2010;89(11):1293-8. DOI: 10.1177/0022034510378427.

**54.** Yamaza T, Ren G, Akiyama K, Chen C, Shi Y, Shi S. Mouse mandible contains distinctive mesenchymal stem cells. J Dent Res 2011;90(3):317-24. DOI: 10.1177/0022034510387796.

**55.** Vermeer J, Renders G, van Duin MA, et al. Bone-site-specific responses to zoledronic acid. Oral Dis 2017;23(1):126-133. DOI: 10.1111/odi.12587.

**56.** Vermeer JA, Renders GA, Everts V. Osteonecrosis of the Jaw-a Bone Site-Specific Effect of Bisphosphonates. Curr Osteoporos Rep 2016;14(5):219-25. DOI: 10.1007/s11914-016-0318-z.

**57.** Matsuura T, Tokutomi K, Sasaki M, Katafuchi M, Mizumachi E, Sato H. Distinct characteristics of mandibular bone collagen relative to long bone collagen: relevance to clinical dentistry. Biomed Res Int 2014;2014:769414. DOI: 10.1155/2014/769414.

**58.** Marx RE, Ehler WJ, Tayapongsak P, Pierce LW. Relationship of oxygen dose to angiogenesis induction in irradiated tissue. Am J Surg 1990;160(5):519-24. DOI: 10.1016/s0002-9610(05)81019-0.

# 7

# General discussion

Radiotherapy, although proven to be an effective treatment modality in head and neck cancers, has inevitable detrimental effects on the surrounding healthy tissues. Irradiation of the oral cavity is known to give acute and chronic adverse local effects such as mucositis, xerostomia, hypogeusia, trismus, radiation caries, candidiasis and osteoradionecrosis (ORN).[1]

Approximately 5% of patients who undergo radiotherapy for head and neck cancer, go on to develop ORN.[2] ORN is typically observed in areas of the mandible that were exposed to high-dose radiotherapy.[3] It is often preceded by local trauma (e.g. tooth extraction) but can also occur spontaneously. The clinical presentation of ORN can range from a small asymptomatic area of bone exposure to severe and extensive necrosis with pathological fracture and fistulae, necessitating surgical intervention and reconstruction.[3]

The pathophysiology of radiation-induced bone damage is complex and not fully understood. In 1983, Marx et al. postulated the pathophysiology of ORN as a '3H'-triad: hypoxia, hypocellularity, and hypovascularity.[4] Subsequent tissue breakdown through persistent hypoxia can cause a chronic, non-healing wound and ultimately result in ORN. Delanian and Lefaix introduced the fibro-atrophic theory including free radical formation, endothelial dysfunction, inflammation, microvascular thrombosis, fibrosis and remodeling, and finally bone and tissue necrosis.[5] Another theory proposed the concept that damage to osteoclasts precede development of vascular alterations and that this suppression of osteoclast function is the initial event in development of ORN.[6] The events in irradiated mandibular bone leading to the occurrence of ORN are not well understood. This thesis addresses the histological and microstructural features present in the irradiated mandible.

Various studies in animal models have shown that high dose irradiation of the mandible causes impaired vascularization, early osteocyte death, initial increase of osteoclast activity followed by long term osteoclast depletion, decreased osteoblast activity and increased bone marrow adiposity.[7-11] In human mandibular bone, these different processes have not previously been investigated systematically and quantitatively. This thesis describes a thorough analysis of the radiation-induced alterations of the mandible

as an important step towards a better understanding of radiation-induced damage of the mandible and ultimately a first necessary step in better understanding the pathogenesis of ORN.

The set-up of the present study was based on bone biopsies obtained from irradiated and non-irradiated edentulous patients, during dental implant surgery facilitating implant-borne mandibular overdentures. In order to interpret the radiation-induced changes in the (edentulous) mandible, first the control group was defined. Since the literature could not provide a solid answer what the effect of edentulism and the extent of resorption, as well as gender had on bone turnover parameters and trabecular structure of the mandible, first an analysis of the non-irradiated mandible was performed.

An important difference between non-irradiated and irradiated patients is the mandibular height. Oral cancer patients often become edentulous after pre-radiotherapy dental screening for oral foci. As a result, the mean time between becoming edentulous and dental implant surgery is shorter in this group, and, therefore, they have less physiologically resorbed mandibles. It was of importance to investigate whether progressive alveolar bone resorption resulted in different microstructural or turnover characteristics. All bone biopsies harvested in non-irradiated patients during dental implant surgery were investigated (Chapter 2). Bone biopsies were analyzed by histomorphometry to assess bone turnover parameters. Micro-CT was used to assess the structural properties. No relationship between trabecular bone volume fraction and mandibular height was seen. However, a significant inverse relation between bone mineral density (BMD) and mandibular height was observed. Because of the limited volume of the bone biopsies, this result was difficult to interpret. A biopsy from the more severely resorbed mandible might contain more bone tissue adjacent to the inferior border that is known to be more highly mineralized.[12] Osteoclast numbers were significantly higher in women, but no significant differences were found between the sexes for any of the other investigated parameters including bone volume fraction. In women, higher turnover parameters (osteoclast number, osteoid surface and osteoid volume) correlated negatively with bone volume fraction. This finding suggests a similar

relationship between a post-menopausal estrogen depletion and osteoporosis to that found in postcranial skeletal sites.[13]

After this first study in non-irradiated patients, the finding of higher BMD in the trabecular bone of the more severely resorbed edentulous mandibles called for further investigation. As mentioned, the limited volume of the bone biopsies impedes extrapolation of this finding for the entire mandible. Therefore, a study was conducted to investigate the effect of mandibular resorption on the trabecular structure in larger areas of mandibular bone in a cadaveric study of edentulous mandibles (5 men and 5 women) with different stages of mandibular resorption (Chapter 3). Trabecular volume BMD was measured in the upper, middle and lower third of the trabecular bone volume in anterior, premolar and molar regions and it turned out that there was no significant difference between these regions, nor a relation between mandibular height and BMD of the trabecular bone volume. The highest BMD in the cortical bone was found inferior-lingually at the midline, inferiorly at the mental foramen region and at the inferior-buccal surface in the molar area which are areas that endure the highest strains.[12] Furthermore, it was found that the trabecular structure of the edentulous mandible exhibits regional differences, with superior trabecular bone volume and quality in the anterior region. In the premolar region, increased resorption coincided with local impairment of the bone quality (lower trabecular thickness and higher trabecular separation). This finding, however, is not relevant for the comparison of irradiated and non-irradiated bone samples in this thesis, as all the bone biopsies were harvested from the interforaminal region, corresponding with the anterior region in the cadaveric study. No difference between male and female mandibles were observed for any of the investigated parameters.

Because hypovascularity is widely accepted to be the key event in the pathogenesis of ORN, the vascularity of the bone samples of the irradiated and non-irradiated patients were investigated (Chapter 4). A quantitative analysis was performed to describe the irradiated mandibular bone marrow's microvasculature in more detail. Overall a significant decrease in vascular area fraction and vascular density in irradiated specimens compared to non-irradiated specimens was found. A significant correlation between vascular density and vascular area fraction with increased time after radiotherapy was

not found. However, a significant negative correlation between time after radiotherapy and percentage of small vessels and a positive correlation between time after radiotherapy with mean vessel perimeter were observed. This may indicate that either the smallest vessels are more affected by irradiation than larger vessels, or that formation of new vessels may be impaired, leading to a more profound hypovascular situation in the later post-irradiation phase. In the literature, a cut-off point of 50 Gy local radiation dose is commonly accepted to identify patients at risk for developing ORN.[14,15] Interestingly, when comparing bone biopsies that had obtained Dmax ≥50 Gy with those of <50 Gy, no significant differences were found in vascular number or vascular area fraction, but the vascular diameter and vascular perimeter were significantly higher in the ≥50 Gy group and the percentage of small vessels was significantly lower. This indicates that a local radiation dose exceeding 50 Gy affects the smaller blood vessels more than the larger, either by a direct effect on the smaller vessels or inhibition of new vessel formation. It must be mentioned that all patients receiving a local dose of more than 50 Gy on the implant bed did receive 20 sessions of hyperbaric oxygen (HBO) therapy prior to dental implant surgery. The effect of HBO treatment on these results is unknown, possibly without HBO the differences in vascularity between patients with a local radiation dose of <50 Gy versus a local radiation dose of ≥50 Gy are more profound.



It is impossible to draw a conclusion from these results on the effect of the hypovascularity on the tissue. The finding that bone biopsies with lower radiation dose have similar vascular area fraction and density as bone biopsies with a higher dose contradicts that hypovascularity in itself is a key event in the pathogenesis of ORN. However, none of the patients in the present study proceeded to develop ORN. The role of the microvasculature in irradiated bone deserves further and more extensive quantitative research to truly appreciate its contribution in mandibular ORN.

To further investigate the effects of irradiation on mandibular bone, in Chapter 5 the effects of radiotherapy on the trabecular structure and parameters of bone turn-over are addressed. The study showed a dramatic decrease in osteoid number, osteoid volume and osteoclast number in irradiated samples compared to non-irradiated controls, with no apparent relationship with Dmax or time after radiotherapy. When

appreciating the micro-CT results, it is quite interesting that a deterioration of trabecular structure, was only observed in bone irradiated with a Dmax <50 Gy. A possible explanation for this, is that higher doses of radiation cause long-term depletion of osteoclasts. Radiotherapy disrupts the balance of bone remodeling by affecting the different bone cells, which vary in radiosensitivity. When, above a certain radiation dose, bone turnover is decreased to an extent that the trabecular structure is preserved (in absence of resorption). This results in a fragile bone matrix that will age but not remodel. Therefore, this bone is pathological in the sense that it has no capacity to renew itself and this could play a role in the pathogenesis of ORN, especially when areas of this bone have become void of osteocytes and are essentially non-vital due to radiation induced osteocyte death, ageing or local injury. A potential bias in this study is the HBO administered to patients with a local dose of >50 Gy on the dental implant bed. Literature on the effect of HBO on bone turnover and trabecular structure in irradiated mandibles is scarce, and solely reported from animal studies. Although a recent review showed there was no consistent evidence for support of HBO in prevention or management of ORN, we cannot exclude a confounding effect from HBO in our analysis.[16]

In Chapter 6, the study focus was on osteocyte apoptosis, bone marrow fibrosis and bone marrow adiposity. Furthermore, the fibrosis and adipose content of the mandibular bone marrow were analyzed. The results show an increase in empty lacunae in irradiated mandibles which is likely a result of osteocyte death in the past. However, no significant increase in apoptotic osteocytes in the irradiated group was observed. Osteocytes irradiated 'in vitro' are relatively sensitive to radiation-induced apoptosis, which is time and dose dependent, and detected as early as 48 hours after radiation.[17] It is conceivable that osteocyte apoptosis is an early sequence of irradiation and is therefore not increased in the irradiated bone biopsies, as the time interval between the last radiotherapy and biopsy in this study was a minimum of 10 months. Osteocyte apoptosis is known to induce osteoclastogenesis.[18,19] In animal and in vitro studies, it has been revealed that irradiation causes an initial increase of osteoclast recruitment and activity.[7-11, 17] In murine models irradiated with high doses, this early, transient increase in osteoclasts is followed by long-term osteoclast depletion.[11,20,21] The persistent presence of empty lacunae in irradiated bone, even many years after irradiation, could in part be due to the

absence of osteoclasts, which leads to the preservation of mineralized matrix that should have been resorbed. No significant increase in bone marrow fibrosis was seen in irradiated specimens compared to non-irradiated specimens. In edentulous mandibles, fibrosis in the bone marrow is a physiologic finding as a result of alveolar healing. The non-irradiated bone biopsies show fibrotic areas in the bone marrow as well, although the morphological aspect was different. Bras et al.[22] also did not find increased fibrosis in the mandibular bone marrow of irradiated non-osteonecrotic mandibular bone. The present study shows that even in mandibular biopsies that received a high dose of irradiation, abundant marrow fibrosis is not a characteristic finding. Perhaps fibrosis comes secondary to trauma and/or marrow inflammation as a reaction to the presence of exposed bone. This, however, contradicts the fibro-atrophic theory as presented by Delanian and Lefaix[5], and suggest that bone marrow fibrosis might rather be a consequence or a co-factor, than a cause of ORN.

A marked increase in adipocyte area in the bone marrow as well as adipocyte diameter was observed in the mandibular bone marrow of irradiated patients. No relation with dose or interval between radiation and biopsy was demonstrated. However, the sample size was rather small. Bone marrow mesenchymal stem cells can differentiate into either osteoblasts or bone marrow adipocytes. Irradiation inhibits proliferation and differentiation of surviving mesenchymal stem cells (MSCs) and osteoprecursor cells into osteoblast cell lineages.[23] Osteogenic differentiation potential of MSC's is less resistant to irradiation than adipogenic potential.[24] In the study described in Chapter 5 the osteoblastic activity was significantly decreased in irradiated human mandibles.



In conclusion, the increased number of adipocytes and the reduced presence of osteoblastic activity that is observed in irradiated human mandibles together with the absence of osteocytes and osteoclasts suggest that radiation disrupts bone homeostasis at different levels. Based on the findings in the studies described in this thesis representing late radiation effects, combined with what is already known from the existing literature, the following could be hypothesized regarding radiogenic bone damage and, in particular, the pathogenesis of ORN: Radiation causes early death of osteocytes,[25] persistent suppression of osteoclastogenesis by lack of signaling from osteocytes and osteoblasts as well as irradiation induced deprivation of osteoclast

precursors,[11, 26] leading to persistence of bone matrix void of osteocytes. The damage to mesenchymal stem cells in bone leads to increased adipogenesis in the bone marrow and decreased osteoblastogenic potential.[27] In this novel theory, the non-vital persisting bone matrix with severely impaired regenerative and remodeling potential may contribute to the vulnerability of the bone to infection and necrosis, particularly when a 'porte d'entrée' is introduced by a disruption of the overlying soft tissue barrier, and could as such be a key event in the pathogenesis of ORN. In this theory, hypovascularity and fibro-atrophy are rather cofactors than key factors in the pathogenesis of radiogenic bone damage and ORN.

## FUTURE PERSPECTIVES

The studies described in this thesis were the first to evaluate the response of human mandibular bone to irradiation on a cellular and structural level. The use of a trephine drill for dental implants offers the unique opportunity to histologically investigate the effects of irradiation on the mandibular bone and bone marrow without the bias of other pathology such as infection, necrosis or cancer in the samples. In order to further investigate the hypothesis on radiation damage of mandibular bone and the pathophysiology of ORN proposed in this thesis, this study should be continued in larger multicenter trials. It would be particularly interesting to follow-up on the irradiated patients after dental implant surgery, to observe whether and in which patients ORN develops. Additional bone samples should be obtained in these ORN patients during debridement surgery to investigate the different aspects of the bone (bone structure, bone turnover, vascularity, marrow fibrosis, osteocyte apoptosis and marrow adiposity) in clinical evident ORN and compare this to the situation prior to ORN. This might help to find specific clues to what characteristics in particular make the bone vulnerable to the development of ORN.

Other areas of interest are stem cell niches in mandibular bone marrow of non-irradiated and irradiated patients, as little is known about the presence and function of stem cells in non-irradiated nor in irradiated mandibular bone marrow. An additional focus should be on vessel sprouting and vascular niches in the bone marrow to further analyze angiogenesis potential in non-irradiated and irradiated mandibular bone. Better insight

on which cells (or the dysfunction of which cells) are more specifically involved in the pathogenesis ORN, will help towards the development of a more targeted approach for its prevention and treatment.

# REFERENCES


1. Vissink A, Jansma J, Spijkervet FK, Burlage FR, Coppes RP. Oral sequelae of head and neck radiotherapy. Crit Rev Oral Biol Med 2003;14(3):199-212. (https://www.ncbi.nlm.nih.gov/pubmed/12799323).
2. Aarup-Kristensen S, Hansen CR, Forner L, Brink C, Eriksen JG, Johansen J. Osteoradionecrosis of the mandible after radiotherapy for head and neck cancer: risk factors and dose-volume correlations. Acta Oncol 2019;58(10):1373-1377. DOI: 10.1080/0284186X.2019.1643037.
3. Chrcanovic BR, Reher P, Sousa AA, Harris M. Osteoradionecrosis of the jaws--a current overview--part 1: Physiopathology and risk and predisposing factors. Oral Maxillofac Surg 2010;14(1):3-16. DOI: 10.1007/s10006-009-0198-9.
4. Marx RE. Osteoradionecrosis: a new concept of its pathophysiology. J Oral Maxillofac Surg 1983;41(5):283-8. (https://www.ncbi.nlm.nih.gov/pubmed/6572704).
5. Delanian S, Lefaix JL. The radiation-induced fibroatrophic process: therapeutic perspective via the antioxidant pathway. Radiother Oncol 2004;73(2):119-31. DOI: 10.1016/j.radonc.2004.08.021.
6. Jacobson AS, Buchbinder D, Hu K, Urken ML. Paradigm shifts in the management of osteoradionecrosis of the mandible. Oral Oncol 2010;46(11):795-801. DOI: 10.1016/j.oraloncology.2010.08.007.
7. Wright LE, Buijs JT, Kim HS, et al. Single-Limb Irradiation Induces Local and Systemic Bone Loss in a Murine Model. J Bone Miner Res 2015;30(7):1268-79. DOI: 10.1002/jbmr.2458.
8. Willey JS, Lloyd SA, Robbins ME, et al. Early increase in osteoclast number in mice after whole-body irradiation with 2 Gy X rays. Radiat Res 2008;170(3):388-92. DOI: 10.1667/RR1388.1.
9. Spiegelberg L, Braks JA, Groeneveldt LC, Djasim UM, van der Wal KG, Wolvius EB. Hyperbaric oxygen therapy as a prevention modality for radiation damage in the mandibles of mice. J Craniomaxillofac Surg 2015;43(2):214-9. DOI: 10.1016/j.jcms.2014.11.008.
10. Damek-Poprawa M, Both S, Wright AC, Maity A, Akintoye SO. Onset of mandible and tibia osteoradionecrosis: a comparative pilot study in the rat. Oral Surg Oral Med Oral Pathol Oral Radiol 2013;115(2):201-11. DOI: 10.1016/j.oooo.2012.09.008.
11. Zhai J, He F, Wang J, Chen J, Tong L, Zhu G. Influence of radiation exposure pattern on the bone injury and osteoclastogenesis in a rat model. Int J Mol Med 2019;44(6):2265-2275. DOI: 10.3892/ijmm.2019.4369.
12. Kingsmill VJ, Boyde A. Mineralisation density of human mandibular bone: quantitative backscattered electron image analysis. J Anat 1998;192 ( Pt 2):245-56. DOI: 10.1046/j.1469-7580.1998.19220245.x.
13. Kanis JA, Melton LJ, 3rd, Christiansen C, Johnston CC, Khaltaev N. The diagnosis of osteoporosis. J Bone Miner Res 1994;9(8):1137-41. DOI: 10.1002/jbmr.5650090802.
14. Tsai CJ, Hofstede TM, Sturgis EM, et al. Osteoradionecrosis and radiation dose to the mandible in patients with oropharyngeal cancer. Int J Radiat Oncol Biol Phys 2013;85(2):415-20. DOI: 10.1016/j.ijrobp.2012.05.032.
15. Tatum SA, Theler JM. Principles and practice of craniofacial bone healing. In: Sataloff RT, Sclafani AP, eds. Sataloff's Comprehensive Textbook of Otolaryngology: Head & Neck Surgery: Facial Plastic and Reconstructive Surgery 1ed. New Delhi: Jaypee Brothers,Medical Publishers Pvt. Limited; 2016:913-928.
16. Sultan A, Hanna GJ, Margalit DN, et al. The Use of Hyperbaric Oxygen for the Prevention and Management of Osteoradionecrosis of the Jaw: A Dana-Farber/Brigham and Women's Cancer Center Multidisciplinary Guideline. Oncologist. 2017 Mar;22(3):343-350. doi: 10.1634/theoncologist.2016-0298. Epub 2017 Feb 16. Erratum in: Oncologist. 2017 Nov;22(11):1413. PMID: 28209748; PMCID: PMC5344641.
17. He F, Bai J, Wang J, Zhai J, Tong L, Zhu G. Irradiation-induced osteocyte damage promotes HMGB1-mediated osteoclastogenesis in vitro. J Cell Physiol 2019;234(10):17314-17325. DOI: 10.1002/jcp.28351.
18. Jilka RL, Noble B, Weinstein RS. Osteocyte apoptosis. Bone 2013;54(2):264-71. DOI: 10.1016/j.bone.2012.11.038.

**19.** Veldhuis-Vlug AG, Rosen CJ. Clinical implications of bone marrow adiposity. J Intern Med 2018;283(2):121-139. DOI: 10.1111/joim.12718.

**20.** Zhang J, Qiu X, Xi K, et al. Therapeutic ionizing radiation induced bone loss: a review of in vivo and in vitro findings. Connect Tissue Res 2018;59(6):509-522. DOI: 10.1080/03008207.2018.1439482.

**21.** Oest ME, Franken V, Kuchera T, Strauss J, Damron TA. Long-term loss of osteoclasts and unopposed cortical mineral apposition following limited field irradiation. J Orthop Res 2015;33(3):334-42. DOI: 10.1002/jor.22761.

**22.** Bras J, de Jonge HK, van Merkesteyn JP. Osteoradionecrosis of the mandible: pathogenesis. Am J Otolaryngol 1990;11(4):244-50. (https://www.ncbi.nlm.nih.gov/pubmed/2240412).

**23.** Han B, Yang Z, Nimni M. Effects of gamma irradiation on osteoinduction associated with demineralized bone matrix. J Orthop Res 2008;26(1):75-82. DOI: 10.1002/jor.20478.

**24.** Georgiou KR, Hui SK, Xian CJ. Regulatory pathways associated with bone loss and bone marrow adiposity caused by aging, chemotherapy, glucocorticoid therapy and radiotherapy. Am J Stem Cells 2012;1(3):205-24. (https://www.ncbi.nlm.nih.gov/pubmed/23671809).

**25.** Fenner M, Park J, Schulz N, et al. Validation of histologic changes induced by external irradiation in mandibular bone. An experimental animal model. J Craniomaxillofac Surg 2010;38(1):47-53. DOI: 10.1016/j.jcms.2009.07.011.

**26.** Zhang J, Wang Z, Wu A, et al. Differences in responses to X-ray exposure between osteoclast and osteoblast cells. J Radiat Res 2017;58(6):791-802. DOI: 10.1093/jrr/rrx02

**27.** Costa S, Reagan MR. Therapeutic Irradiation: Consequences for Bone and Bone Marrow Adipose Tissue. Front Endocrinol (Lausanne) 2019;10:587. DOI: 10.3389/fendo.2019.00587.

# 8

# Summary

# Samenvatting

# SUMMARY

Radiotherapy is an effective treatment modality for head and neck cancers, but has the disadvantage that it also induces damage to the surrounding healthy tissues. The mandibular bone is known to be susceptible to irradiation damage, which can result in compromised wound healing and ultimately osteoradionecrosis (ORN). ORN is most frequently seen in the mandible and is a serious complication, presenting as an area of exposed bone of at least three months duration with no tendency of healing. ORN usually occurs between 4 months and 3 years after radiotherapy, but can present even decades after radiotherapy. More severe cases of ORN may need surgical intervention (resection) including reconstruction.

There is no general consensus on the pathogenesis of radiation-induced bone damage and ORN. Proposed theories state that vascular impairment, hypocellular tissue and local hypoxia, as well as an irradiation-induced dysregulation of fibroblasts with deposition of abnormal fibro-atrophic tissue may predispose to ORN. Scientific evidence for these theories in irradiated human mandibular bone is scarce, inconclusive and generally derived from animal studies.

The aim of this thesis was to investigate the effects of radiotherapy on the human mandible at tissue level, in order to elucidate the disruptions of the bone physiology that might precede and contribute to the development of ORN. The goal was to broaden the current perspective by focusing on different aspects of the bone: the vascularity, the trabecular structure, bone turnover and the bone marrow.

Bone tissue was obtained from irradiated and non-irradiated edentulous patients during dental implant surgery in the anterior mandible for implant-borne overdentures. In irradiated patients, mandibular resorption is generally less severe than in non-irradiated patients, because frequently these patients have become edentulous shortly before the start of their cancer treatment. Unlike the non-irradiated group, the indication for dental implants in irradiated patients is usually not progressive resorption of the mandible, but impaired oral function secondary to the adverse effects from their cancer treatment, such as altered oral or mandibular anatomy and xerostomia. Because

edentulism in itself initiates a process of atrophy in the mandible, it was important to define the characteristics of (non-irradiated) mandibular bone in progressive stages of physiological resorption.

In Chapter 2 the mandibular bone of non-irradiated individuals was analyzed using histomorphometry and micro-CT. There was no significant difference between men and women for any of the measured parameters (including bone volume fraction) in cortical nor trabecular bone, except for the number of osteoclasts, which was higher in women than in men. Only in women, bone volume was negatively associated with turnover, which suggests a similar relationship between a post-menopausal estrogen depletion and osteoporosis to that found in postcranial skeletal sites. A higher bone mineral density was observed in the trabecular bone of the more severely resorbed edentulous mandibles, which called for further investigation.

A second study was undertaken using larger volumes of bone from cadaveric human mandibles (Chapter 3). In this study, molar, premolar and anterior segments of the edentulous mandible were analyzed using micro-CT. No significant differences were found between men and women in any of the measured regions. Cortical bone mineral density (BMD) increased towards the inferior border of the mandible. There was no significant relation between mandibular height and BMD in any of the regions. Overall, cortical BMD was higher in areas with highest strains and lower in areas subject to the most mandibular resorption. Only in the premolar region, impaired bone quality was associated with increased mandibular resorption. Trabecular bone volume was higher and trabecular bone structure is superior in the anterior region of the edentulous mandible which might explain improved primary stability of dental implants in this region.



In Chapters 4, 5 and 6 the effects of radiotherapy on mandibular bone were investigated. In irradiated patients, vascular density and vascular area fraction of the mandibular bone marrow were lower. In bone samples with a local point dose (Dmax) of ≥50 Gy (often mentioned in the literature as a threshold value of irradiation above which ORN may develop) the mean vascular diameter and perimeter was higher than in samples with a Dmax <50 Gy, whereas the percentage of smaller vessels was lower. A longer

interval between radiotherapy and biopsy was also associated with a larger mean vessel perimeter and lower percentage of smaller vessels. This may indicate that either the smallest vessels are more affected by irradiation than larger vessels, or, that formation of new vessels may be impaired, leading to a more profound hypovascular situation in the later post-irradiation phase.

Radiotherapy dramatically impaired bone turnover in the mandible. However, deterioration of the trabecular structure only affected bone irradiated with a Dmax of <50 Gy. No difference in bone trabecular structure parameters was seen between non-irradiated bone and irradiated bone with a Dmax of ≥50 Gy.

Apoptotic osteocytes and empty lacunae were counted as a measure for osteocyte death. Apoptotic osteocytes were not increased in the irradiated bone compared to the non-irradiated bone. However, the amount of empty lacunae was significantly higher. The bone marrow adiposity was significantly increased in the irradiated bone but no difference was observed in bone marrow fibrosis.

In conclusion, with increasing radiation dose, bone homeostasis gets disrupted at different levels. Based on the results of this study and the existing literature on radiation damage to bone, we speculated on the following order of events after irradiation: Osteocyte death is an early event after irradiation. A lack of osteocyte and osteoblast signaling, as well as an irradiation induced deprivation of osteoclast precursors, leads to persistent lack of osteoclastogenesis. Irradiation-induced damage to the mesenchymal stem cells in bone decreases their osteoblastogenic potential and increases marrow adipogenesis. Subsequently, a fragile bone matrix void of osteocytes persists, which, in a dose-dependent absence of regenerative and remodeling potential, is vulnerable to infection and necrosis, particularly when a disruption of the overlying soft tissue barrier is introduced This could as such be a key event in the pathogenesis of ORN.

# SAMENVATTING

Radiotherapie is een veel toegepaste effectieve behandeling van hoofd-halskanker, maar veroorzaakt ook schade aan de omliggende gezonde weefsels. In kaakbot kan schade door bestraling leiden tot een gestoorde wondgenezing en osteoradionecrose (ORN). ORN wordt vooral gezien in de onderkaak en betreft een ernstige complicatie van radiotherapie. De diagnose ORN wordt gesteld als in bestraald gebied gedurende ten minste drie maanden blootliggend bot zonder genezingstendens aanwezig is. ORN kan aanleiding geven tot pijnklachten, fistels in de mond en van de huid en pathologische fracturen van de kaak. Doorgaans ontstaat ORN tussen 4 maanden en 3 jaar na de laatste bestraling, maar het kan zelfs decennia na de laatste radiotherapie nog optreden. In ernstige gevallen zijn chirurgische behandeling (kaakresectie) en reconstructie geïndiceerd.

Er bestaat geen consensus over wat precies de effecten van bestraling op het bot zijn die uiteindelijk kunnen leiden tot het ontstaan van ORN. De in de literatuur beschreven theorieën stellen, dat een door bestraling veroorzaakte beschadiging van de bloedvaten, verlies van cellen in het weefsel en het plaatselijk optreden van een zuurstoftekort, dan wel een ontregeling van fibroblasten met afzetting van littekenweefsel, het optreden van ORN kunnen induceren. De wetenschappelijke onderbouwing van deze theorieën is mager, niet eenduidig en vooral gebaseerd op dierexperimenteel onderzoek.

Het doel van dit proefschrift was om de effecten van bestraling in humaan onderkaakbot in kaart te brengen, om zo op weefselniveau inzicht te krijgen in de processen die mogelijk bijdragen aan het ontstaan van ORN. In dit onderzoek werd het bestaande perspectief verbreed door te kijken naar de verschillende aspecten van botweefsel: de microvascularisatie, de trabeculaire structuur, de botombouw en het beenmerg.

Tijdens het plaatsen van tandwortelimplantaten in de onderkaak bij bestraalde en niet-bestraalde tandeloze patiënten (ten behoeve van een implantaat-gedragen gebitsprothese) werden botbiopten afgenomen. Bij niet-bestraalde patiënten werden de implantaten geplaatst vanwege een slecht functionerende volledige gebitsprothese op een sterk geslonken onderkaak, hetgeen doorgaans het gevolg was van langdurige

tandeloosheid. Patiënten die bestraald gaan worden, krijgen voorafgaande aan hun behandeling een tandheelkundig onderzoek, en als blijkt dat er slechte, niet te behouden gebitselementen aanwezig zijn, worden deze voor aanvang van de bestraling verwijderd, omdat dan de wondgenezing nog niet door de bestraling wordt beïnvloed. Omdat deze patiënten vaak kort voor de bestraling tandeloos zijn geworden, is de onderkaak van bestraalde patiënten is veelal minder geslonken dan die van niet-bestraalde patiënten. De reden van het plaatsten van tandwortelimplantaten bij bestraalde patiënten is meestal niet omdat de kaak is geslonken, maar problemen met het dragen van een gebitsprothese voortkomend uit de behandeling van de tumor, zoals veranderde anatomie in de mond en monddroogte.

Omdat tandeloosheid gepaard gaat met een progressieve afname van het kaakbotvolume, was het van belang om eerst de eigenschappen van het bot van de geslonken onderkaak te definiëren. In Hoofdstuk 2 wordt een onderzoek beschreven waarin botbiopten van gezonde, niet-bestraalde personen werden geanalyseerd met behulp van histomorfometrisch onderzoek en micro-CT. Er werden tussen mannen en vrouwen geen significante verschillen gezien met betrekking tot de onderzochte parameters (met name ook niet in het botvolume), met uitzondering van het aantal osteoclasten; dit was bij vrouwen hoger dan bij mannen. In het trabeculaire bot van de sterker geslonken onderkaken werd een relatief hogere botmineraaldichtheid aangetoond. Nader onderzoek in grotere volumes kaakbot is nodig om dit mogelijke verband nader te onderzoeken.

Om deze reden werd een humaan kadaveronderzoek uitgevoerd waarin het bot van de onderkaak nader werd bestudeerd (Hoofdstuk 3). In deze studie werd de tandeloze onderkaak verdeeld in drie regio's (molaar, premolaar en incisief) en met behulp van micro-CT geanalyseerd. Er werden tussen mannen en vrouwen geen significante verschillen gevonden met betrekking tot de metingen in de voornoemde regio's. Er werd in geen van de regio's een significante relatie gezien tussen de hoogte van de onderkaak en de BMD van het trabeculaire bot. De corticale BMD was hoger in de gebieden met de hoogste belasting en lager in de gebieden met de meeste resorptie van het kaakbot.

In Hoofdstukken 4, 5 en 6 werden de effecten van bestraling op het kaakbot onderzocht. Bij bestraalde patiënten werd een lagere vaatdichtheid gevonden en een kleinere fractie vaatoppervlak van het beenmerg gezien. In bot met een lokale puntdosis (Dmax) van ≥50 Gy (in de literatuur vaak genoemd als drempelwaarde van bestraling waarboven het risico op het ontstaan van ORN toeneemt) was de gemiddelde diameter en omtrek van de bloedvaten hoger dan in de botbiopten met een Dmax <50 Gy, en het aandeel kleinere bloedvaten (gedefinieerd als bloedvaten met een lumen van <400 $\mu m^2$) lager. Een langere tijdsduur tussen de laatste bestraling en afname van het botbiopt was gecorreleerd met een grotere gemiddelde vaatomtrek en een lager percentage kleinere vaten. Dit zou kunnen betekenen dat ofwel de kleinere vaten gevoeliger zijn voor bestralingsschade, ofwel dat de nieuwvorming van (kleine) vaten wordt belemmerd, hetgeen leidt tot een meer uitgesproken gebrek aan bloedvaten in de latere post-bestralingsfase.

De botombouw in de onderkaak bleek door bestraling drastisch te verminderen. Een verslechtering van de trabeculaire structuur werd echter alleen gevonden in bestraald bot met een Dmax van <50 Gy. Er werden geen significante verschillen gezien in de parameters voor de trabeculaire structuur tussen niet-bestraald bot en bestraald bot met een Dmax van ≥50 Gy.

Er werd geen toename van osteocyten in apoptose waargenomen in de bestraalde patiënten, vergeleken met de niet-bestraalde patiënten, maar het aantal lege lacunae was in bestraald bot wel significant hoger. Het aantal adipocyten in het beenmerg was significant verhoogd na bestraling. Er werd geen verschil waargenomen in de hoeveelheid fibrose in het beenmerg van bestraald en niet-bestraald bot.

Concluderend kan worden gesteld, dat bij toenemende stralingsdosis de fysiologische processen in het botweefsel op verschillende niveaus verstoord raken. Gebaseerd op de resultaten van deze studie en de kennis uit de literatuur kan de volgende hypothese over de door bestraling geïnduceerde schade aan het botweefsel van de onderkaak worden geponeerd. Een vroeg effect van bestraling is de sterfte van osteocyten. Door gebrek aan signaaleiwitten van osteocyten, en door directe bestralingsschade aan osteoclastprecursors, blijft de osteoclastogenese uit. Onder invloed van de bestraling

neemt de differentiatie van mesenchymale stamcellen in het beenmerg tot osteoblasten af. In plaats daarvan differentiëren deze tot adipocyten. Er blijft een fragiele botmatrix bestaan waarin zich gebieden bevinden zonder of met zeer weinig osteocyten. Door het (dosisafhankelijk) gebrek aan remodellerend en regeneratief vermogen, is deze acellulaire botmatrix gevoelig voor infectie en necrose, vooral wanneer er een beschadiging van de overliggende weke delen optreedt. Dit zou als zodanig een belangrijke factor kunnen zijn bij het ontstaan van ORN.

# 9

List of abbreviations

Contributing authors and chapter information

List of publications

Acknowledgements / Dankwoord

About the author

# LIST OF ABBREVIATIONS

| | |
|---|---|
| 3D-CRT | 3-dimensional conformal radiotherapy |
| A | Anterior |
| Ad | Adipocytes |
| ASA classification | American Society of Anaesthesiologists physical status classification |
| ASBMR | American Society for Bone and Mineral Research |
| BS | Bone Surface |
| BV | Bone volume |
| BV/TV | Bone volume fraction |
| Ct | Cortical |
| CBCT | Cone-beam computer tomography |
| Dmax | Maximum radiation point dose |
| DXA | Dual energy X-ray absorptiometry |
| e.Lc | Empty lacunae |
| Fb | Fibrosis |
| Gy | Gray |
| HA | Hydroxyapatite |
| HBO | Hyperbaric oxygen |
| IMRT | Intensity modulated radiotherapy |
| IQR | Interquartile range |
| IR | Ionizing radiation |
| M | Molar |
| Ma | Marrow |
| Micro-CT, μCT | Microcomputed tomography |
| MRONJ | Medication-related osteonecrosis of the jaw |
| N | Number |
| Ocl | Osteoclasts |
| OMJ | Osteomyelitis of the jaw |
| ORN | Osteoradionecrosis |
| OS | Osteoid surface |
| Ot | Osteocytes |
| OV | Osteoid volume |
| PM | Premolar |
| Po | Porosity |
| ROI | Region of interest |
| Sp | Separation |
| Tb | Trabecular |
| Th | Thickness |
| TRAP | Tartrate resistant acid phosphatase |

| | |
|---|---|
| 3D-CRT | 3-dimensional conformal radiotherapy |
| TV | Total volume |
| VAF | Vascular area fraction |
| VD | Vascular density |
| VOI | Volume of interest |

## *Histomorphometric indices*

| | |
|---|---|
| BV/TV | Bone volume fraction |
| Ad.T.Ar/Ma.Ar | Fraction of adipose tissue per bone marrow area |
| Fb.T.Ar/Ma.Ar | Fraction of fibrotic tissue per bone marrow area |
| Ma.Ar/Tt.Ar | Fraction of bone marrow per total area |
| N.e.Lc/B.Ar | Number of empty lacunae per bone area |
| N.Ocl/BS | Osteoclasts per mm |
| N.Ot/B.Ar | Number of osteocytes per bone area |
| N.Pos.Ot/B.Ar | Number of apoptotic osteocytes per bone area |
| N.Pos.Ot/N.Tt.Ost | Number of apoptotic osteocytes per total amount of osteocytes |
| OS/BS | Osteoid surface fraction |
| OV/TV | Osteoid area fraction |

## *CBCT indices*

| | |
|---|---|
| BMD | Bone mineral density |
| BV/TV | Bone volume fraction |
| Conn. Dens | Connectivity density |
| Ct.Po | Cortical porosity |
| Ct.Th | Cortical thickness |
| DA | Degree of anisotropy |
| SMI | Structure model index |
| Tb.N | Trabecular number |
| Tb.Sp | Trabecular separation |
| Tb.Th | Trabecular thickness |
| Tb.TV/TV | Trabecular tissue volume fraction |

# CONTRIBUTING AUTHORS

*E. Bloemena (EB)*
Amsterdam UMC and Academic Centre for Dentistry Amsterdam (ACTA), location Vrije Universiteit Amsterdam, Department of Oral and Maxillofacial Surgery/Oral Pathology, Amsterdam, The Netherlands.

*G.J. Blom (GB)*
Amsterdam UMC, location Vrije Universiteit Amsterdam, Department of Radiation Oncology, Amsterdam, The Netherlands.

*N. Bravenboer (NB)*
Amsterdam UMC, location Vrije Universiteit Amsterdam, Department of Clinical Chemistry, Amsterdam, The Netherlands.

*C.M. ten Bruggenkate (CtB)*
Amsterdam UMC and Academic Centre for Dentistry Amsterdam (ACTA), location Vrije Universiteit Amsterdam, Department of Oral and Maxillofacial Surgery/Oral Pathology, Amsterdam, The Netherlands.
Alrijne Hospital, Department of Oral and Maxillofacial Surgery, Leiderdorp, The Netherlands.

*D. van Dijk (DvD)*
Amsterdam UMC, location Vrije Universiteit Amsterdam, Department of Clinical Chemistry, Amsterdam, The Netherlands.

*H.W. van Essen (HvE)*
Amsterdam UMC, location Vrije Universiteit Amsterdam, Department of Clinical Chemistry, Amsterdam, The Netherlands.

*A.M. Kullaa (AK)*
Institute of Dentistry, University of Eastern Finland, Kuopio campus and Educational Dental Clinic, Kuopio University Hospital, Kuopio, Finland.

*I. Lichters (IL)*
Academic Centre for Dentistry Amsterdam (ACTA), Department of Functional Anatomy, Amsterdam, The Netherlands.

*D.H.F. Rietveld (DR)*
Amsterdam UMC, location Vrije Universiteit Amsterdam, Department of Radiation Oncology, Amsterdam, The Netherlands.

*L. van Ruijven (LvR)*
Academic Centre for Dentistry Amsterdam (ACTA), Department of Functional Anatomy, Amsterdam, The Netherlands.

*E.A.J.M. Schulten (ES)*
Amsterdam UMC and Academic Centre for Dentistry Amsterdam (ACTA), location Vrije Universiteit Amsterdam, Department of Oral and Maxillofacial Surgery/Oral Pathology, Amsterdam, The Netherlands.

# CHAPTER INFORMATION

*Chapter 2*

*Published as:*

Dekker H, Schulten EAJM, ten Bruggenkate CM, Bloemena E, van Ruijven L, Bravenboer N. Resorption of the mandibular residual ridge: A micro-CT and histomorphometrical analysis. Gerodontology. 2018; 35: 221–228.

*Authors' contributions:*

Study design: HD, ES, CtB, EB, NB
Conduct of study: HD, LvR, NB
Collection of data: HD
Analysis and management of data: HD
Preparation of manuscript: HD
Review of manuscript: ES, CtB, EB, LvR, NB

*Funding sources:*

Department and institutional funds.

*Conflict of interest:*

None

*Chapter 3*

*Published as:*

Dekker H, Schulten EAJM, ten Bruggenkate CM, Bloemena A, van Ruijven L, Bravenboer N. Regional differences in microarchitecture and mineralization of the atrophic edentulous mandible: A microcomputed tomography study. Arch Oral Biol. 2022; 133: 105302

*Authors' contributions:*

Study design: HD, ES, LvR, NB
Conduct of study: HD, LvR
Collection of data: HD
Analysis and management of data: HD
Preparation of manuscript: HD
Review of manuscript: ES, CtB, EB, LvR, NB

*Funding sources:*

Department and institutional funds.

*Conflict of interest:*

None

*Chapter 4*

*Published as:*

Dekker H, Bravenboer N, van Dijk D, Bloemena E, Rietveld DHF, ten Bruggenkate CM, Schulten EAJM. The irradiated human mandible: A quantitative study on bone vascularity. Oral Oncol. 2018; 87: 126–130.

*Authors' contributions:*

Study design: HD, NB, EB, DR, CtB, ES.
Conduct of study: HD, DvD, NB, EB
Collection of data: HD, DvD
Analysis and management of data: HD, DvD
Preparation of manuscript: HD
Review of manuscript: NB, DvD, EB, DR, CtB, ES

*Funding sources:*

Department and institutional funds.

*Conflict of interest:*

None

*Chapter 5*

*Published as:*

Dekker H, Schulten EAJM, van Ruijven L, van Essen HW, Blom GJ, Bloemena E, ten Bruggenkate CM, Kullaa AM, Bravenboer N. Bone microarchitecture and turnover in the irradiated human mandible. J Craniomaxillofac Surg. 2020; 48: 733–740.

*Authors' contributions:*

Study design: HD, ES, LvR, GB, EB, CtB, AK, NB
Conduct of study: HD, LvR,, HvE, NB
Collection of data: HD
Analysis and management of data: HD
Preparation of manuscript: HD
Review of manuscript: ES, LvR, GB, EB, CtB, AK, NB

*Funding sources:*

Department and institutional funds.

*Conflict of interest:*

None

*Chapter 6*

*Published as:*

Dekker H, Schulten EAJM, Lichters I, van Ruijven L, van Essen HW, Blom GJ, Bloemena E, ten Bruggenkate CM, Kullaa AM, Bravenboer N. Osteocyte apoptosis, bone marrow adiposity and fibrosis in the irradiated human mandible. Adv Radiat Oncol. 2022; 7: 10095.

*Authors' contributions:*

Study design: HD, ES, GB, EB, CtB, AK, ES
Conduct of study: HD, IL, HvE, NB
Collection of data: HD, IL
Analysis and management of data: HD
Preparation of manuscript: HD
Review of manuscript: ES, IL, LvR, HvE, GB, EB, CtB, AK, NB

*Funding sources:*

Department and institutional funds.

*Conflict of interest:*

None

# LIST OF PUBLICATIONS

## In this thesis

**Dekker H**, Schulten EAJM, Lichters I, van Ruijven L, van Essen HW, Blom GJ, Bloemena E, ten Bruggenkate CM, Kullaa AM, Bravenboer N. Osteocyte apoptosis, bone marrow adiposity and fibrosis in the irradiated human mandible. Adv Radiat Oncol. 2022; 7: 10095.

**Dekker H**, Schulten EAJM, ten Bruggenkate CM, Bloemena E, van Ruijven L, Bravenboer N. Regional differences in microarchitecture and mineralization of the atrophic edentulous mandible: A microcomputed tomography study. Arch Oral Biol. 2022; 133: 105302

**Dekker H**, Schulten EAJM, van Ruijven L, van Essen HW, Blom GJ, Bloemena E, ten Bruggenkate CM, Kullaa AM, Bravenboer N. Bone microarchitecture and turnover in the irradiated human mandible. J Craniomaxillofac Surg. 2020; 48: 733-40

**Dekker H**, Bravenboer N, van Dijk D, Bloemena E, Rietveld DHF, ten Bruggenkate CM, Schulten EAJM. The irradiated human mandible: A quantitative study on bone vascularity. Oral Oncol. 2018; 87: 126-30

**Dekker H**, Schulten EAJM, ten Bruggenkate CM, Bloemena E, van Ruijven L, Bravenboer N. Resorption of the mandibular residual ridge: A micro-CT and histomorphometrical analysis. Gerodontology. 2018; 35: 221-8

## Other publications

Sridhar Reddy P, Villikka K, Kashyap B, **Dekker H**, Schulten EAJM, Mikkonen JJW, Turunen M, Koistinen AP, Bravenboer N, Kullaa AM. Microstructural changes in the irradiated and osteoradionecrotic bone: a SEM study. Ultrastruct Pathol. 2024; 48: 128-136.

Palander A, Fauch L, Turunen MJ, **Dekker H**, Schulten EAJM, Koistinen A, Bravenboer N, Kullaa A. Molecular Quantity Variations in Human-Mandibular-Bone Osteoid. Calcif Tissue Int. 2022; 111: 547-558.

Kashyap B, Naumanen K, Mikkonen J, **Dekker H**, Schulten E, Bloemena E, Pasonen-Seppänen S, Kullaa A. Irradiation Alters the Expression of MUC1, CD44 and Hyaluronan in Oral Mucosal Epithelium. Biomedicines. 2022; 10: 2816.

Kashyap B, Mikkonen JJW, Bhardwaj T, **Dekker H**, Schulten EAJM, Bloemena E, Kullaa AM. Effect of smoking on MUC1 expression in oral epithelial dysplasia, oral cancer, and irradiated oral epithelium. Arch Oral Biol. 2022; 142: 105525.

Reddy Padala S, Saikia D, Mikkonen JJW, Uurasjärvi E, **Dekker H**, Schulten EAJM, Bravenboer N, Koistinen A, Chauhan A, Singh SP, Kullaa AM. Irradiation Induced Biochemical Changes in Human Mandibular Bone: A Raman Spectroscopic Study. Appl Spectrosc. 2022; 76: 1165-1173.

Padala SR, Kashyap B, **Dekker H**, Mikkonen JJW, Palander A, Bravenboer N, Kullaa AM. Irradiation affects the structural, cellular and molecular components of jawbones. Int J Radiat Biol. 2022; 98: 136-47.

Lodders JN, Leusink FKJ, Ridwan-Pramana A, Winters HAH, Karagozoglu KH, **Dekker H**, Forouzanfar T, Schulten EAJM. Long-term outcomes of implant-based dental rehabilitation in head and neck cancer patients after reconstruction with the free vascularized fibula flap. J Craniomaxillofac Surg. 2021; 49: 845-854.

**Dekker H**, Bun RJ, Mulder DC, Breeuwsma N, van der Rhee JI, Guimerà N, Quint W, Vermeer MH, Bouwes Bavinck JN. Human papillomavirus 16-positive supraclavicular cutaneous squamous cell carcinoma metastatic to the level IV supraclavicular lymph nodes. JAAD Case Rep. 2020; 11: 822-5.

Fauch L, Palander A, **Dekker H**, Schulten EAJM, Koistinen A, Kullaa A, Keinänen M. Narrowband-autofluorescence imaging for bone analysis. Biomed Opt Express. 2019; 10: 2367-82.

Ukkonen H, Vuokila S, Mikkonen JJW, **Dekker H**, Schulten EAJM, Bloemena E, Koistinen A, Valdez TA, Kullaa A, Singh SP. Biochemical Changes in Irradiated Oral Mucosa: A FTIR Spectroscopic Study. Biosensors. 2019; 9: 12.

Lampi T, **Dekker H**, ten Bruggenkate CM, Schulten EAJM, Mikkonen JJW, Koistinen A, Kullaa AM. Acid-etching technique of non-decalcified bone samples for visualizing osteocyte-lacuno-canalicular network using scanning electron microscope. Ultrastruct Pathol. 2018; 42: 74-79.

Asikainen PJ, **Dekker H**, Sirviö E, Mikkonen J, Schulten EAJM, Bloemena E, Koistinen A, Ten Bruggenkate CM, Kullaa AM. Radiation induced changes in the microstructure of epithelial cells of the oral mucosa: a comparative light and electron microscopic study. J Oral Pathol Med. 2017; 46: 1004-10.

Ruslin M, **Dekker H**, Tuinzing DB, Forouzanfar T. Assessing the need for a protocol monitoring weight loss and nutritional status in orthognathic surgery based on patients experiences. J Clin Exp Dent. 2017; 9: e272-5

Singh SP, Parviainen I, **Dekker H**, Kullaa, AM. Raman Microspectroscopy Demonstrates Alterations in Human Mandibular Bone after Radiotherapy. J Anal Bioanal Tech. 2015; 6: 2155-72.

Karagozoglu KH, **Dekker H**, Rietveld DHF, de Bree R, Schulten EAJM, Forouzanfar T, van der Waal I. Proposal for a new staging system for osteoradionecrosis of the mandible. Med Oral Patol Oral Cir Bucal. 2014; 19: e433-7.

Van Keulen JW, de Vries JP, **Dekker H**, Gonçalves FB, Moll FL, Verhagen HJ, van Herwaarden JA. One-year multicenter results of 100 abdominal aortic aneurysm patients treated with the Endurant stent graft. J Vasc Surg. 2011; 54: 609-15.

Bastos Gonçalves F, de Vries JP, van Keulen JW, **Dekker H**, Moll FL, van Herwaarden JA, Verhagen HJ. Severe proximal aneurysm neck angulation: early results using the Endurant stentgraft system. Eur J Vasc Endovasc Surg. 2011; 41: 193-200.

Het signaleren van het compartimentsyndroom in de extremiteiten. **H. Dekker**.
In: Procedures in de spoedeisende hulp. IM Spaans et al. 1e druk. Houten: Bohn Stafleu van Loghum; 2010.

# DANKWOORD

Prof. dr. E.A.J.M. Schulten, Bert. Het is inmiddels bijna 14 jaar geleden dat ik kwam solliciteren voor het onderzoek, met daaraan gekoppeld een opleidingsplaats MKA-chirurgie. Ik ben u dankbaar dat u mij deze kans heeft gegeven. Het is een lange weg geweest naar de voltooiing van dit werk. Zonder uw steun zowel in goede als in minder goede tijden, was dit proefschrift zoals het er nu ligt, er niet geweest.

Prof. dr. E. Bloemena, Elisabeth. Ik ben trots en dankbaar dat u mij bij wilde staan op mijn wetenschappelijke reis. Ik durf te zeggen dat in ieder geval in dit land en waarschijnlijk ook ver daarbuiten, niemand te vinden is met meer kennis van de orale pathologie dan u. Zowel persoonlijk als professioneel heb ik diep respect voor u.

Dr. N. Bravenboer, Nathalie. Jij bent absoluut de drijvende kracht achter dit project geweest. Samen op jouw kamertje kletsten we over van alles en nog wat en bedachten we ook nog nieuwe experimenten. Door de jaren heen heeft onze wetenschappelijke samenwerking tot een warme vriendschap geleid. Bedankt voor alle input, support, koffiemomentjes en fijne gesprekken. Ik hoop dat wij in de toekomst zowel wetenschappelijk als vriendschappelijk verbonden zullen blijven.

Prof. dr. Chr. M. ten Bruggenkate, Chris. Bedankt dat u mij mogelijkheid hebt geboden dit proefschrift te realiseren. Het oogsten van de botbiopten voor de controlegroep deden we samen in Leiderdorp, de Wagner CD in de stereo, en met een moordend tempo werden op de tonen van 'die Walküre' de potjes gevuld. Ik heb ervan genoten om met u samen te werken.

Prof. dr. A. Kullaa, dear Arja, thank you and your colleagues for the valuable input in our study. I very much enjoyed our collaboration and our meetings in Amsterdam. The Moomin birthday button book has been one of my daughter's favorites and we still read it occasionally. I look forward to continuing working together, and hopefully someday I can visit Kuopio and see your lab and the beautiful Finnish scenery.

Geachte leden van de promotiecommissie: prof. dr. J. Klein Nulend, prof. dr. R. de Bree, prof. dr. J.P.R. van Merkesteyn, prof. dr. J.G.A.M. de Visscher en prof. dr. dr. P.A.W.H. Kessler. Hartelijk dank voor uw belangstelling in mijn manuscript en voor de tijd en moeite die u heeft genomen om dit zorgvuldig te beoordelen.

Lieve Marjan en Elisabeth, mijn paranimfen. Marjan, al sinds 2010 mijn partner in crime. Wij hebben samen ontelbaar veel kilometers afgelegd: door vreemde landen en over besneeuwde bergen, over hoge pieken en door diepe dalen. Dit alles natuurlijk opgeleukt door ontelbaar veel potjes Yathzee, cappu'tjes en glaasjes wijn. Bedankt voor je vriendschap, en bedankt dat je mij ook nu weer bij wil staan tijdens de verdediging van mijn proefschrift. Elisabeth, mijn AIOS maatje. Vanaf het moment dat wij elkaar ontmoetten op het interfacultair tandheelkunde congres in Lunteren, hadden wij een klik. Jij deed geneeskunde, ik tandheelkunde en uiteindelijk samen in opleiding. Lief en (opleidings-)leed hebben wij met elkaar gedeeld, en nu sta je weer naast me. Ik ben dankbaar dat je mijn paranimf wil zijn.

Graag wil ik ook alle patiënten bedanken die hun weefsel beschikbaar wilden stellen ten behoeve van het onderzoek.

Dr. L. van Ruijven, beste Leo. Jouw onuitputtelijke geduld om mij vertrouwd te maken met de ingewikkelde materie van de micro-CT is bewonderenswaardig. Vele uren heb ik gespendeerd bij de scanner op de 12e, al dan niet met baby, en nooit was je te beroerd om mee te komen kijken als ik weer eens voor de zoveelste keer vastliep met meten of scannen. Dank je voor het delen van je kennis en kunde, en voor alle hulp die je mij hebt geboden tijdens het onderzoek.

Dr. E.C.J. Phernambucq, drs. G. Blom en drs. D.H.F. Rietveld, Erik, Gerrit en Derek. Dank jullie wel voor jullie input vanuit de afdeling Radiotherapie en de onmisbare hulp bij het berekenen van de stralingsdoses.

Tijdens het promotietraject heb ik vele studenten mogen begeleiden bij hun onderzoeksstage. In het bijzonder wil ik graag noemen Zeineb, Emma, Loreine, Dennis,

Astrid, Jorieke en Inez. Dank voor jullie enthousiasme en inzet voor het onderzoek. Het was een plezier met jullie samen te werken.

Beste Huib, mede Beatles-fan en koffie enthousiast. Dank voor je geduld en je onmisbare hulp bij het verwerken van de botbiopten. En dat je altijd om mijn grappen lachte, ook als ze slecht waren.

Beste Paulien, Ina en Mirjam. Veel dank voor de vele coupes die jullie voor mij gesneden en gekleurd hebben.

Lieve collega's van het derma-lab! Jullie verdienen natuurlijk een speciaal plekje in mijn dankwoord. Want hoe ongelooflijk saai het labwerk ook was, het was bij jullie altijd een feestje. In het bijzonder Hanneke en Maria, en mijn vrienden Erik, Jeroen, Lambert, Taco en Niels, van 'er is altijd nog plan B', dank voor de gezellige tijd!

Lieve meiden van de poli's Dijklander Purmerend, ZMC en KMC. Jullie maken elke dag gezellig! Bedankt dat jullie mij altijd opvrolijken met een lekker koffietje of een sappige roddel, Sky Radio Love Songs voor mij opzetten (Celine Dion!) en dat jullie stuk voor stuk zulke leuke mensen zijn!

Lieve Theo, collega en vriend. Dank dat ik altijd op je kan rekenen. Het is mij een eer en een genoegen met je samen te mogen werken.

Lieve Marnix en Ewoud, jullie zijn de beste maten die ik mij kan wensen. Bedankt voor jullie vertrouwen in mij. Ik hoop dat wij nog vele jaren met elkaar ons mooie vak kunnen uitoefenen.



Lieve vrienden en familie, dank jullie wel dat jullie er waren door de jaren heen. Ik hoef mij nooit eenzaam te voelen.

Lieve blondies, Sally, Kerren, Gwen en natuurlijk mijn lieve nichtje Annechien. Stuk voor stuk zulke mooie sterke vrouwen. Onze levens zijn zo verschillend verlopen, maar

zo leuk om elkaar af en toe te zien om bij te kletsen. Bedankt voor jullie vriendschap. Ik hoop nog steeds op een reünie in 'Le Monde'…

Lieve Annelien. 'Beter een goede buur dan een verre vriend' is in ons geval een understatement. Jij bent veel meer dan alleen een buur en vriend. Of ik nou hulp nodig heb met de kinderen, geen melk meer in huis heb of gewoon zin heb in een prettig gesprek, een aflevering 'per seconde wijzer' of een glas wijn, bij jou mag ik altijd aanbellen. Dank je wel dat je er bent!

Lieve Judith, lieve zus. Soms voel je zo ver weg maar op de belangrijke momenten ben je dichtbij. Jouw warme gezin met Phi Son, Otis, Loé en Rumi is een baken van rust en liefde, ik heb oneindig veel respect voor wat jullie samen hebben opgebouwd. Dank voor alle heerlijke bordjes saoto en pho, en jullie gastvrijheid voor mij en voor mijn kinderen. Ik hou van jullie.

Lieve Jasper, lieve broer. Wat heb jij hard gewerkt en wat ben ik trots op jou! Met je twee prachtige en lieve dames Emmelie en Sofie hebben jullie het samen voortreffelijk voor elkaar. Dank dat ik ondanks je drukke schema altijd op je handigheid kan rekenen, of het nou een klus is aan mijn auto of ik hulp nodig heb om iets aan de muur te schroeven, je staat altijd voor mij klaar. Love you.

Lieve pap en mam. Waar moet ik beginnen. De weg hier naar toe is niet altijd even makkelijk geweest. Ondanks alle obstakels hebben jullie mij altijd onvoorwaardelijk gesteund, en dat doen jullie nog steeds. Zonder jullie was dit proefschrift er niet geweest. Ik ben jullie enorm veel dank verschuldigd voor jullie liefde, steun en geloof in mij. Ik hou van jullie. Dit proefschrift is voor jullie.

Mijn lieve allerliefsten, Cézanne, Brent en Beau. Jullie zijn mijn zon, mijn maan en mijn sterren, jullie zijn mijn alles. Jullie zijn zulke prachtige en unieke individuen en ik ben zo ontzettend trots dat ik jullie moeder mag zijn. Mama houdt tachtigmiljoenhonderdduizend ontelbaar veel van jullie. Als jullie dat maar nooit vergeten.

# ABOUT THE AUTHOR

Hannah Dekker was born in Hoorn, the Netherlands on February 12th, 1981. After graduation from secondary school she started her medical education at the VU University Amsterdam in 2000. During her bachelor study, she was an editor for the student edition of the Dutch Medical Journal (Nederlands Tijdschrift voor Geneeskunde – studenteneditie).

After obtaining her MD degree, she worked for three years as a surgical resident, respectively in the Emergency Department of Amsterdam University Medical Centers (Amsterdam UMC, location VUmc) and in the Department of Surgery of the St. Antonius Hospital in Nieuwegein/Utrecht.

In the fall of 2010, she began her PhD research under the supervision of prof. dr. E.A.J.M. Schulten, prof. dr. E. Bloemena, dr. N. Bravenboer and prof. dr. C.M. ten Bruggenkate. In 2011, she started her dental education at Academic Centre for Dentistry Amsterdam (ACTA) where she obtained her DDS degree in 2014.

She started her Oral and Maxillofacial Surgery residency in the Department of Oral and Maxillofacial Surgery, Amsterdam UMC, location VUmc, in January of 2015 (supervisor: prof. dr. E.A.J.M. Schulten). Her non-academic rotation was performed in the Medical Center Alkmaar (supervisor: drs. I.G.H. van der Tol, 2018).

In July 2019 she was registered as an oral and maxillofacial surgeon. She works as a consultant in Zaandam Medical Center (ZMC) and Dijklander hospital in Purmerend.

Hannah is the proud mother of Cézanne (2017), Brent (2018) and Beau (2019).